Investigating the T cell-specific role of Interleukin-4 receptor alpha (IL-4Rα) in tuberculosis (TB)

by **Robert Pierre Rousseau**

RSSROB010

Thesis presented for the Degree of Doctor of Philosophy (Ph.D.) in Clinical Sciences in Immunology

February 2024

Supervisor: Associate Professor Suraj P Parihar

Co-Supervisors: Dr Catherine Riou and Professor Frank Brombacher

International Centre for Genetic Engineering and Biotechnology (ICGEB) Cape Town

Centre for Infectious Diseases Research in Africa (CIDRI-Africa)

Institute of Infectious Diseases and Molecular Medicine (IDM)

Division of Immunology, Department of Pathology, Faculty of Health Sciences, University of Cape Town, South Africa

Declaration

I, **Robert Pierre Rousseau**, hereby declare that the work on which this thesis is based, is entirely my own (except where acknowledgements indicate otherwise) and that neither the whole body of work, nor an part of it has been, is being, or is to be submitted for another degree in this or any other university.

I grant permission to the university to reproduce the purpose of research either the whole or any portion of the contents in any manner whatsoever.

Signature: Signed by candidate

Date: 08 February 2024

Acknowledgements

Firstly, I would like to thank my supervisor, **A/Prof Suraj Parihar** for granting me the opportunity to study a PhD. I will always remember the way we met by chance, and he kindly invited me into his office and it snowballed into where I am today. His incredible guidance and advice throughout this journey have been pivotal, and I am thankful for his training, advice and his time. It has been a fantastic four years.

I would also like to thank **Prof. Frank Brombacher** and **Prof Robert J Wilkinson** for providing space in their labs, and providing me with a funding. Without which this degree would not have been possible. Their encouragement, and advice is well appreciated. I would also like to extend a gracious thanks to **Dr Catherine Riou**, the wizard of flow, for all the time that she allowed me to spend in her office. Her open door policy and scientific mentorship, has fashioned me into a critical thinker, and instilled indelible traits that I will take forward in my career. Her flow training has proved invaluable. An enormous thanks **Dr Mumin Ozturk** for being there at the start, and spent many hours training me on various lab techniques. You helped set the foundation from which I was able to springboard into the rest of this degree. His selflessness, and dedication are traits that I aim emulate.

I am extremely fortunate to have met so many talented and smart colleagues over the years.

I would like to thank to give a special thanks to **Dr Rudranil Hazra, Dr Shelby-Sara Jones-Addinal, Sibongiseni Poswayo,** and **Saiyukthi Naidoo**. You all provided help to me in many ways during my scientific journey. Without you guys, there many experiments which I would simply not be able to perform. I would like to thank members of the Brombacher group and CIDRI labs for their efforts, assistance and advice in the background are all appreciated.

I would like to thank my parents **Pierre Rousseau** and **Marian Rousseau** for instilling a love for science in me at an early age. I am thankful for their support, and tireless encouragement. I would like to thank my sister, **Meghan Valerio**, for her support and always being there to check in on me. I am extremely fortunate to have such an incredibly supportive family.

Thanks to my friends and roommates **Alistair Muskett**, **Fraser Muskett**, **Tayna Carlisle** and **Etienne van den Berg** for celebrating my small victories and making a home a place I want to come back to. I would like to thank, **Melissa Wain**, for being my pillar of support. Thank-you for being patient with my early mornings, late nights, and absent weekends. Your words of encouragement and acts of love have kept me moving forward more than you realise. Thank you for reminding me that there is a finish line and helping me cross it.

Publications

1. Anca F. Savulescu, Nashied Peton, Delia Oosthuizen, Rudranil Hazra, Robert P. Rousseau, Musa M Mhlanga and Anna K. Coussens. **Quantifying spatial dynamics and regulators of *Mycobacterium tuberculosis* phagocytosis by primary human macrophages using microfabricated patterns** (Cell Reports Methods, 2023, Nov, 3 (11):100640)

2. Julius E. Chia, Robert P. Rousseau, Mumin Ozturk, Sibongiseni KL Poswayo, Frank Brombacher and Suraj P. Parihar. **Differential role of IL-4Rα-deficient Foxp3 T cells in listeriosis and tuberculosis** (Submitted, Frontiers Immunology)

3. Mumin Ozturk, Maxine Hoft, Robert P Rousseau, Frank Brombacher and Suraj P. Parihar. **IL-4Rα deletion on dendritic cells decreased *Mtb* burdens and lung pathology during chronic infection** (in preparation)

4. Robert P. Rousseau, Sibongiseni KL. Poswayo, Mumin Ozturk, Saiyukthi Naidoo, Rudranil Hazra, Robert J Wilkinson, Catherine Riou, Frank Brombacher and Suraj P. Parihar. **The deletion of IL-4Rα on T cells increased host susceptibility to tuberculosis despite intact Th1 responses** (in preparation)

List of Abbreviations

AIDS: Acquired Immunodeficiency Syndrome

AF: Alexa Fluor

AM: Alveolar Macrophages

APC: Antigen-presenting cells

APC: Allophycocyanin

AP: Alkaline phosphatase

ATP: Adenosine Triphosphate

BAL: Bronchoalveolar lavage

BCG: Bacillus Calmette Guérin

Bcl6: B cell lymphoma 6 protein

BMDM: Bone Marrow Derived Macrophages

CCL: Chemokine (C-C motif) ligand

CCR: CC- Chemokine Receptor

CD: Cluster of Differentiation

CFU: Colony Forming Units

CXCR: C-X-C chemokine receptor

DC: Dendritic cells

DC-SIGN: DC-Specific Intracellular Adhesion Molecule-3 Grabbing Nonintegrin

DPI: Days post infection

DNA: Deoxyribonucleic Acid

ECM: Component of Extracellular Matrix

ELISA: Enzyme-linked Immunosorbent Assay

FACS: Fluorescence-activated cell sorter

FcγR: Fc gamma receptor

FBS: Foetal bovine serum

FITC: Fluorescein isothiocyanate

G-CSF: Granulocyte colony stimulating factor

GM-CSF: Granulocyte macrophage-colony stimulating factor

GTP: Guanosine triphosphate

γδ: Gamma delta T cells

H&E: Haematoxylin and eosin

HGF: Hepatocyte growth factor

HIV: Human Immunodeficiency Virus

HRP: Horseradish peroxidase

iBALT: Inducible bronchus associated lymphoid tissue

ICOS: Inducible T cell co-stimulator

ICS: Intracellular Cytokine Staining

IFN-γ: Interferon-gamma

IL-: Interleukin

IM: Interstitial Macrophage

IN: Intranasal

iNOS: Inducible nitric oxide synthase

KLRG1: Killer cell lectin-like receptor G1

LN: Lymph Node

LPS: Lipopolysaccharide

***M.bovis*:** *Mycobacterium bovis*

Met: Mesenchymal-epithelial transition factor

MDR-TB: Multidrug-resistant TB

MCP-1: Monocyte chemoattractant protein-1

MHC: Major Histocompatibility complex

MMP: Matrix Metalloproteinase

***Mtb*:** Mycobacterium tuberculosis

MYD88: Myeloid differentiation primary response gene 88

NHP: Non-human Primate

NK: Natural Killer

NO: Nitric oxide

PE: R-phyoerythrin

PerCP: peridinin chlorophyll protein

PCR: Polymerase Chain Reaction

PD-1: Programmed Cell Death Protein 1

PHOX: Phagocyte oxidase

PI3P: Phosphatidylinositol 3-phosphate

PMN: Polymorphonuclear leukocytes

PRR: Pattern-recognition receptors

PAMP: Pattern-recognition receptors

RAC1: Ras-related C3 botulinum toxin substrate 1

RBC: Red Blood Cell

RNIs: Reactive nitrogen intermediates

ROS: Reactive Oxygen Species

STAT: Signal transducer and activator of transcription

SEM: Standard error of the mean

S. mansoni: *Schistosoma mansoni*

TB: Tuberculosis

T-bet: T-box expressed in T cells

T_{CM}: Central memory T cell

TCR: T cell receptor

T_{EM}: Effector memory T cell

Th1: T helper 1

TGF-β: Transforming Growth Factor β

TLR: Toll like receptor

TNF: Tumor necrosis factor

TLR: Toll-like receptors

T_{reg}: T regulatory cell

T_{RM}: Tissue Resident memory T cell

WHO: World Health Organization

WPI: Weeks post Infection

XDR-TB: Extensively Drug resistant TB

Table of Contents

Table of Figures

Chapter 1: Literature Review

Chapter 3: Results

Chapter 4: Discussion

List of Tables

Abstract

Protective immunity to tuberculosis (TB) is dependent on the ability of the host to mount a robust T cell response. The main effector T cells which contribute to protection in TB include T helper (Th) Th1 and Th17 T cells. The Th2 response, associated with IL-4Rα mediated signalling, remains largely overlooked in TB. The role of IL-4Rα in TB appears to be different according to cell type. Deletion of IL-4Rα on macrophages has no effect on disease, but deletion of the receptor on B cells, leads to better control. This thesis aimed to explore the T cell-specific role of IL-4Rα in TB disease by making use of T cell specific knockout model, iLCK^{Cre}IL-4Rα$^{-/lox}$. We found that absence of IL-4Rα on T cells results in a delay in the recruitment of T cells to the lung. This was demonstrated by decreased CD4 and CD8 T cell numbers during acute infection compared to littermate controls. Consequently, the bacilli are able to better establish infection and proliferate in the lung, shown by increases in lung mycobacterial burden at both acute and chronic stages of infection. However, no differences are observed in the spleen, indicating deletion of IL-4Rα does not have a role in the dissemination of TB. In the absence of IL-4Rα, T cells express higher amounts of T-bet or RORγt transcription factors, indicating stronger Th1 and Th17 responses, respectively. The stronger pro-inflammatory responses do not clear the pathogen, and instead contribute to immunopathology. During chronic infection, we observed higher amounts of IL-17 as well as a corresponding increase in neutrophils, which in turn lead to a decrease in alveolar free space. The promotion of increased Th1 CD4 T cells resulted in greater amounts of terminally differentiated (CD44^{+}KLRG1^{+}) which have a poor proliferative capacity despite secreting large amounts of IFN-γ. KLRG1 expression is also associated with a reduced ability to migrate into the lung parenchyma, the site of disease. We also found that these (CD44^{+}KLRG1^{+}) expressed reduced amounts of CXCR3, CD69, and CD103, which are all markers associated with poorer migration into the lung parenchyma. Importantly, these factors result in decreased survival in T cell-specific IL-4Rα mice. In conclusion this study demonstrates that absence of IL-4Rα on T cells promotes a predominant Th1/Th17 response, that results in delayed recruitment into the lung tissue, which ultimately proves detrimental for the host.

Chapter 1:
Literature Review

1.1 Tuberculosis

1.1.1 The Global burden of tuberculosis

Mycobacterium tuberculosis (*Mtb*), the etiological agent of tuberculosis (TB), is an ancient pathogen which has afflicted humans for centuries. TB remained the leading cause of death due to infectious disease, until 2021 where it came second to SARS-CoV2. According to the 2022 WHO tuberculosis report, it is estimated that 10.6 million became ill with TB, and that 1.6 million people died as a result of TB in 2021 [1]. Of note, for the 2020-2021 period, TB cases numbers may have been underestimated due to the emergence of the COVID-19 pandemic, where access to health service was restricted. Importantly, during the COVID-19 pandemic, a reversal of the trend in the estimated number of TB deaths (Fig. 1.1A) and incidence of multi-drug-resistant/rifampicin resistant-tuberculosis (MDR/RR-TB) cases (Fig. 1.1B) was also observed, likely associated to essential TB services disruption.

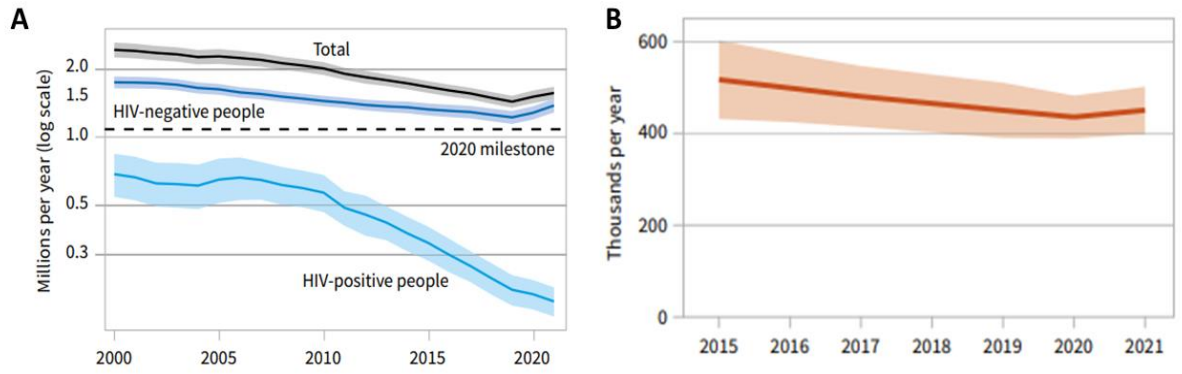

Figure 1.1: The 2020-2021 period saw a reversal in the trend in global estimates for (A) TB induced deaths (B) Incidence of MDR/RR-TB. Shaded are represents 95% uncertainty interval. (Adapted from the WHO Global Tuberculosis Report 2022 [1])

The large number deaths illustrate that TB remains a significant public health problem globally, with the largest burden of disease found in developing countries [2] (Figure 1.2). The vast majority of TB cases and TB deaths occur in Africa and South-East Asia. These regions combined accounted for approximately 87% of incident cases and 82% of deaths related to TB, including both HIV-positive and HIV-negative patients. Adult men are disproportionality affected by TB and account for 56.5% of all TB cases in 2021, whereas woman and children accounted for 32.5% and 11%, respectively.

An association between countries with high burdens of disease and low socioeconomic status is well established. Furthermore, socioeconomic status is also linked to treatment outcome. Several factors associated with low economic status contribute to the vulnerability of these

communities to TB, including high HIV burden, undernutrition, limited access health care facilities, increased non-adherence to treatment [3-7].

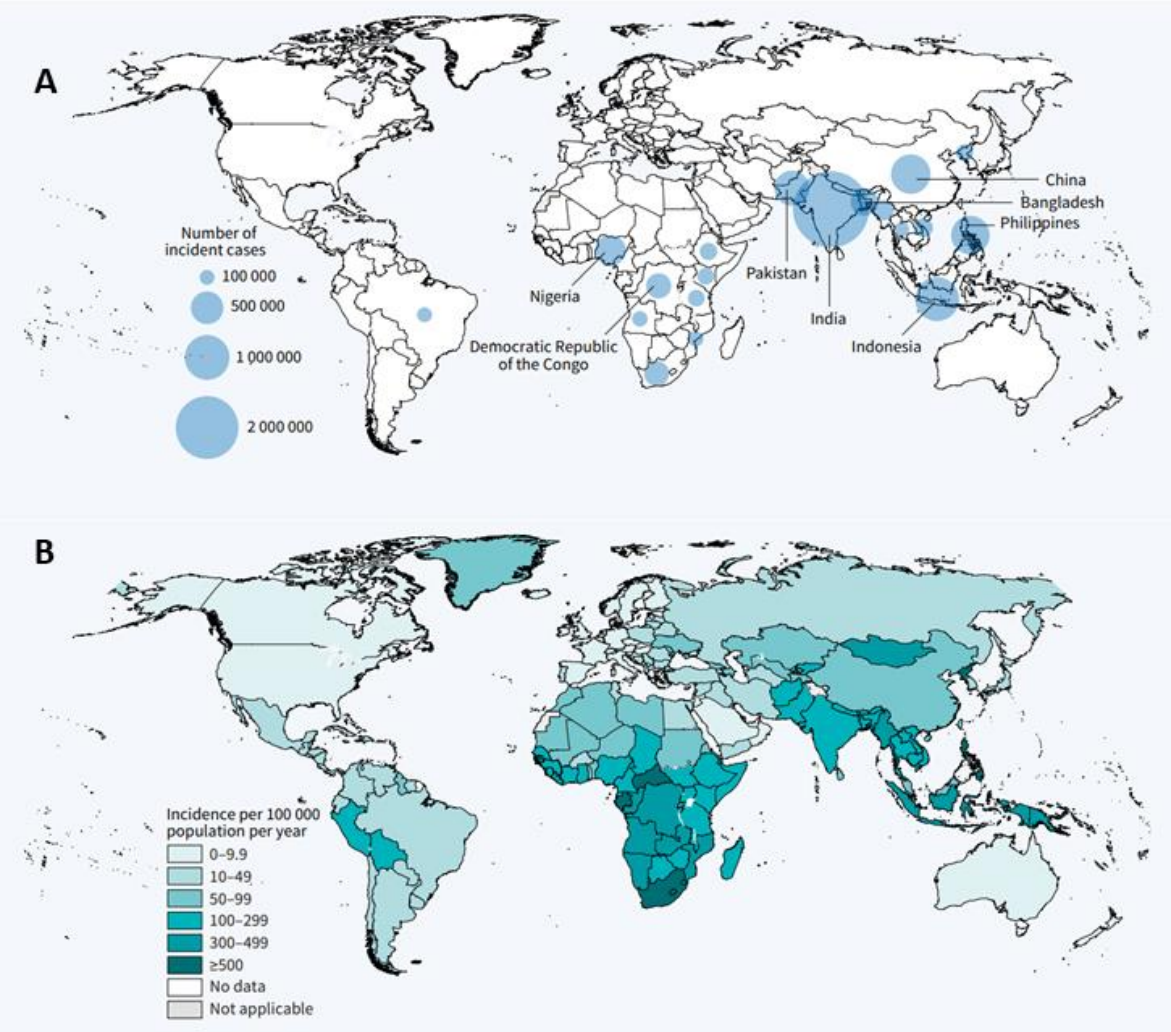

Figure 1.2: Global burden of TB disease. (A) – Estimated incidence of TB for countries with at least 100000 cases. (B) – Estimated Incidence of TB as a proportion of population. (Adapted from the WHO Global Tuberculosis Report 2022 [1])

Despite the high burden of the disease, TB is a treatable disease. Yet about 50% of TB patients succumb to the disease due to a lack of access to treatment [1]. TB treatment is complex. The complexity of TB treatment is related to specific microbiological characteristics of this pathogen, including its ability to 1) grow in a matrix-encased multicellular community (called biofilms), 2) reside intracellularly in macrophages and 3) transition into a non-replicating, dormancy state [8-11]. Consequently, TB treatment necessitates a prolonged and multidrug regimen, spanning over 6 months. The first 2 months involves an initial bactericidal phase of rifampicin, isoniazid, pyrazinamide and ethambutol. Over the remaining 4-month period, only isoniazid and rifampicin are administered to ensure sterilization [8, 12]. Patients who undergo this treatment approach have a high rate (86%) of successful outcome [1]. Long treatment

periods often increase the risk of non-adherence to prescribed regimen. Contributing factors may include logistical issues, such as difficulty and cost of transport to the clinic or clinic supply shortage. It may also include the drug-related side effects [3, 5, 6]. Recently, studies have shown that the treatment duration can be reduced to 4 months using rifampentine, with moxifloxacin [13]. Resistance to the first-line drugs, rifampicin and isoniazid, is referred to as multi-drug resistant TB (MDR-TB). *Mtb* resistant to the first-line drugs, as well as any fluoroquinolone and either bedaquiline or linezolid, is referred to as extensively drug-resistant TB (XDR-TB) [14]. Drug-resistant TB requires between 9-20 months of treatment with costly medication, and has a lower success rate compared to drug-susceptible TB (success rate of 56% for MDR-TB and 39% for XDR-TB) [14]. In 2021, the WHO reported 166,991 cases of combined total of MDR-TB and XDR-TB, a 6.4% increase from 2020 [1]. The emergence of drug-resistance TB remains a challenge and necessitates better understanding of the disease to derive better treatment strategies.

The WHO has created a global watchlist of 30 countries with high TB burdens, high TB/HIV and high MDR/RR-TB burden countries. 49 countries, included on at least one of these lists, account for an estimated 86-90% of the total TB cases reported in 2021. South Africa is listed on all three of these watchlists, underscoring the need for better, testing, diagnosis and treatment strategies.

1.1.2 Pathogenesis and Immunopathology of TB

1.1.2.1 *Mycobacterium Tuberculosis*

Mtb is non-motile, acid-fast, rod-shaped bacillus ranging in approximately 0.2-0.5 x 1 μm. The baciili are surrounded by a protective envelope comprised of the cytoplasmic membrane, a cell wall and matrix of glucans and proteins that form a waxy capsule (Figure 1.3) [15, 16].

The distinctive feature of mycobacterial cell wall is the myco-membrane, which is enriched in mycolic acids and is a major contributor to the impermeability of the envelope. A study that highlights the protective nature of the myco-membrane showed that it is between 10-100 times less permeable to β-lactam antibiotics compared to the envelope of gram-negative bacteria, such as *Escherichia coli* and *Pseudomonas aeruginosa* [17]. The structure of mycobacterial cell wall is a major reason underpinning the resistant of *Mtb* to numerous drugs.

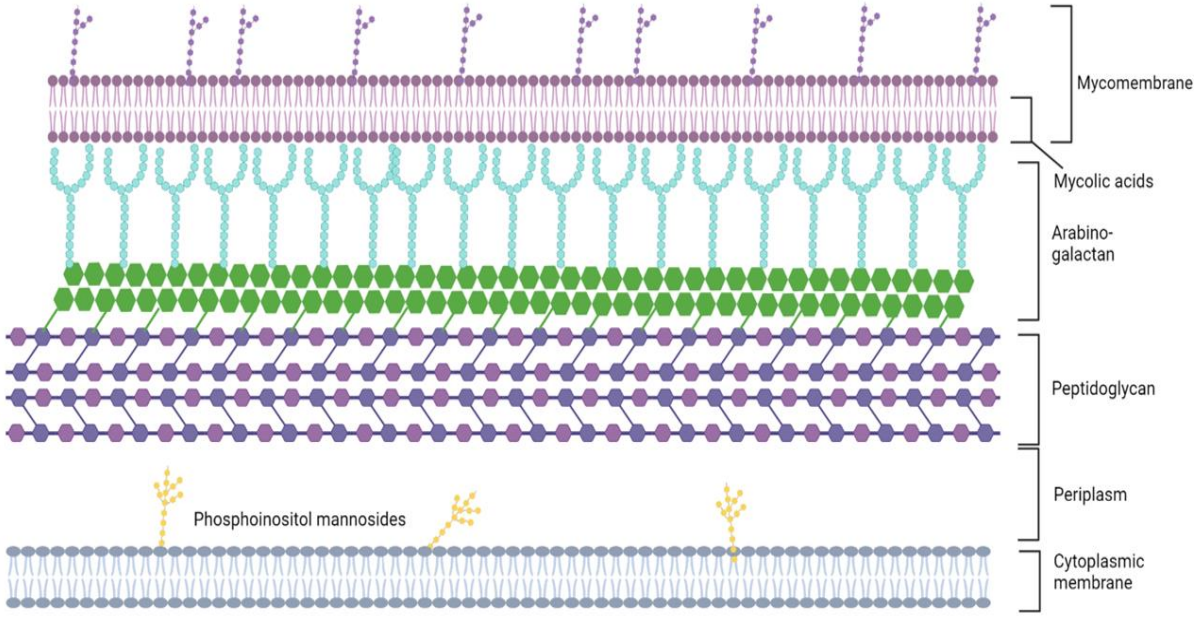

Figure 1.3: Schematic representation of the cell envelope of Mycobacterium tuberculosis
(Adapted from [15]. Image generated in Biorender)

1.1.2.2 Initial events after *Mtb* infection.

TB infection is primarily caused by the inhalation of *Mtb*-containing aerosol droplets (Figure 1.4). Transmission of Mtb requires that *Mtb*-containing droplets are aerosolized from the site of disease. This is mediated by pulmonary TB patient's cough, sneezes, shouts or even tidal breathing [18, 19]. The infectious aerosol droplets range between 1-5 µm in size, and are capable of remaining airborne [20] and culturable. Once it is inhaled, *Mtb* droplets enter the lung and are deposited in the distal alveolar space. The initial host response involves the recruitment of phagocytic cells, primarily composed of resident alveolar macrophages (AM) and neutrophils. The invading bacilli are then engulfed by AMs or dendritic cells (DCs) [21]. Once the *Mtb* bacilli have been phagocytosed, they are either killed or are able to persist and replicate within these macrophages which could result in primary disease or after a latent period, could progress to active disease [22]. *Mtb* makes use of the virulence factor, a type VII ESX-1 secretion system, that interplays with the host IL-1R and allows the infected AM to traverse the epithelial boundary into the lung interstitium [23]. The consequence of this is that the AMs help disseminate the infection, and that bacteria are delivered into the lung tissue before the arrival of additional recruited monocytes. *Mtb* is an adaptable pathogen capable of evading and suppressing immune mechanisms, enabling its persistence within the host.

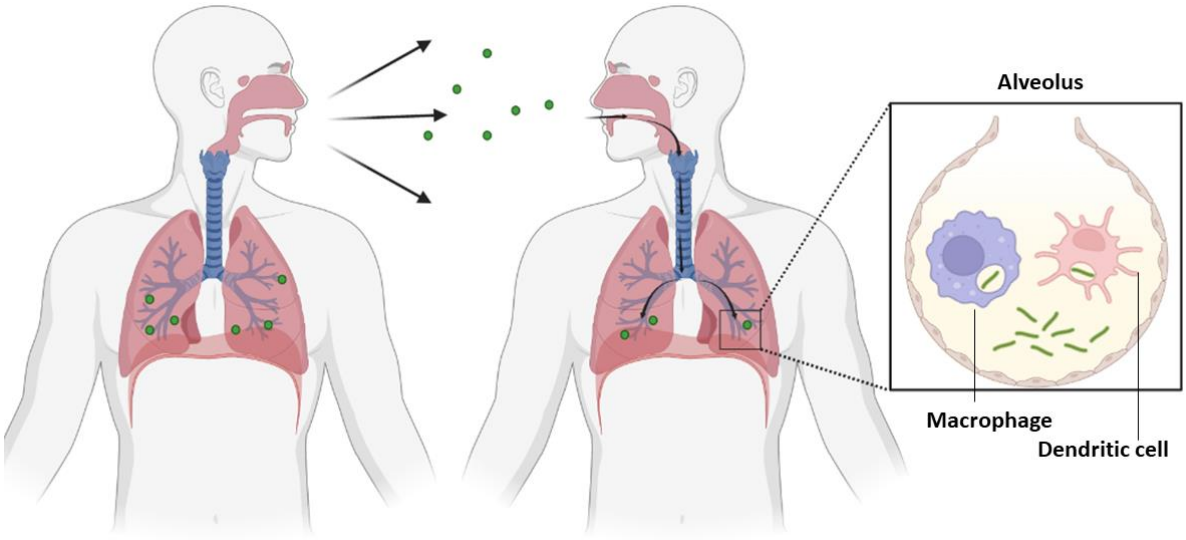

Figure 1.4: *Mtb* Bacilli are spread from an infected person to another through the air: The green dots represent Mtb containing droplet nuclei. Once inhaled the bacilli are deposited in the alveoli where it comes into contact and is taken up by with alveolar macrophages or other phagocytes such as dendritic cells. (Image adapted from [24] and generated in biorender).

These evasion strategies encompass various tactics, such as inhibiting the maturation of the phagolysosome through ESX-3 type VII secretion system, blocking acidification within the macrophage, disrupting antigen processing and presentation by transcriptionally downregulating major histocompatibility complex (MHC) class II, and masking toll-like-receptors (TLRs) ligands from the microbial surface [25-31]. These survival strategies allow *Mtb* to replicate within the macrophages which remain quiescent, ultimately leading to macrophage necrosis. As a result, bacteria are released to the extracellular space, where they can be phagocytosed by other AMs allowing the cycle to repeat [32-34].

1.1.2.3 The granuloma, the hallmark of TB.

This cycle of infection and necrosis of macrophages within the lung interstitium, results in the release of inflammatory chemokines which recruit neutrophils, monocytes and other immune cell populations. The accumulation of immune cells leads to the formation of a granuloma (Figure 1.4), the defining hallmark of tuberculosis disease [35, 36]. The core of the TB granuloma is comprised of Mtb-infected macrophages. The very center of the granuloma is constituted of necrotic material, called the caseum, often described as cheese-like. The core of infected macrophages is then surrounded by epithelioid macrophages [35, 37] These epithelioid macrophages are characterized by specific morphological features including diffuse cytoplasm and elongated nuclei. These morphological alterations result from transcriptional changes inducing epithelial-like modules such as E-cadherin. Consequently, this process leads to the

interdigitation and tight adherence of epithelioid macrophages to one another [35, 38]. This core of macrophages acts as a scaffold and is surrounded by a cluster of lymphocytes, typically referred to as the lymphocyte cuff. Some parts of the granuloma can have areas where the peripheral lymphocytes are organized adjacent to antigen presenting cells (iBALT), facilitating antigen presentation to T cells at the site of disease [39, 40]. The organized structure of the granuloma effectively contains the pathogen, preventing active disease. However, the granuloma is a double edged sword, while it might contain the pathogen from spreading, it can also act as niche for the *Mtb* bacilli, allowing the bacteria to survive in a relatively dormant state for a long period of time [41]. The strategy of isolating the pathogen within a granuloma also shields it from the host's T-cell immune response. This is because the CD4 and CD8 T cells are restricted from infiltrating and gaining access to the core of the granuloma where *Mtb* reside, as well as localized T cell suppression driven by TGF-β and IL-10 [38, 42-44]. It is important to note that TB granulomas come in various types, distinguished by differences in inflammation profiles, cellular composition, and the timing of their formation relative to the onset of infection [45-49]. These different granulomas vary in their capacity to promote bacterial survival or hinder it [45-48]. granulomas are commonly categorized as (1) foreign body type, (2) solid, caseous and cavitary, and (3) Nascent, caseous, fibrotic and calcified granulomas.

The prevailing line of thinking was that formation of granuloma is primarily orchestrated by type 1 cytokines TNF and IFN-γ [50-52]. However, a recent study examining the transcriptional profiles of granulomas in non-human-primates (NHPs) at different timepoints showed an inverse correlation between bacterial burden and T cells expressing the Th-1 associated T-bet expression [48], highlighting the complex regulation of granuloma formation. For example, coordinated type 1 and type 17 responses within the granuloma were found to strongly correlate with low bacterial burden, suggesting that a well-coordinated interplay of IL-17, TNF and IFN-γ is required. [47]. In Schistosoma, granuloma formation is driven by IL-4 and IL-13 dependent pathways. Cronan and colleagues made use of single-cell RNA sequencing in zebra fish to demonstrate that TB granulomas have both type 1 and type 2 markers present [37]. The results of this study show that type 2 markers, such IL-4 and IL-13 might play a role in granuloma, and not just type 1. They also found that eosinophils contributed to IL-4 production. The study further shows that macrophages within the core of the granuloma that express type 1-associated IL-1β, CXCl11 and iNOS transcripts did not express markers typically associated with epithelioid macrophages such as E-cadherin and ZO-1. The authors conclude that type 2 signals

may play a non-negligeable role in driving the formation of the epithelioid core of macrophages. Moreover, another study in NHPs by Grant and colleagues showed that high bacterial burden granulomas often appear early, exhibit elevated expression of IL-4, IL-5 and IL-13 and are enriched with mast cells [47]. The authors asserted that the type 2 signaling pathways drive the tissue remodeling to wall off the pathogen, but instead allow for a permissive environment for mycobacterial growth. These studies demonstrate that a better understanding of type 2 immunity in TB disease could unveil critical targets for host-directed therapies.

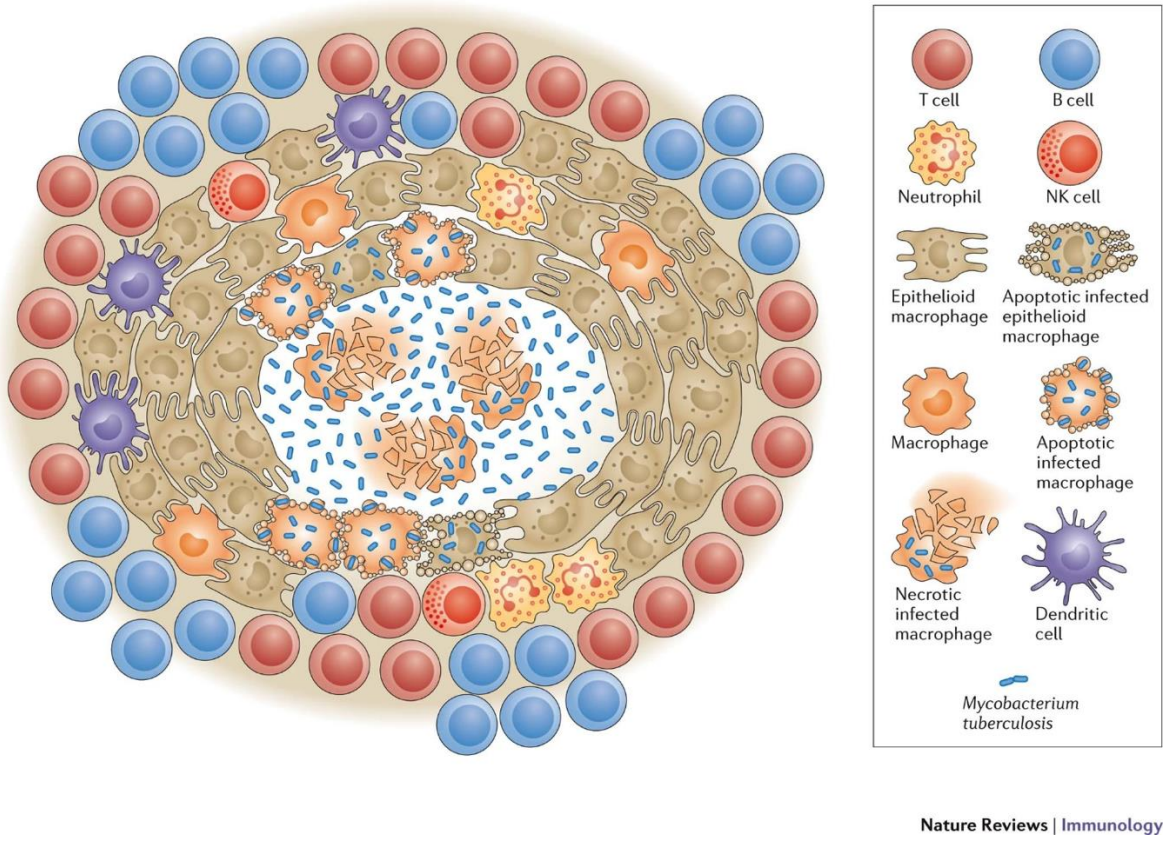

Figure 1.5:The hallmark of tuberculosis, the granuloma. The schematic shows how the structure is highly organized and composed of heterogeneous population of immune cell populations. Image used from Cadena, et al. (2017)[53].

1.1.2.4 The role of T cells in TB

The uptake of *Mtb* and *Mtb*-containing fragments is facilitated by DCs and monocyte derived DCs, which subsequently migrate to draining lymph nodes (LN) to process and present antigens to naïve T cells [54-56]. The DCs migration is controlled by IL-12p40, IL-12p70, CCL19 and CCL21 [51, 57-59]. Dissemination of *Mtb* to the LN is carried out by *Mtb*-infected DCs, and occurs 8-10 days after initial infection [60]. Studies in the murine model have shown

that once *Mtb* is in the LN, *Mtb*-specific T cell are primed and become activated, proliferate and differentiate into effector cells, as demonstrated by their ability to produce IFN-γ, express activation markers (such as CD44, and CD69), and undergo several rounds of division measured using CFSE assay [60-62]. These effector cells also downregulate the LN homing marker, CD62L allowing their migration at the site of disease (e.g., the lung in pulmonary TB infection) 15 – 18 days after infection [40, 62, 63]. In humans, *Mtb*-specific T cells responses can take between 2-8 weeks after initial infection [54]. The response of T cells to *Mtb* infection in the lungs is substantially delayed when compared to some other respiratory pathogens such as RSV or Influenza, in which the adaptive response is mounted between 7-8 days [64, 65]. Moreover, the delay in the T cell response allows the *Mtb* bacilli to grow and establish infection before the onset of the adaptive immune response. The bacterial growth peaks at 3 weeks in the mouse lung, after which it enters a steadier state of growth. The exact cause delay in the adaptive response is driven by multiple factors. One contributing factor to the delayed response, is the hinderance of effective T cell priming due to *Mtb* induced impaired DC function. This is accomplished in several different ways. *Mtb* impedes lysosomal fusion by secreting EsxH and EsxG via the ESX-3 type VII secretion system [66]. These virulence components manipulate the host endosomal sorting complex required for transport (ESCRT) resulting in suboptimal antigen processing and loading of peptides onto MHC [66-68]. The prevention of MHC-I and MHC-II upregulation in infected host cells by mycobacterial lipoproteins, the ability of antigen presenting cells (APCs) to present peptide to T cells is impaired [69-71]. Priming of T cells by APCs requires not only recognition of the MHC-peptide complex by the T cell receptor (TCR) but also effective co-stimulation, the absence of which results in T cell dysfunction or anergy [72]. Differences in co-stimulation result in differences in effector T cell responses. For example, interaction of CD80/CD86 with CD28 is essential for robust Th1 responses [73]. This is effectively demonstrated by knockout of CD28, which results in a dampened Th1 response leading to uncontained bacterial growth and increased necrosis during *Mtb* infection [73]. Although the mechanism is not exactly understood, *Mtb* downregulates CD80, CD86 and CD40 during chronic *Mtb* infection, ultimately hindering the ability of T cells to carry out effector functions [74]. Overall, these mechanisms result in the delay of the adaptive response and provides the mycobacteria the time to proliferate and establish infection in the lung.

1.1.2.4.1 T helper (Th) T cells

CD4 T cells play a central role in orchestrating immune response to pathogens. Several types of CD4 cells have been described based on their cytokine secretion potential and lineage-

specific master transcription factors which inform functional capacity. A visual representation of the classification can be found in (Figure 1.5). Th1 express IFNγ and T-bet and Th2 cells express IL-4/IL-5/IL-13 and GATA3 [75, 76]. Th17 are identified by the production of IL-17 and RORγt, T_{FH} express IL-21 and Bcl6 and Th22 produce IL-22 [77-79]. T_{regs} are identified by expression of the transcription factor FoxP3, and the production of IL-10 and TFG-β [80]

Th1 responses are characteristic of intracellular pathogens, while a Th2 response is usually associated with helminth infections. Th17 is commonly associated with bacterial and fungal infections, while T_{FH} is required for germinal center formation and T_{regs} help modulate CD4 and CD8 T cell effector responses, to prevent excessive inflammation and immunopathology [79].

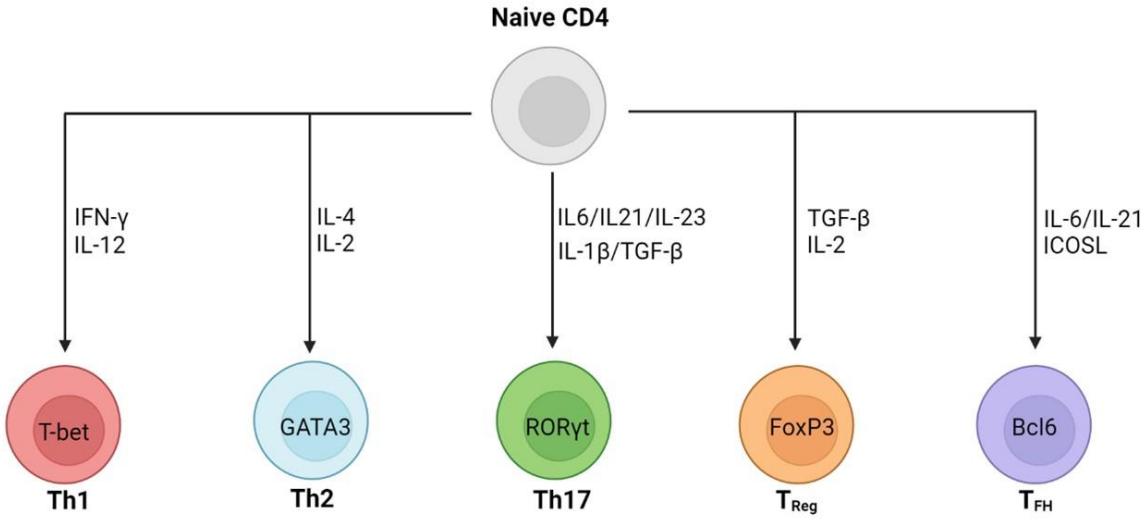

Figure 1.6: Schematic illustrating the development of Naive CD4 T cells into various T helper (Th) subsets. The schematic shows the master transcriptional regulator associated with each subset, as well as the cytokines which drive polarization. Figure is based off of Leung et al., (2010) [81]

1.1.2.4.2 Th1 T cells

There is a longstanding perspective that Th1 T cells fulfill a pivotal role in protective TB immunity, which will be discussed in further detail later in this review. IFN-γ and il-12 drive the development of Th1 functions. Th1 differentiation is characterized by the expression of the transcription factor T-bet, and IFN-γ and TNF. IFN-γ signaling activates STAT1 which induces T-bet, resulting in a signal feedback loop. IL-12 signaling results in STAT4 activation which is also important for Th1 development [76].

Knockout (KO) mouse models have been a useful tool in understanding immune mechanisms in TB. KO models have allowed for extensive studies in TB and have convincedly established that the essential role of CD4 T cells in response to *Mtb* infection, particularly T-helper 1 (Th1) CD4 T cells. Indeed, several studies reported increased pulmonary pathology and early mortality following Mtb infection in mice deficient in MHC II, IFN-γ, IL-12, T-bet or CD4 T cells [82-89]. In humans, increased tuberculosis susceptibility has been shown in person with genetic disorders disrupting IFN signaling pathways [90] and immunosuppressed patients such as HIV-infected individuals with depleted levels of CD4 T cells [91, 92]. Furthermore, BCG vaccination of NHPs is protective against *Mtb* challenge. The major underlying reasons for protection was rapid clonal expansion of purified protein derivative (PPD)-specific IFN-γ CD4 T cells, and a few CD8 T cells which rapidly accumulated in the lung upon infection [93] This is one of the reasons why a robust Th1 response, comprising of a strong IFN-γ response is a major target for TB vaccine design [94].These findings highlight the importance of CD4 T cells in controlling TB disease.

Part of the reason why CD4 T cells are so important in TB immunity is their pivotal role in orchestrating and triggering other immune cell populations. Secretion of IFN-γ by CD4 T cells is considered essential for host survival, along with TNF. These cytokines promote production of nitric oxide (NO) within infected macrophages, enhancing their antimicrobial function[95]. CD4 T cells producing IFN-γ have other immune effects, including: (1) helping macrophage autophagy, which can cause *Mtb*-containing autophagosomes to mature into autophagolysosomes [96], (2) Inducing the turnover of DCs, thereby decreasing persistent antigen presentation which prevents T cell exhaustion [97] and (3) limiting the expansion of IL-17 producing T cells [98].

TNF also has several roles in TB immunity. As discussed above, along with IFN-γ, it promotes bactericidal activities in macrophages, but the effect of this cytokine goes beyond that. TNF promotes the expression of several chemokines such as CXCL10, CXCL13 and CCL2 [80]. These chemokines recruit more immune cells and is linked to the maintenance of the granuloma.

Th1 CD4 T cell is also required to enhance CD8 effector functions by promoting expression of granzyme A and B, IFN-γ and TNF. CD4 T cells help CD8 T cells to downregulate inhibitory receptors such as PD-1, and LAG3 which put the brake on cytolytic activity, while simultaneously upregulating CX3CR1, which is associated with more efficient tissue

infiltration [99]. More recently, the synergistic effects of CD4 and CD8 T cells have shown to restrict bacterial growth, preventing CD8 T cell exhaustion and promoting survival of infected mice [100].

These studies highlight the substantial role of Th1 CD4 T cells in TB immunity. However, while Th1 CD4 T cells are necessary, they are not sufficient to control Mtb infection. Interestingly, a study by Sakai and colleagues found that CD4 T cells residing in the lung parenchyma ($CXCR3^+$ $KLRG1^-$ $CX3CR1^-$) produce less IFN-γ than intravascular CD4 T cells ($KLRG1^+$ $CX3CR1^+$), but have a better protective capacity [101]. The authors assert that this observation indicates that the ability of CD4 T cells to migrate into the tissue and interact with infected macrophages, is likely more important than their capacity to produce IFN-γ. The authors noticed that CD4 T cells that migrate into the lung parenchyma, termed lung-homing, tend to express high levels of PD-1, and argue that the prevalence of this co-inhibitory marker could partly explain their limited capacity to produce IFN-γ. In a follow up study, Sakai and colleagues made use of a PD-1 KO mouse model to further investigate their findings and found that the PD-1 deletion resulted in lower amounts of lung-homing CD4 T cells and the generation of hyperactive IFN-γ+ CD4 response, which increased immunopathology and lead to early mortality [102]. Similarly, an earlier study showed that deletion of PD-1 resulted in much higher amount of *Mtb*-specific CD4 T cells, but also in increased mortality of the mice [103]. Moreover, increased IFN-γ production by CD4 T cells is directly implicated in TB-Immune Reconstituted Inflammatory syndrome (TB-IRIS), further confirming that a strong IFN-γ CD4 response can be pathogenic [104]. Similarly, elevated production of TNF is also associated with increased immunopathology [105]. These studies indicate that the pro-inflammatory T cell response needs to be regulated, to control immunopathology.

Despite the well-recognized role of IFN for Mtb control, reports have indicated that the IFN-γ+ CD4 T cell mediated response is not the only axis involved for protection against TB [102, 106]. However, the contribution of IFN-γ-independent mechanisms of Mtb protection are still understudied. For example adoptive transfer of IFNγ-deficient, but T-bet+ CD4 T cells adoptively transferred into C57BL/6 mice provided the same level of protection against *Mtb* infection as WT CD4 T cells [106].The study also found that the adoptive transfer of Th1 skewed, IFN-γ deficient T cells, was more effective at providing protection against *Mtb* than the partially effective Th17 CD4 T cells, while the Th2 generated CD4 T cells proved ineffective. It is worth noting that the adoptive transfer of Th2 skewed CD4 T cells into C57BL/6 mice suppressed the priming of the endogenous population of the antigen-specific

cells[106]. This study strongly indicates that IFN-γ-independent pathways can restrict *Mtb* growth. While also demonstrating that not all effector T helper responses are equal when it comes to TB immunity. Similarly, the MVA85A vaccine trial, which despite eliciting a strong and durable Th1 cytokine expressing CD4 T cells, did not elicit sufficient protection [107]. A recent study from the Stanley group made use of co-culture system to further investigate this mechanism. By making use of wild-type and IFN-γ-KO T cells extracted from *Mtb* infected mouse lungs, and co-cultured with bone-marrow-derived-macrophages infected with *Mtb in vitro*. The study found that CD4 T cell derived GM-CSF causes HIF-1α activation in macrophages, driving M1 and glycolytic transcripts that lead to increased bactericidal activity, further highlighting the role of IFN-γ-independent mechanisms for Mtb control [108].

1.1.2.4.3 Th2 T cells

Simplistically, Th1 and Th2 are differentiated by the ability to secrete different cytokines. Th1 produce mainly IFN-γ, TNF and IL2 while Th2 are characterized by IL-4, IL-13 and IL-5 production. The IL-4, IL-13, as well as IL-5 genes are all clustered one locus, which is located on chromosome 5 in humans (5q31) and spans a 160 kb region[109]. In the mice, it is situated on chromosome 11 and spans a 120 kb region[110]. The IL-4 and IL-13 genes are similar in structure and comprising of 4 exons and 3 introns, and also share many cis- and trans-regulatory elements [111].

The expression of IL-4 and IL-13 is controlled by a locus control region (LCR) which spans a region of rad50, a DNA damage response gene that is also in the Th2 cytokine locus. The LCR contains several DNase I-hypersensitive sites which regulate the expression of Th2 cytokines [112-114]. Levels of Th2 cytokines are substantially reduced in LCR-deficient mice [115]. IL-4 and IL-13 have several cellular sources including CD4 T cells, γδ T cells, basophils, mast cells, eosinophils, type 2 innate lymphoid cells (ILC2), NK T cells and innate skin like keratinocytes [116-125]. IL-4 is primarily recognized for its pivotal role in governing the polarization of antigen-stimulated naïve CD4 T cells, steering them towards the Th2 phenotype. In addition, IL-4 also effectively suppresses the production of IFN-γ in $CD4^+$ T cells, thereby attenuating the Th1 immunity [117, 126].

The master regulator associated with Th2 polarization is the canonical transcription factor GATA3, although its functions extend beyond this role [127]. GATA3 upregulation is initiated through IL-4/STAT6 axis. Th2 polarization is initially driven by GATA3 and activated STAT5 which modify the Th2 cytokine locus. This signaling pathway enhances the expression of IL-4, further amplifying the feedback loop as it induces greater GATA3 expression. Nevertheless,

there is evidence that the IL-4/STAT6 signaling axis is not indispensable for Th2 polarization. Indeed, mouse KO models deficient in either IL-4Rα or STAT6 are still capable of producing Th2 response, although fewer IL-4 producing CD4 T cells were detected. This suggests that alternative pathways can also contribute to Th2 polarization and response [128].

IL-4/IL-13 induced signaling happens either through type 1 or type 2 receptors. The type 1 receptor comprises of IL-4Rα and common gamma chain (γC). Whereas the type 2 receptor is composed of IL-4Rα and IL-13Rα1. IL-4 can bind both type 1 and type 2 receptors, but IL-13 can only bind type 2. IL-4 binds to IL-4Rα rapidly and with high affinity (K_D = 20 – 300 pM); resulting in the recruitment γC or IL-13Rα1 forming a complete heterodimeric signaling complex [129]. In contrast, IL-13 to IL-13Rα with moderate affinity (K_D =10 nM), in turn this binding event recruits IL-4Rα which stabilizes the interaction, and increases the affinity of IL-13 to the receptor complex (K_D =30 pM) [130-133]. Lymphocytes express low amounts of IL-13Rα, so IL-4/IL-13 signaling is predominantly through the type 1 receptor.

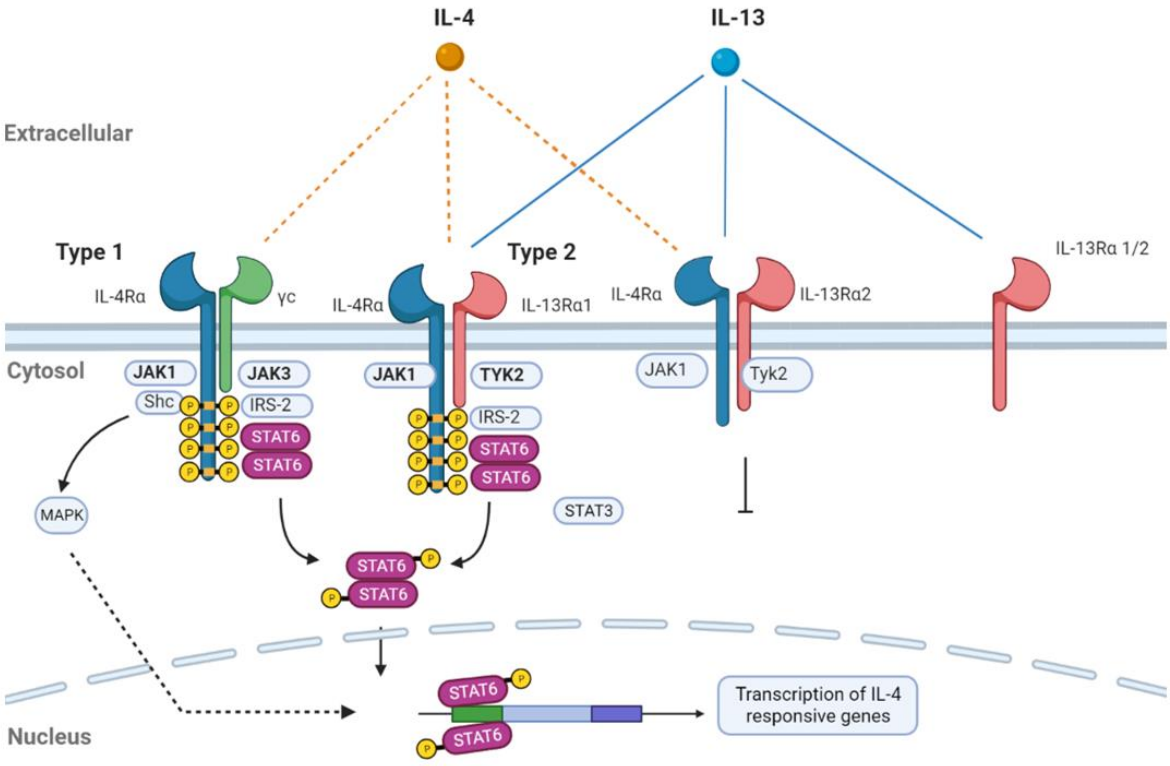

Figure 1.7: Schematic depicting the differences between the Type 1 and Type 2 receptors in IL-4 signaling. IL-4 signaling through the Type 1 receptor, consisting of IL-4Rα and the common γ chain activates JAK1 and JAK3. The Type 2 receptor made up of IL-4Rα and IL-13Rα1 and can bind both IL-4 and IL-13 and is associated with JAK1 and TYK2. Shc which binds to Y497 is capable of driving MAPK cascade. In both Type 1 and Type 2 receptor systems, STAT6 binds to phosphorylated sites at Y575, Y603 and Y631. The phosphorylated STAT6 homodimer then passes into the nucleus where it mediates gene expression. The downstream signaling of IL-13Rα2, previously called a decoy receptor, is not fully understood. Image is based on [134, 135] and was generated in Biorender.

The ability of CD4 T cell to polarize in one Th function or another is largely dependent on the pathogen associated molecular patterns (PAMPs) that is encountered by the DCs [136]. DCs which encounter Gram-negative bacteria respond by secreting IL-6, and IL-12. Naïve T cells then respond by polarizing into either Th1 or Th17 cells [63, 137]. As described in the previous section, this is also the typical response to *Mtb* as well. Th2 responses are typically associated with helminth infections. Adoptive transfer of DCs that have been exposed to helminth extract will drive Th2 responses in the receiving mouse [138]. However, Th2 development in response to *Mtb*, *Mtb* antigens or BCG has also been observed [139, 140]. *Mtb* infection with H37Rv is reported to induce the IL-1β production in DCs, thereby directing Th2 responses, and facilitated progression of diseases by dampening Th1 responses [140]. Interestingly, neither BCG nor H37Rv containing mutations in ESAT-6 or RD-1 elicit IL-1β production, and as such did not induce Th2 responses. Certain antigens appear to "favour" a response, as seen when by a bias of CD4 T cells to produce IL-4 when cultured with a human monocyte derived DCs stimulated with the 30 and 38 kDa *Mtb* antigens [141]. Certain epitopes of the same protein seemingly drive distinct helper subsets. A study making use of the 16 KDa heat shock protein of *Mtb* found that the peptide sequence p91-110 preferentially drove Th1 polarization, while p21-40 preferentially dove Th2 polarization [142]. To further complicate our understanding of this bias, there is evidence that different strains tend to drive different Th1 responses. *In vitro* infection of monocytes with the virulent HN878 strain of *Mtb* induced greater amounts of IL-4 and IL-13, whereas the monocytes infected with CDC1551 secreted more IL-12. This strain specific effect was demonstrated to be due to be lipid mediated. Monocytes that are infected either with HN878 or CDC1551 drive naïve T cells to a more Th2 or Th1 phenotype respectively [143]. The authors further suggest that the virulence of Beijing strain family, of which HN878 is a part of, is in part due to the pathogen's propensity to prevent the host from driving an effective Th1 response. These studies demonstrate that there are mixed responses in TB and that these are not necessarily Th1 and Th17 but can also involve Th2 responses. Moreover, the drivers of these effects are multifactorial, as they can be host driven, or pathogen driven as seen by the immune prevalence of certain epitopes, or due to variation in strain.

The long-held view of the importance, albeit insufficient of Th1 responses in TB, gave rise to the view that an underlying Th2 response plays a subversive role in TB. This is a controversial view as there is evidence for and against it. Early studies done in C57BL/6 mice by Robert North, who wished to explore Th2 responses showed that there is no difference in mycobacterial burden between IL-4 KO, IL-10 KO and WT mice [144]. A follow up study

made use of C57BL/6 mice deficient in either IL-4 + IL-13, IL-4Rα or STAT6, and found there to be very little difference in bacterial burden compared to controls [145]. North argued that these data are indicative that the Th1 response to *Mtb* infection is not being held back by the Th2 response. Interestingly, an IL-13 overexpressing (IL-13^{tg}) model on the C57BL/6 background is more susceptible to TB infection compared to littermate controls, with all transgenic mice succumbing to infection within 140 days post infection [146]. The IL-13^{tg} mice were found to have decreased IL-12p40 and increased TNF in lung homogenates at 63 days post infection compared to controls. In addition, the IL-13^{tg} were found to develop centrally necrotizing granulomas, which resembled the cellular architecture of granulomas seen in human TB patients. Characterized by a core of dead and dying cells, surrounded by epithelioid macrophages and foamy macrophages. These were then encircled by CD3+ T cells which were then encircled fibrous rim of collagen fibers which allow for a visually distinct border between the granuloma and the adjacent lung tissue. Lastly the IL-13^{tg} mice were found to have very high levels of alternatively activated macrophages, which have impaired effector mechanisms against *Mtb*. Deletion of IL-4Rα in the IL-13 overexpressing mouse abrogates the TB tissue pathology effect. Another difference seen in the Th1 vs Th2 paradigm in TB is the effect that these helper effects have on macrophages. As noted earlier in this review, the secretion of IFN-γ by Th1 CD4 T cells causes classical activation of the macrophages which results in the increased ability to kill intracellular pathogens. This in part is due to an increase in NO and reactive nitrogen intermediates but is also due to increased autophagy. IFN-γ causes this phagosome-lysosome fusion through certain cell signaling cascades such as LRG-47 and PI3K. In contrast, IL-4 and IL-13 cause alternative activation of macrophages, which have reduced bactericidal ability. IL-4Ra mediated signaling inhibits anti-microbial autophagy processes in macrophages, and is STAT6 dependent.[147] IL-4Rα driven alternative activation increases production of Arg1, which shares a common substrate L-Arginine with iNOS [148]. This interferes with NO production and as a result, alternatively activated macrophages have lower levels of NO and reduced capacity to destroy intracellular pathogens [149].

The importance of the genetic background in mice when performing immunological studies. C57BL/6 and BALB/c mice are typically regarded as Th1 and Th2 dominant strains respectively [150-152]. Characterization experiment have shown that BALB/c mice have tendency to early secretion of large amounts of IL-4 in response to infection with *Leishmania major*, causing the down regulation of the IL-12 receptor on CD4 T cells, and thus unresponsive IL-12 signaling [153]. Another report purports that IL-12 signaling in BALB/c is defective,

resulting in naïve CD4 T cells being more resistant to Th1 polarization [154]. Although the both BALB/c and C57BL/6 mice are classified as resistant strains within the TB disease model, C57BL/6 are able to better control *Mtb* infection compared to BALB/c [155] owing to their underlying genetic differences.

Kinetic studies in BALB/c mice infected with a high dose of H37Rv demonstrate that TB disease in mice typically consist of 2 phases, the first is the acute phase which lasts till the 28th day, after which the second, chronic or progressive phase begins. The chronic phase is characterized by interstitial fibrosis, focal necrosis and pneumonia. These kinetic studies showed that the acute phase consisted of a strong Th1 response evidenced by expression of IFN-γ and IL-12 in the first 3 weeks and coincided with *Mtb* growth reaching a stationary phase. [156, 157]. On the other hand, IL-4 was detected at consistently low levels until day 28, thereafter IL-4 levels steadily rose until day 60, where levels started increasing substantially. This initiation of a strong Th2 response coincides with reactivating pulmonary TB in the chronic stage of infection, where the rate of *Mtb* growth goes exits a stationary phase and begins to increase till at least 60 days post infection [157]. The observation that progressive TB infection is associated with a steady increase of IL-4 in BALB/c mice, prompted a follow up study where the authors make use of an IL-4 KO. Infection of IL-4 deficient mice on the BALB/c resulted in mice lower bacterial burden and decreased lung pathology [157]. This study also showed how TNF in the presence of IL-4 exacerbates tissue damage and leads to increased mortality, an effect that is not seen in the IL-4 KO mouse. In NHPs as previously discussed in section 1.1.2.3, granulomas with the highest bacterial burden were characterized by a strong Th2 response, with high levels of IL-4 and GATA3.

The role of IL-4Rα mediated signaling in human TB is not thoroughly explored. However, increased IL-4 expression correlates with increased lung damage [158-160]. Increased IL-4 mRNA and IL-4 to IFN-γ ratio has been observed in active TB patient blood, but not BAL, compared to Latent TB infected patients (LTBI) [161]. The same study made use of PBMCs from the blood of patients with active TB for a set of *in vitro* experiments. The researchers made use of a study with *Mtb* infected monocyte-derived macrophages (MDMs) that were cultured alone or with PBMCs pulsed with purified protein derivation (PPD) or PPD and recombinant IL-4. The group of MDMs co-cultured with the PBMCs primed with PPD and IL-4 had higher CFU compared to PPD alone group. This was in part IL-4 driven, substantial increase in T_{regs}, decreased IFN-γ secretion from CD4 T cells and alternative activated macrophages as seen by increased DC-SIGN. These effects are reversed upon neutralization

using anti-IL-4 antibody [161]. Moreover, patients that express the mutation, structural variant of the IL-4Rα (I50V), results in more efficient signaling, have greater degree of lung pathology [162]. These studies show the potential of IL-4 mediated signaling to play a subversive role in the immune response to TB.

Up until this point, all IL-4 and IL-4Rα KO models discussed in this review have been global (null) knockouts. To uncover the role of IL-4 mediated signaling in TB, another approach involves the use of cell-specific knockout models. The first cell specific IL-4Rα deficient mouse model used for TB was the LysM^{Cre}IL-4Rα$^{-/lox}$ on the BALB/c background in which IL-4Rα has been partially deleted in macrophages and neutrophils. The rationale behind the use of this model, was the observation that alternatively activated macrophages, an IL-4Rα driven process, are associated with reactivation of latent TB in mice. The study found that the deletion of IL-4Rα on macrophages resulted in ½ a log increase in CFU in the lung at the acute (4 weeks), but no differences at the chronic (18 weeks) phase of TB. The study also found that no difference in survival to high dose infection, nor any differences in histopathology at both acute and chronic phase between LysM^{Cre}IL-4Rα$^{-/lox}$ and littermate controls [163]. Interestingly, despite the link between IL-4Rα and Arg1 activity, no differences were seen in this study in both the cell-specific and global IL-4Rα KO compared to controls. This is despite LysM^{Cre}IL-4Rα$^{-/lox}$ animals has been shown to have increased NO production in other disease models, including *L. major* and *N. brasiliensis* [164, 165]. High induction of iNOS, and Arg1 in cell-specific, global IL-4Rα KO and WT mice was observed regardless of whether the infective dose was high or low, or which strain was used. This implies that during *Mtb* infection there is an IL-4Rα-independent pathway for induction of Arg1, possibly due to increases in IL-6, IL-10 and G-CSF. The authors understood that collectively this data indicates that the macrophage specific role of IL-4Rα in TB is dispensable.

The B cell specific role of IL-4Rα was investigated making use of the mb1^{cre}IL-4Rα$^{-/lox}$ model on the BALB/c background. Indeed, the role of B cells in TB is underexplored and whether B cells are protective or detrimental in TB in contentious. Reports range from the ability of B cells to mediate lung immunopathology [166], necessity for antigen specific T cell responses [167], to facilitating dissemination of *Mtb* [168] and even being neutral [169]. Using B cell deficient mice, it was revealed that B cells participate in the formation of the TB granuloma [166] and with the B cell depleting anti-CD20 antibody in NHPs [170]. Making use of the mb1^{cre}IL-4Rα$^{-/lox}$, the authors found that bacterial burden in the lung and spleen was lower than littermate controls, and WT BALB/c mice at chronic TB. The adoptive transfer of IL-4-

responsive B cells into mb1^{cre}IL-4Rα$^{-/lox}$ mice returned the bacterial burden similar to WT control mice. The histopathology of B cell-specific IL-4Rα deficient mice indicated they had smaller lesions in the lung as well as decreased iNOS expression at both acute and chronic TB. Lastly, culturing *Mtb*-infected macrophages in the supernatants of *Mtb*-exposed B cells from KO mice, resulted in the macrophages producing higher levels of NO, IL-1β and TNF compared to controls. Indicating that the cytokine milieu in the supernatants of IL-4Rα-deficient B cells induces favourable bactericidal effects within macrophages. Collectively, the study demonstrates that IL-4Rα on B cells has a detrimental role on TB pathogenesis. Our unpublished studies have shown that IL-4Rα deficient T regs had no difference in TB whilst IL-4Rα deficient DCs showed a protective effect in mice. However, the T cell-specific role of IL-4Rα remains to be elucidated in TB.

1.2 Project rationale

Despite the availability of anti-TB drugs as well as the BCG vaccine against TB, TB remains a significant global health challenge. TB infection is widespread with a 2014 mathematical modelling study estimated that approximately 1.7 billion people are latently infected with *Mtb* [171]. Among those who have latent TB infections (LTBI) only a small fraction (5-10%) progress to active TB [172]. This demonstrates that the host is able to limit disease severity. Despite decades of research very little is known about what host defense factors allow for progression from latent to active TB, and immune correlates of protection against TB disease remains a contentious subject. A better understanding in various elements of the immune system and the interplay between these elements are critical to determine what constitutes protective immunity against TB. This highlights a knowledge gap, and we believe that ongoing efforts into better understanding the immune response to TB might uncover future, potential host treatment strategies both in the form of therapeutics to supplement traditional therapy but will also assist in vaccine design strategies. A large focus of the immune response to TB is on T cells. Understanding the immunobiology of T cells in the context of *Mtb* infection will provide insight into the correlates of protection that is so critically desired.

One way in which this can be investigated is by taking a closer look at the role of IL-4Rα on T cells and the role it plays in TB. IL-4 and IL-4-mediated signaling has been reported has having a subversive role in TB. The specific way in which IL-4 undermines the TB response is underexplored but is attributed to CD4 Th2 responses being associated with recrudescent TB, the improper control of intracellular bacteria by alternatively activated macrophages, and early appearing granulomas allowing for permissive environment for *Mtb*.

T cells are a major source of IL-4, induction of which is generated through IL-4Rα mediated feedback loop. Thus, using T cells in which the IL-4Rα has been deleted will theoretically allow for investigating the local effect of IL-4 on T cells, but more broadly how T cell produced IL-4 might effect immune responses to *Mtb* infection. Given the subversive role that IL-4 mediated signalling has reported in TB, the T cell specific role of IL-4Rα provides a promising candidate for exploring this. Previous studies of the T cell-specific role of IL-4Rα have been demonstrated in *Leishmania major* [173], *Leishmania donovani* [174], atopic dermatitis [175], *Schistosoma mansoni* [176], and *Nippostrongylus brasiliensis* [177]. In *L. major* infection, the absence of IL-4Rα on T cells, allowed for a strong Th1 response to be mounted which resulted in better control of the infection of the intracellular pathogen [173]. Given *Mtb* is an intracellular pathogen, we hypothesize that ablation of IL-4Rα will result in a greater degree of Th1 polarization which will have a protective effect in *Mtb* infection. To this end, we designed a study using a mouse model ($iLCK^{Cre}IL4Ra^{-/lox}$) in which the IL-4Rα is deleted on all T cell populations (CD4, CD8, NKT and γδ T cells) [176] to elucidate the overall T cell specific role of IL-4Rα both *in vitro* and *in vivo*.

1.3 Aims and objectives

The overall aim of this study is to investigate the role of IL-4Ra signaling on T cells during tuberculosis. The specific objectives that were used to answer this question were as follows:

1. Investigating the role of IL-4Rα expressed by T cells during *Mtb* infection using IL-4Ra-deficient T cell mice model.
2. To determine the mechanism(s) responsible for driving the phenotype in T cell-specific IL-4Rα deficient mice in TB.

Chapter 2:
Methods

2.1 Mouse Strains

iLCK^{Cre}IL-4Rα$^{-/lox}$ mice were generated by backcrossing iLCK^{Cre} mice with BALB/c mice as previously described [176]. The iLCK^{Cre} mice were kindly gifted by DR C.B. Wilson, University of Washington. These were then intercrossed with IL-4Rα$^{flox/flox}$ and global knockout IL-4Rα$^{-/-}$ mice for nine generations. This was done in an effort to delete IL-4Rα exon 7 and exon 9 in all LCK expressing cells (T cells). The IL-4Rα$^{-/lox}$ mice which lacked the transgene iLCK^{Cre} were used as controls for each experiment. All mice were generated and housed in specific pathogen free (SPF) conditions within the University of Cape Town, Animal Research Facility, under guidelines previously approved by the University of Cape Town Research Ethics Committee and the South African Veterinary Council (SAVC). All mice were 8-12 weeks old and were sex matched for each independent experiment. All procedures were conducted in the Research Animal Facility Biosafety Level 2 (BSL2).

2.2 Ethics Statement

All experiments performed in this study were done following the Animal Research Facility approved protocols (Permit No: 019/023 and 022/024). In addition, all procedures were performed in accordance with the regulations under the South African National Standard (SANS 10386:2008).

2.3 Genotyping

The genotype of iLCK^{Cre}IL-4Rα$^{-/lox}$ was confirmed by PCR using genomic DNA extracted from ear clippings, and the following primer sequences in Table 2.1.

Table 2.1: Primers for genotyping T cell-specific IL-4Rα deficient mice

Target	Primer sequence
IL-4Rα WT Forward	5'-TGA CCT ACA AGG AAC CCA GGC-3'
IL-4Rα WT Reverse	5'-CTC GGC GCA CTG ACC CAT CT-3'
IL-4Rα KO Forward	5' - GGC TGC TGA CCT GGA ATA ACC - 3'
IL-4Rα KO Reverse	5' - CCT TTG AGA ACT GCG GGC T - 3'
Cre Forward Primer	5'- GAG GGT GGA ATG AAA CTC TCG GT -3'
Cre Reverse Primer	5'- CAG GTA TGC TCA GAA AAC GCC TGG -3'

Optimal conditions for genotyping included an initial denaturation step (94°C for 1 min). Followed by 40X cycles of denaturation (94°C for 30 sec), annealing (57-60° for 20 sec) and

extension (72°C for 1 min). This was lastly finished by a final extension (72°C for 1 min). PCR products were then visualised on 1.6% agarose gel (SYBR Safe DNA gel stain, Thermofisher). Expected band sizes for iLCK^{Cre}IL-4Rα$^{-/lox}$ included KO product (471 bp), WT product (600 bp), and Cre product (517 bp).

2.4 *Mycobacterium tuberculosis* culture and infection

Mtb strains HN878 and H37Rv were passaged through BALB/c mice to maintain virulence and glycerol stocks were generated as previously reported [178]. All mice were infected intranasally as previously described [163]. In brief, a glycerol stock was removed from -80°C storage and allowed to thaw, and washed twice with phosphate buffered saline (PBS) and resuspended in sterile saline at a concentration of ~2000 CFU/ml. Thereafter, 25µl of the inoculum was administered to each nostril of mice under anaesthesia. Dosage was confirmed by plating the homogenised lung tissue of 3-4 mice on Middlebrook 7H11 (10% v/v OADC and 0.5% v/v glycerol) plates (BD Biosciences) one day post infection. The inoculum was also plated on 7H11 to further confirm that the correct dosage was achieved. At indicated timepoints (4 weeks or 18 weeks), mice were euthanised to collect spleen and lung into sterile saline (0.4% v/v Tween-80) and homogenised. The homogenates were then diluted in 10-fold increments and plated on Middlebrook 7H11 (10% v/v OADC and 0.5% v/v glycerol) plates (BD Biosciences). After a period of 21 days at 37°C, the colonies on each plate were enumerated.

2.5 Histopathology and Immunohistochemistry.

At indicated timepoints a lobe of the lung was collected and fixed in 4% phosphate-buffered formalin. For each experiment the lobe chosen was kept consistent. The fixed tissue was then embedded in paraffin wax and subjected to cryo-sectioning using the Leica TP 1020 benchtop processor. Four different 3 µm thick sections were obtained for haematoxylin and eosin (H&E) and two 3 µm thick sections for iNOS staining. All slides were scanned at 40X magnification in the Olympus VS120 virtual microscope. Image analysis included calculating alveolar free space and measuring iNOS-postivley stained area using Qupath-0.4.3 software. The total alveolar free space per section was calculated by subtracting the H&E stained area from the rest of the lung. The average of the four sections for each lobe was then taken. iNOS area was calculated by determining area positively stained with diaminobenzidine (DAB).

2.6 Enzyme-linked Immunosorbent Assay (ELISA)

Various cytokines and chemokine concentrations (IL-1α, IL-1β, IL-2, IL-4, IL-6, IL-10, IL-12p40, IL-12p70, IL-13, IL-17, IL23, IFN-β, IFN-γ, TGF-β, CCL2, CCL3, CCL5, CXCL1, CXCL2, CXCL5 and GM-CSF) were determined using ELISA. Lung homogenates were

centrifuged at 3000 x g for 5 min, and the supernatant was collected and passed through two rounds of filtration (0.2 µm) before used in the ELISA assay. The coating and detection antibodies as well as recombinantly produced proteins used as standards were obtained from BD biosciences, Biolegend and R&D scientific. All ELISA were performed according to manufacturer instructions. Horseradish peroxidase (HRP) or alkaline phosphatase (AP) with 1mg/ml 4-nitrophenyl disodium salt-hexahydrate was used for detection. Absorbance readings for AP plates were detected at 405nm with a reference of 495nm. Absorbance readings for the HRP plates were detected at 450nm with a reference of 540nm. All absorbances were measured using the VersaMAX^{TM} microplate spectrophotometer (Molecular Devices, Sunnyvale, California).

2.7 Nitric Oxide measurement

Nitric oxide (NO) in lung homogenates was measured using Greiss assay. Standards of sodium nitrite (Na_2NO_3) were prepared at a 1mM starting concentration, and then with a two-fold serial dilution in 96 well plate. Lung homogenates are added to the plate in a 1:1 ration with 50µl 1% sulfanilamide ($C_6H_8N_2O_2S$) in 2.5% phosphoric acid (H_3PO_4) and incubated for 5-10 minutes in the dark. Thereafter, 25µl of 0.1% napthyl ethylenediamine in 2.5% phosphoric acid and incubated for another 5-10 minutes. When the colour of the samples had visibly developed, relative to the standards, the plate was read in the VersaMAX^{TM} microplate spectrophotometer (Molecular Devices, Sunnyvale, California) at an absorbance of 540nm, using a reference wavelength of 690 nm.

2.8 Flow cytometry- Surface staining and intracellular cytokine staining

Lung tissue was collected, chopped with a scalpel and placed in lung digestion buffer (DNase I, Collagenase type I in DMEM). Lung tissue was digested for 1 hour at 37°C with end-over-end turning. Suspensions were passed through a 100µm a cell strainer, and incubated for 5 minutes with red cell lysis buffer (150mM NaCl, 10mM $KHCO_3$ and 0.1mM EDTA-Na_2). The cell suspension was then passed through a 70µm cell strainer (SPL Life Sciences) and washed with complete medium. Similarly, single cell suspensions of mediastinal lymph node and spleen were generated by passing the tissue through a 70 µm strainer, subjected to red cell lysis buffer for 5-10 minutes, before passing the suspension through a 40µm strainer. Cells were then counted in Trypan Blue (Sigma) with CytoSMART (Corning) automated cell counter. Cells were seeded at $1x10^6$ cells/well in V-bottom (Corning) plate. Cells were then washed once with PBS before stained with a viability marker (575V Viability Dye, BD Biosciences). After 15 minutes incubation at room temperature, the reaction was quenched using FACS

buffer (0.5% w/v BSA in PBS) and surface stained using fluorochrome labelled monoclonal (Table 2.2) antibodies in Panel 1-4 (Appendix) for 20 minutes at 4°C before fixing with PBS (2% w/v paraformaldehyde).

For intracellular cytokine staining (ICS) experiments. Single cell suspensions of lung or spleen were seeded at a density of $2x10^6$ cells/well and cultured with either 10µg/ml *Mtb* lysate (BEI NR 12822), 2µg/ml a peptide pool of 300 *Mtb*-derived peptides Mtb300 [179, 180], or 5µg/ml anti-CD3 (Clone:1435-2C11; Biolegend) and 1µg/ml CD28 (Clone:37.51;Biolegend) was used for 6 hours at 37°C with 5% CO_2. For the final 6 hours, 10 µg/ml of Brefeldin A (Sigma-Aldrich) to block Golgi bodies releasing cytokines in the supernatants. Cells were washed with PBS and surface stained with fluorochrome labelled monoclonal antibodies (Table 2.2) in Panels 5-7 (Appendix). Cells were then fixed and permeabilised using the ebioscience™ FoxP3/Transcription staining buffer set (Invitrogen Life Technologies) as per manufacturer instructions for 45 minutes at 4°C in the dark. Intracellular stains where then performed using antibodies listed in Appendix. Cells were then washed again in FACS buffer and acquired on LSRFortessa™ (BD Biosciences) acquiring 200,000 to 300,000 cells. Final analysis was performed in FlowJo® software v10.9.0 (Tree Star Inc) containing FlowSOM v3.0.18. All flow cytometry analysis was performed on live cells.

Flow cytometric analysis. For tSNE projections of WT/KO CD4 T cells, at least 2000 live, CD3+CD19-CD4+ T cells were selected using iLCK^{Cre}IL-4Rα$^{-/lox}$ and IL-4Rα$^{-/lox}$ (n= 5mice/group) and concatenated into one FCS file. FlowSOM analysis was performed, and the resulting clusters were overlayed on the tSNE projections. The percentage of the T cells from each mouse (iLCK^{Cre}IL-4Rα$^{-/lox}$ and IL-4Rα$^{-/lox}$) in each cluster was quantified and displayed.

Table 2.2: Flow Cytometry antibodies - murine

Specificity	Flurochrome	Clone	Supplier
CD3	A700	17A2	Biolegend
	PE-Dazzle	17A2	Biolegend
CD4	Bv421	RM4-5	BD Biosciences
CD8	Bv510	53-6.7	Biolegend
	APC	53-6.7	Biolegend
CD19	PerCP-Cy5.5	ID3	Biolegend
CD44	FITC	IM7	Biolegend
CXCR5	PE-Cy7	2G8	Biolegend
IL-4Ra	PE	I015F8	Biolegend
TCRγδ	biotin	GL3	Biolegend
biotin	PE-Dazzle	n/a	Biolegend
CD62L	APC	MEL-14	Biolegend
NK1.1	APC-cy7	PK136	Biolegend
PD-1	FITC	29F.1A12	Biolegend
CD103	PerCP-Cy5.5	M290	Biolegend
KLRG1	Bv786	2FI/KLRG1	Biolegend
CD69	BV510	H1.2F3	Biolegend
CD127	PE-Cy7	SB/199	Biolegend
CXCR3	PE	CXCR3-173	Biolegend
Ly6G	FITC	1A8	Biolegend
Ly6C	PerCP-Cy5.5	AL-21	Biolegend
MerTK	Bv786	108928	Biolegend
CD11b	Bv421	M1/70	Biolegend
CD64	PE-Cy7	X54-5/7	Biolegend
CD103	PE	M290	Biolegend
MHCII	A700	M5/114.15.2	Biolegend
CD11c	APC	HL3	Biolegend
SiglecF	APC-cy7	E5-2440	Biolegend
F4/80	PE-Cy7	BM8	Biolegend
CD169	APC-cy7	3D6.112	Biolegend
RORγt	PerCP-Cy5.5	Q31-378	BD Biosciences
GATA3	PE-Cy7	L50-823	BD-Biosciences
T-bet	PE	4B10	Biolegend
FoxP3	APC	MF-14	Biolegend
Ki67	PE	11F6	Biolegend
IFN-γ	A700	XMG1.2	Biolegend
TNF	APC-cy7	MP6-XT22	Biolegend
IL-17	Bv650	TC11-18H10.1	Biolegend
IL-2	PE	JES6-5H4	Biolegend
IL-4	PerCP-Cy5.5	11B11	Biolegend

2.9 Bone-marrow derived macrophages generation

Bone-marrow derived macrophages (BMDM) were generated as previously described [181] from IL-4Rα$^{-/lox}$ mice. In brief, bone marrow cells were flushed out of femurs of uninfected mice (8-12 weeks old). These precursor cells were cultured in PLUTZNIK media (DMEM containing 10% FCS, 5% horse serum, 30% L929 conditioned media, 2 mM L-glutamine, 1 mM sodium pyruvate, 50 μM β-mercaptoethanol and 100 U/ml penicillin and 100 μg/ml streptomycin) for 7 days at 37˚C and 5% CO_2. The cells were rinsed once with PBS to remove non-adherent cells. BMDMs were then harvested and plated at desired concentrations.

2.10 T cell isolation and co-culture

iLCK^{Cre}IL-4Rα$^{-/lox}$ and IL-4Rα$^{-/lox}$ mice were infected intranasally with 100CFU of *Mtb* HN878 for 12 weeks. The mice were euthanised and lungs were collected to generate a single cell suspension as described in 2.8. T cells were purified from lung single cell suspensions using MojoSort^{TM} mouse CD3-negative selection T cell isolation kit (Biolegend) and was used according to the manufacturer instructions. The purity of the cells was determined for each experiment and was typically 93-95%. The T cells were added to BMDMs which were infected the prior day at an MOI of 1. After 48 hours of co-culture cells were harvested for either flow cytometry or were lysed by 0.1% Triton-X100, and plated of 7H11 plates to enumerate CFU.

Funding Acknowledgements

I would like to sincerely thank all sources that helped fund this project. Sources for personal support include the National Research Foundation (NRF) SARCHI Grantholder-linked Bursary (2020-2022), VC Research Doctoral Scholarship (2020-2021), UCT Doctoral Research Scholarship (2020-2021), UCT Doctoral GAP Funding (2020-2022), and CIDRI PhD scholarship supported by CIDRI-Africa (2023). We would also like acknowledge the funding that supported consumables, and facilities. Funding sources include the NRF, South African Medical Research Council (SAMRC), and funding from the Wellcome Trust which supported the BSL3 core facility (203135/Z/16/Z).

Chapter 3:

Results

3.1 Tuberculosis infection increased the expression of IL-4Rα on CD4 T cells

The iLCK^{Cre}IL-4rα$^{-/lox}$ mice was used to investigate the function of IL-4Rα specifically on T cells. Our laboratory previously characterized this mice model which confirmed that IL-4Rα expression reduced on CD4, CD8, Natural Killer T cells and γδ T cells when compared to the littermate control (IL-4Rα$^{-/lox}$) and global (IL-4Rα$^{-/-}$) knockout mice [176]. It must be noted that expression of IL-4Rα in the iLCK^{Cre}IL-4rα$^{-/lox}$ mice model was unaffected in non-T cell population. We sought to find out whether the IL-4Rα signalling on T cells influence the outcome in the acute and chronic *Mtb* infection. Using flow cytometry, we compared the surface expression of IL-4Rα on T cell populations in the iLCK^{Cre}IL-4rα$^{-/lox}$ and littermate control animals, after intranasal infection with 100 CFU of the HN878 hypervirulent *Mtb* strain. Mice were sacrificed at acute 4 weeks (4wpi) and at chronic 18 weeks post infection (18wpi) (Figure 1A) and IL-4Rα expression was assessed in the lungs. The expression of IL-4Rα increased on the CD4 T cells in both the iLCK^{Cre}IL-4rα$^{-/lox}$ and IL-4Rα$^{-/lox}$ littermate control, however, as expected knockout animals showed decreased IL-4Rα expression iLCK^{Cre}IL-4rα$^{-/lox}$ mice compared to the control animals during infection compared to uninfected controls (Figure 1B). The reason that IL-4Rα is detected in the knockout is due to inefficiency in the Cre recombinase system. There was no significant difference in expression of IL-4Rα expression on CD4 T cells at 4wpi compared to 18wpi. IL-4Rα expression on CD8 T cells was significantly increased when comparing both acute and chronic timepoints to uninfected controls of IL-4Rα$^{-/lox-}$, but no significant changes were seen in the expression of IL-4Rα on the CD8 T cells of iLCK^{Cre}IL-4rα$^{-/lox}$ (Figure 1C). These observations are further demonstrated by mean GMFI of IL-4Rα expression on these CD4 and CD8 T cells at naïve, 4wpi and 18wpi (Figure 1D-E). These data show that *Mtb* infection does induce expression of IL-4Rα on CD4 T cells compared to the naïve state, however, the expression of IL-4Rα does not differ significantly during the course of infection. In order to see if the observed change in expression of IL-4Rα on T cells during *Mtb* infection was as a result of analysing T cells in the lung, the major site of disease, we decided to assess splenic T cells (Figure 2A-D). Splenic CD4 T cells from the knockout showed a similar trend as seen in the lung. All together, these data indicate that infection with *Mtb* cause an increase in the expression of IL-4Rα on CD4 T cells.

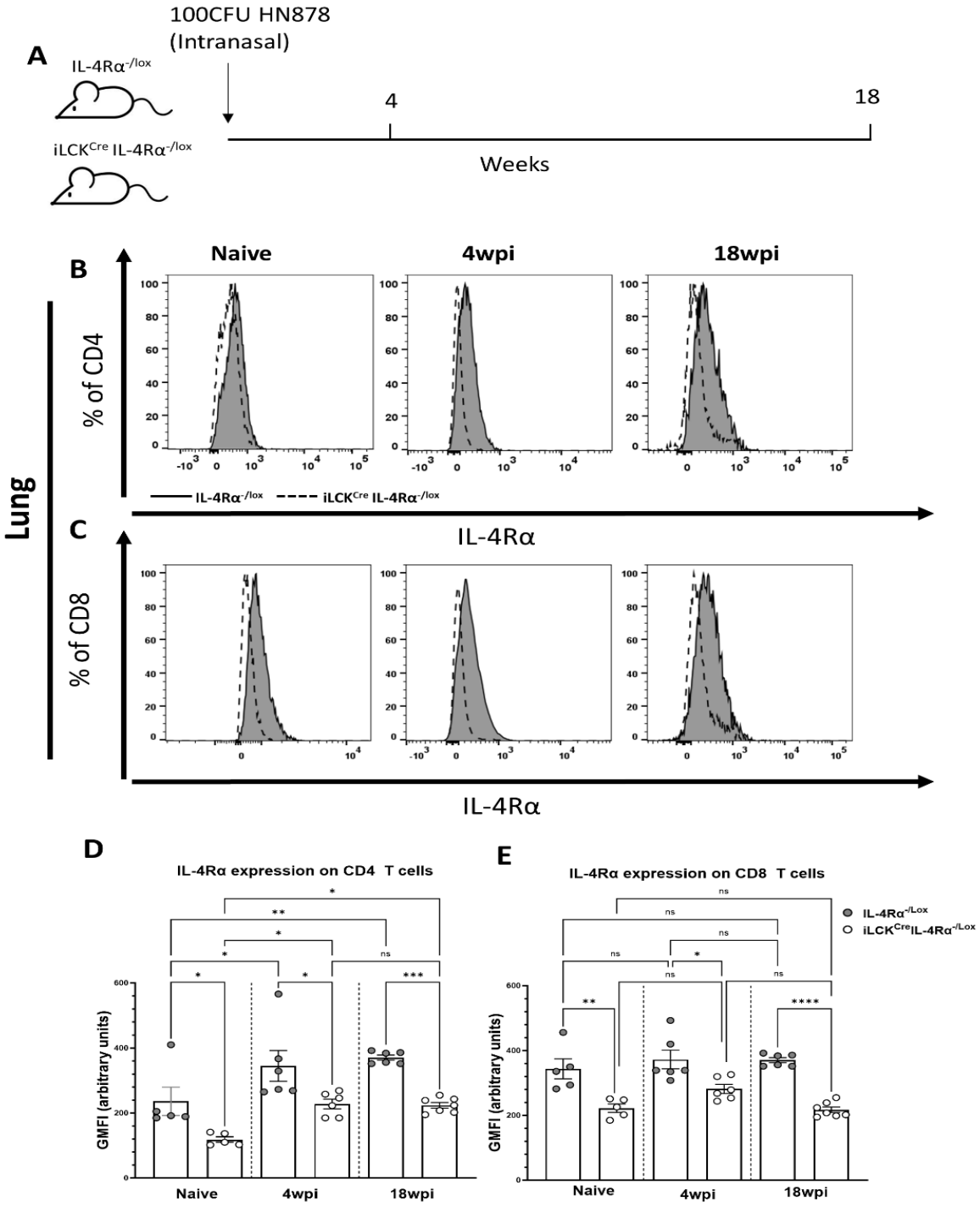

Figure 1: *Mtb* infection drives IL-4Rα expression on T cells in the lung over time. (A) Mice were infected with 100CFU of the HN878 intranasally and euthanised at the acute (4wpi) and chronic (18wpi) infection as indicated in the layout. Expression of IL-4Rα was measured by flow cytometry. Representative histograms displaying IL-4Rα expression of on **(B)** CD4 T cells and **(C)** CD8 T cells in the lungs of uninfected mice as well as in acute and chronic TB. Grey histogram represents IL-4Rα$^{-/lox}$ while the white histogram represents iLCK^{Cre}IL-4Rα$^{-/lox}$. IL-4Rα expression displayed as GMFI on **(D)** CD4 T cells and **(E)** CD8 T cells derived from the lung. Grey dots represent IL-4Rα$^{-/lox}$ and white dots represent iLCK^{Cre}IL-4Rα$^{-/lox}$ mice. Data represented as mean ± SEM of n=5 mice/group, and experiments were performed twice (naïve) and four times (infected). Statistical analysis was performed using one-way-ANOVA with Tukey's post-test. *p<0.05, **p<0.001,***p<0.0001, ****p<0.00001 and ns, no significant differences.

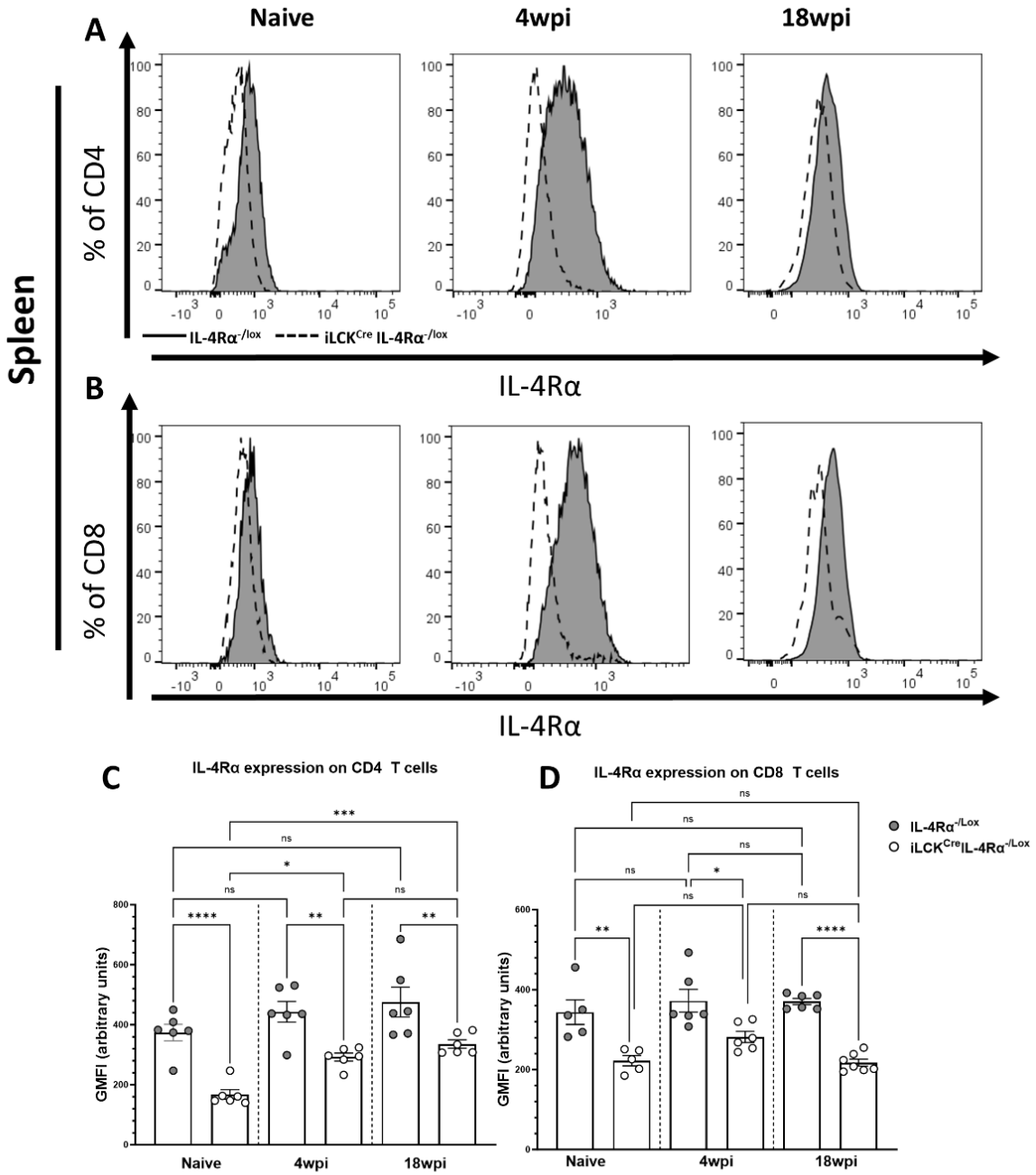

Figure 2: IL-4Rα expression on T cells during *Mtb* infection in the spleen over time. Representative histograms displaying IL-4Rα expression on splenic **(A)** CD4 T cells and **(B)** CD8 T cells. Grey histogram represents IL-4Rα$^{-/lox}$ while the white histogram represents iLCK^{Cre}IL-4Rα$^{-/lox}$. IL-4Rα expression displayed as GMFI on splenic **(C)** CD4 T cells and **(D)** CD8 T cells as mentioned in the lung tissues Grey dots represent IL-4Rα$^{-/lox}$ and white dots represent iLCK^{Cre}IL-4Rα$^{-/lox}$. Data represented as mean ± SEM of n=5 mice/group, and experiments were performed twice in naïve and four times in infected mice. Statistical analysis was performed using one-way-ANOVA with Tukey's post-test. *p<0.05, **p<0.001,***p<0.0001,****p<0.00001 and ns, no significant differences

3.2 Mice with IL-4Rα deficient T cells are susceptible to *Mtb* infection

To determine the functional consequence of IL-4Rα deficient T cells in TB, we assessed survival of the iLCK^{Cre}IL-4rα$^{-/lox}$ and IL-4Rα$^{-/lox}$ littermate control during *Mtb* infection (Figure 3A). Mice were infected via intranasal route with 150 CFU of the hypervirulent HN878 and euthanized at the humane endpoint, determined by a decrease in 20% of the maximum weight. iLCK^{Cre}IL-4rα$^{-/lox}$ mice succumbed earlier to infection than littermate controls, (Figure 3A). This result suggests that IL-4Rα on T cells plays a role in mediating survival during TB.

Given that the enhanced mortality of iLCK^{Cre}IL-4rα$^{-/lox}$ mice, we investigated the acute and chronic stages of infection. The disease severity in mouse models could be assessed by monitoring change in body weight over time. The iLCK^{Cre}IL-4rα$^{-/lox}$ mice showed a significant difference in body weight percentage at the chronic but not in acute stage of infection (Figure 3B), indicating potential host dependence of IL-4Ra signalling on T cells in chronic TB. We observed no significant differences in lung or spleen weight at either acute or chronic stages of infection (Figure 3C-D). The bacterial burden in the iLCK^{Cre}IL-4rα$^{-/lox}$ was significantly increased in the lungs at both the acute and chronic time point, but not in the spleen (Figure 3E-F). This demonstrates the IL-4Rα deficient T cells decreased the ability of host to control mycobacterial load in the lung but have no role in dissemination of *Mtb* into the spleen.

Tissue pathology remains an important way of characterizing disease phenotype and provide insight into the mechanisms which drive disease. To this end, we asked if the increased bacterial burden in the lungs correlates with tissue pathology. As *Mtb* infection progresses, adjacent alveolar spaces are infiltrated by inflammatory cells such as neutrophils and macrophages. This thickening of alveolar walls and filling of these spaces is termed alveolitis. Thus, by measuring alveolar free space we can get an indication on the degree of tissue pathology within the lung. Haematoxylin and eosin (H&E) staining allows visualisation of alterations in tissue structure. At 4wpi infection, we observed lesions in both iLCK^{Cre}IL-4rα$^{-/lox}$ and IL-4rα$^{-/lox}$ control mice (Figure 4A), as shown by dotted lines, but no significant differences in alveolar free space were detected upon quantification (Figure 4B). In contrast at 18wpi, lung sections showed a visible decrease in the amount of free space and significant decrease in alveolar space in the iLCK^{Cre}IL-4rα$^{-/lox}$ when compared to the IL-4rα$^{-/lox}$ mice (Figure 4A-C). *Mtb* infected macrophages in the lung are able to kill the invading bacilli through production of Nitric Oxide (NO) radicals. IFN-γ leads to the upregulation of inducible nitric oxide synthase (iNOS), which in turn enhances NO production [182]. We assessed whether inducible nitric oxide synthase (iNOS) correlates with lung mycobacterial burdens by immunohistochemistry. At 4wpi, there

was a significant decrease in the amount of iNOS expression in iLCK^{Cre}IL-4rα$^{-/lox}$ which correlates with enhanced lung burdens, whilst iNOS expression remained unchanged at chronic phase (Figure 4D-F).

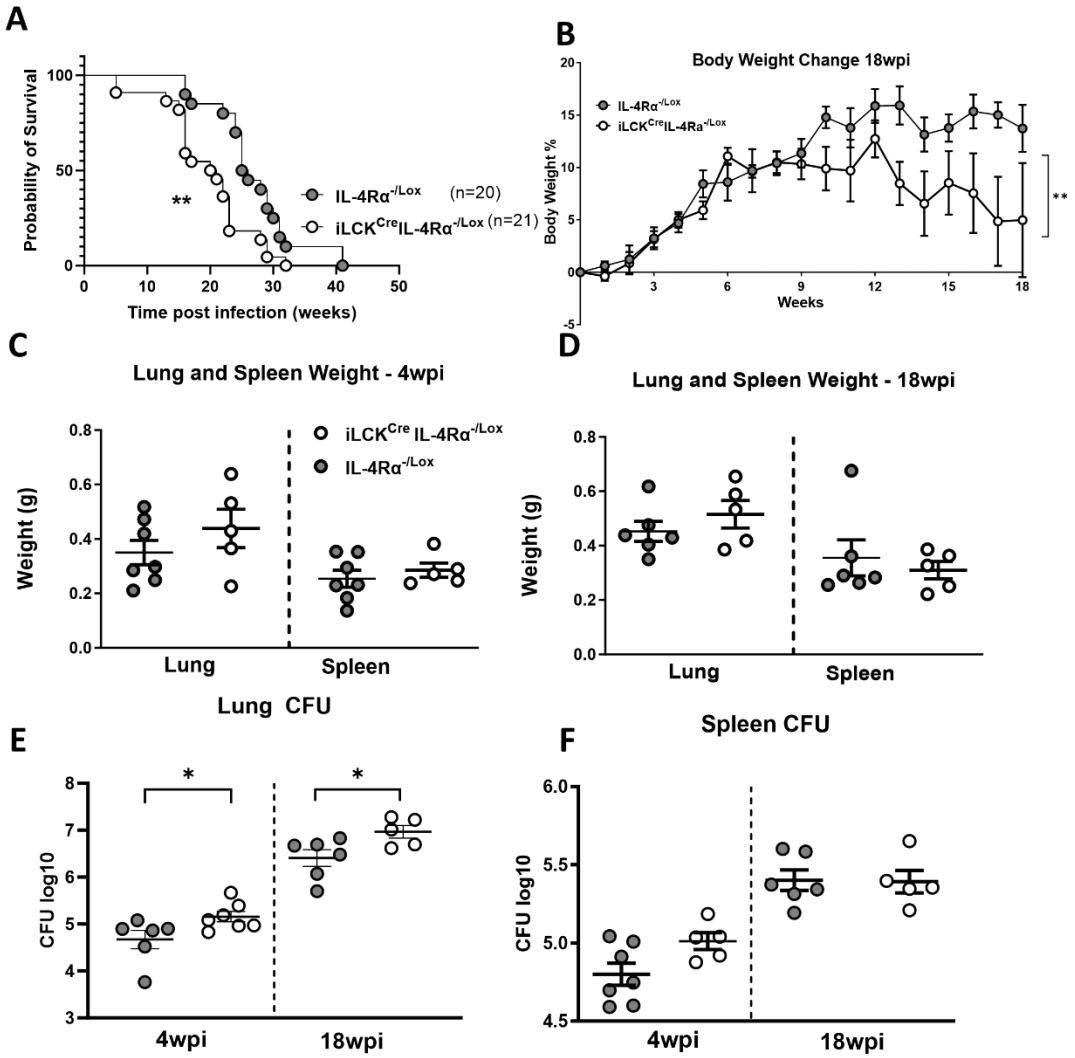

Figure 3: Absence of IL-4Rα on T cells increased mortality during Mtb infection. (A) iLCK^{Cre}IL-4Rα$^{-/lox}$ and IL-4Rα$^{-/lox}$ littermate controls were intranasally infected with 150 CFU of HN878 Mtb strain for survival study (n=19-20mice/group). **(B)** Change in percentage of body weight is displayed for 18wpi. **(C-F)** iLCK^{Cre}IL-4Rα$^{-/lox}$ and IL-4Rα$^{-/lox}$ littermate controls were intranasally infected with 100 CFU of HN878 and euthanized at either 4 weeks or 18 weeks after infection. Lung and spleen weight was measured at **(C)** 4 weeks and at **(D)** 18 weeks after infection. Lung weight index was measured for **(E)** 4 weeks and **(F)** 18 weeks after infection. Represented data of two to four independent experiments. **(B-F)** Data represented as mean ± SEM of n=5 mice/group, and experiments were performed four times Statistical significance was determined by (A) two-tailed Mantel-Cox survival with log-rank test or (B) two-way ANOVA **P<0.001.

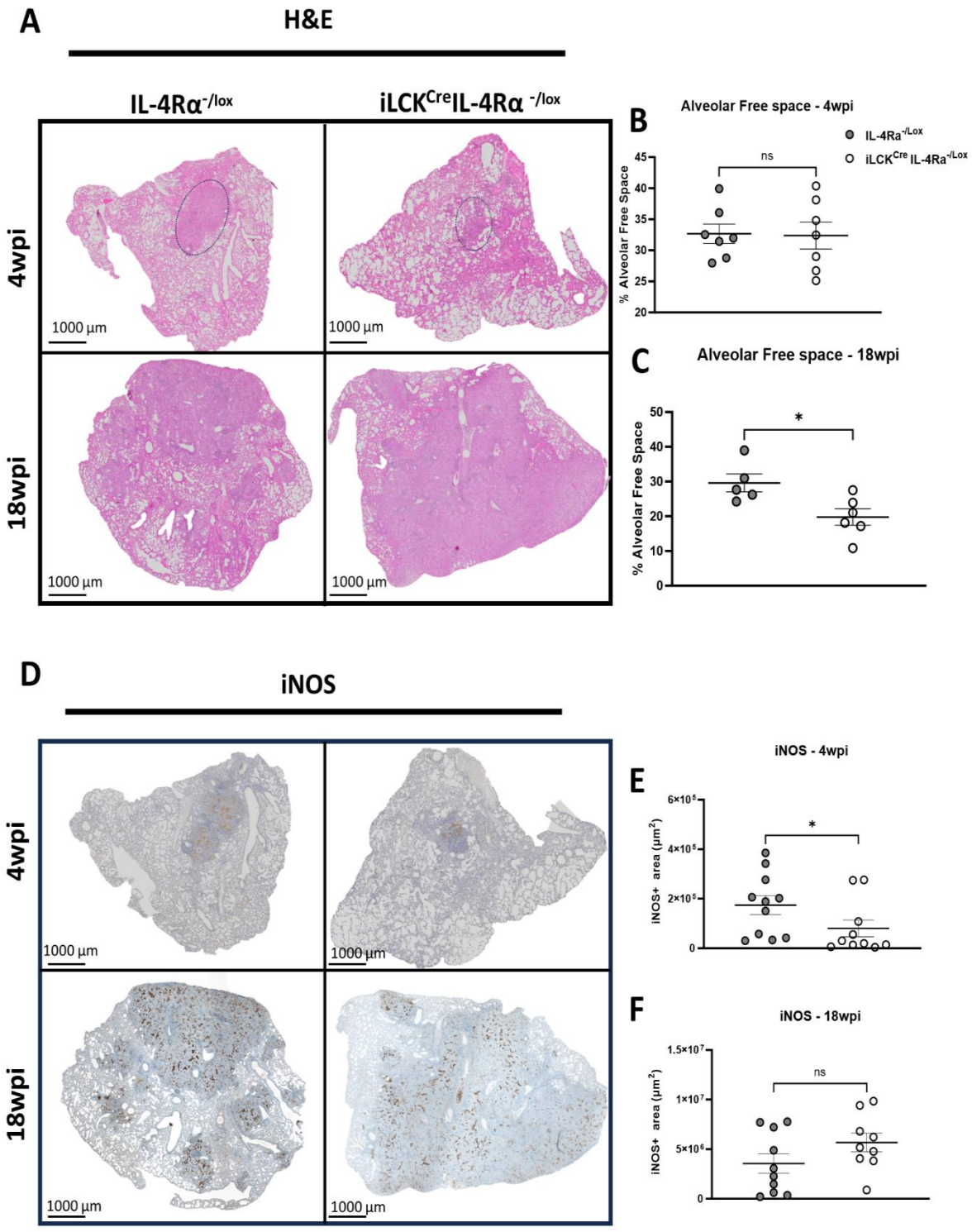

Figure 4: Increased mycobacterial burden and tissue pathology in iLCK^{Cre}IL-4Rα$^{-/lox}$ mice during chronic *Mtb* infection. iLCK^{Cre}IL-4Rα$^{-/lox}$ and IL-4Rα$^{-/lox}$ littermate controls were intranasally infected with 100 CFU of HN878 at and euthanized either 4 weeks or 18 weeks after infection to determine mycobacterial burden in the (A) Lung and (B) spleen (C) Representative H&E histopathology of lung sections (40x) along with (D) quantification of alveolar free space at 4- and 18wpi. (E) Representative iNOS histopathology (40x) along with (F) quantification of iNOS^{+} area at 4- and 18wpi. Data represented as mean ± SEM of n=5-7 mice/group, and experiments were performed 2-4 times. Statistical significance was analysed by unpaired student t-test. *p<0.05

3.3 Immune cell responses are altered in iLCK^{Cre}IL-4rα$^{-/lox}$ during *Mtb* infection

To gain further insight into the increased susceptibility of iLCK^{Cre}IL-4rα$^{-/lox}$ to *Mtb* infection, a better understanding of immune response and the immune cell populations was required. Single-cell suspensions of the lungs from iLCK^{Cre}IL-4rα$^{-/lox}$ and IL-4rα$^{-/lox}$ were prepared to determine immune cell populations using flow cytometry. The total number of cells in the lungs, revealed by Cytosmart automated cell counter, showed no statistically significant differences at either time points (Figure 5A-B). The lymphoid population showed a substantial decrease in the amount of T cells recruited to the lung at 4wpi. The almost 38% contraction in the amount of T cells in the lung is a sign of significantly altered immune response at the acute time point (Figure 5C-D). Other lymphoid populations were not significantly altered by the deletion of IL-4Rα on T cells in iLCK^{Cre}IL-4rα$^{-/lox}$ mice. We noted with interest that γδ T cells are not altered, despite also lacking the IL-4Rα. Indicating that if the differences of T cells recruited to lung is related to the absence of IL-4Rα, it only affects the αβ-T cells. Curiously the amount of T cells recruited to the lung had stabilised by 18wpi with no perturbations observed in the different lymphoid population at this time point (Figure 5E-F). We further sought to examine if there were any differences in the amount of CD4 and CD8 T cells in the lung at acute and chronic time points. This revealed that there were significant decreases in both CD4 and CD8 T cells at acute stage of infection but not at the chronic stage of infection (Figure 5G). Comparing the ratio of CD4 to CD8 T cells is predictive test used to gain insight into immune activation status [183]. Normal CD4 to CD8 ratio in blood is 1.5-2.5, with higher ratio tending to indicate immune activation while a lower ratio associated with immunodeficiency or autoimmune manifestations. The ratio of CD4 to CD8 in the bronchoalveolar lavage (BAL) of TB patients can range from 1-3.5 depending on age and other malignancies [184]. We compared the live CD4 to CD8 T cells at both timepoints and found that iLCK^{Cre}IL-4rα$^{-/lox}$ mice had significant increased ratio of CD4 to CD8 T cells at acute stage of infection but not at chronic stage (Figure 5H). Although the CD4:CD8 ratio in the iLCK^{Cre}IL-4rα$^{-/lox}$ is in line with what is reported in BAL, the statistically significant relative increase in CD4 to CD8 T cells suggest underlying differences in immune activation driven by the absence of IL-4Rα. The difference in the ratio of CD4 to CD8 T cells, in conjunction with the relatively reduced recruitment of T cells to the site of disease suggest a dysregulated immune response particularly in acute phase of infection.

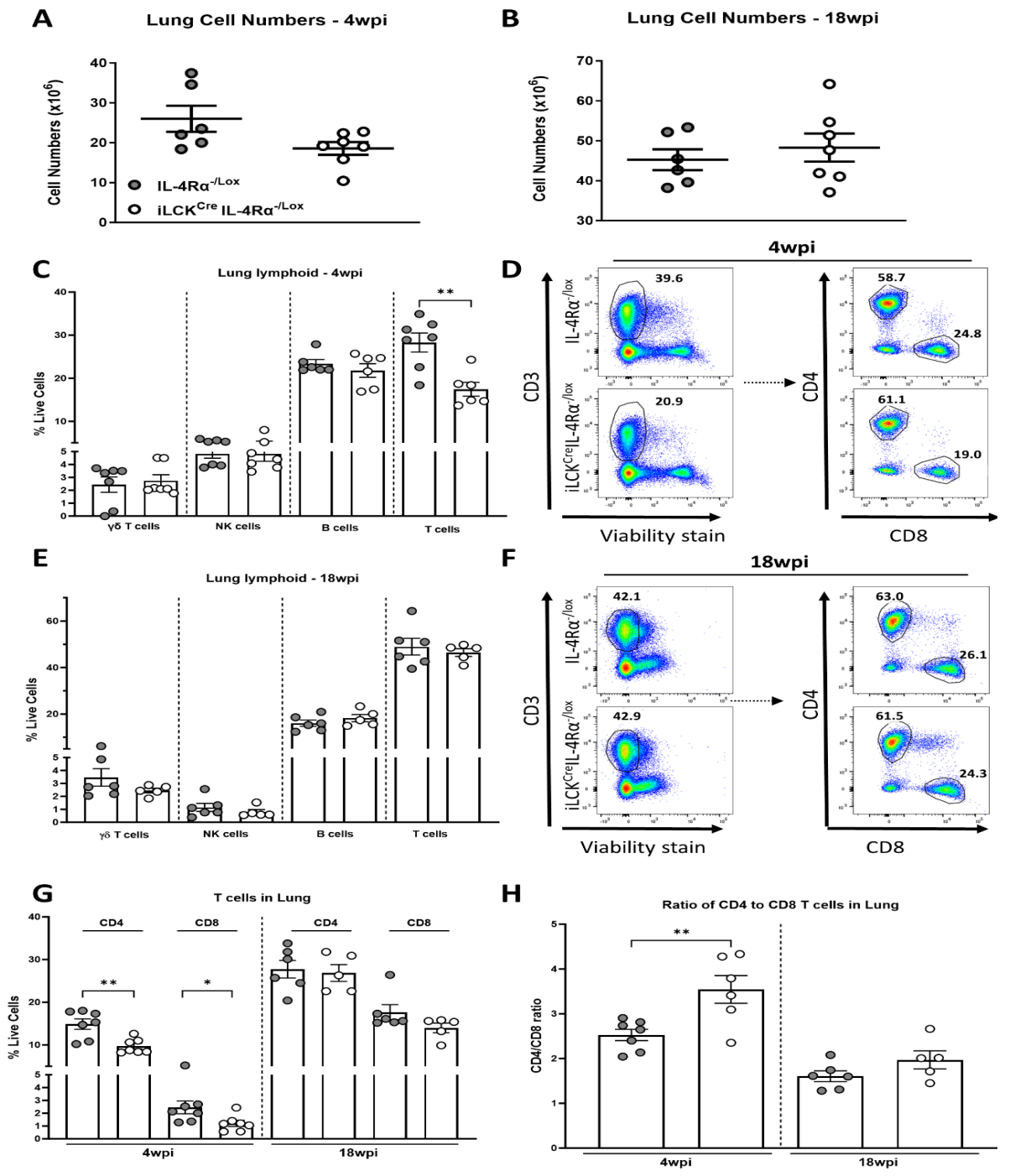

Figure 5: IL-4Rα deficiency results in reduced recruitment of T cells to the lung in acute but not in chronic *Mtb* HN878 infection. Total lung cell numbers were enumerated in the lungs of mice at **(A)** 4 weeks and **(B)** 18 weeks post-infection. Single cell suspensions was analysed by flow cytometry to track lymphoid populations at **(C)** 4 weeks **(D)** representative flow plots. **(E)** Lymphoid populations at 18 weeks post infection. **(F)** Representative flow plots. **(G)** CD4 and CD8 T cells are displayed at 4 weeks and 18 weeks post infection. **(H)** Ratio of CD4 to CD8 T cells in the lung at indicated timepoints. Cell populations are displayed as percentage of live cells. Lymphoid populations were determined using the following surface markers. Gamma-delta T cells (γδ T cells): $CD3^+$ γδ TCR^+; NK Cells: $CD3^-$ $NK1.1^+$; B cells: $CD3^-CD19^+$, T cells: γδ TCR^-,$NK1.1^-$,$CD19^-CD3^+$; CD4 T cells: γδ TCR^-,$NK1.1^-$,$CD19^-CD3^+CD4^+$; CD8 T cells: γδ TCR^-,$NK1.1^-$,$CD19^-CD3^+CD8^+$. Data represented as mean ± SEM of n=5-7 mice/group, and experiments were performed 2-4 times. Statistical significance was analysed by unpaired student t-test. *p<0.05, **p<0.001

3.4 iLCK^{Cre}IL-4rα$^{-/lox}$ mice show no differences in lymphoid populations in the mediastinal lymph nodes during *Mtb* infection

The adaptive immune response to *Mtb* infection takes about 2 weeks from the onset of infection in the lung till the priming of T cells in the lymph node (LN), and a further 1-2 weeks before these adaptive response is detected in the lung [60, 185]. The mediastinal lymph node (MLN) is the local draining lymph node for the lung and is thus the site at which *Mtb*-specific T cell responses are initiated. Given the substantial differences in the amount of CD4 and CD8 T cells recruited to the lung during the acute stage of infection, we assessed the lymphoid populations within the mediastinal lymph node, to assess whether the decreased recruitment to the lung is due to an impaired priming of T cells. Total number of cells as determined by cytosmart automated cell counter, revealed no differences between the iLCK^{Cre}IL-4rα$^{-/lox}$ and IL-4rα$^{-/lox}$ at during both acute and chronic stages of infection (Figure 6A-B). Flow cytometry revealed that where no differences in the lymphoid populations within the MLN at both acute and chronic stages of infection (Figure 6C-D). A decreased number of CD8 T cells, but not CD4 T cells was detected in the MLN during acute infection with *Mtb* whereas no differences in CD4 T cells or CD8 T cells were observed in chronic stage. In contrast to the lungs, no differences in the ratio of CD4 to CD8 T cells were observed in the MLN during infection (Figure 6F). The overall lack of differences in lymphoid populations between the iLCK^{Cre}IL-4rα$^{-/lox}$ and the IL-4rα$^{-/lox}$ mice during the course infection, suggests that the differences observed in the lung was not due to impaired T cell priming in the MLN except a small decrease in CD8 T cells in the MLN, similar to the lungs, during acute TB infection. Overall this demonstrates deficiency of IL-4Rα on T cells does not cause major differences in the lymphoid populations in the MLN.

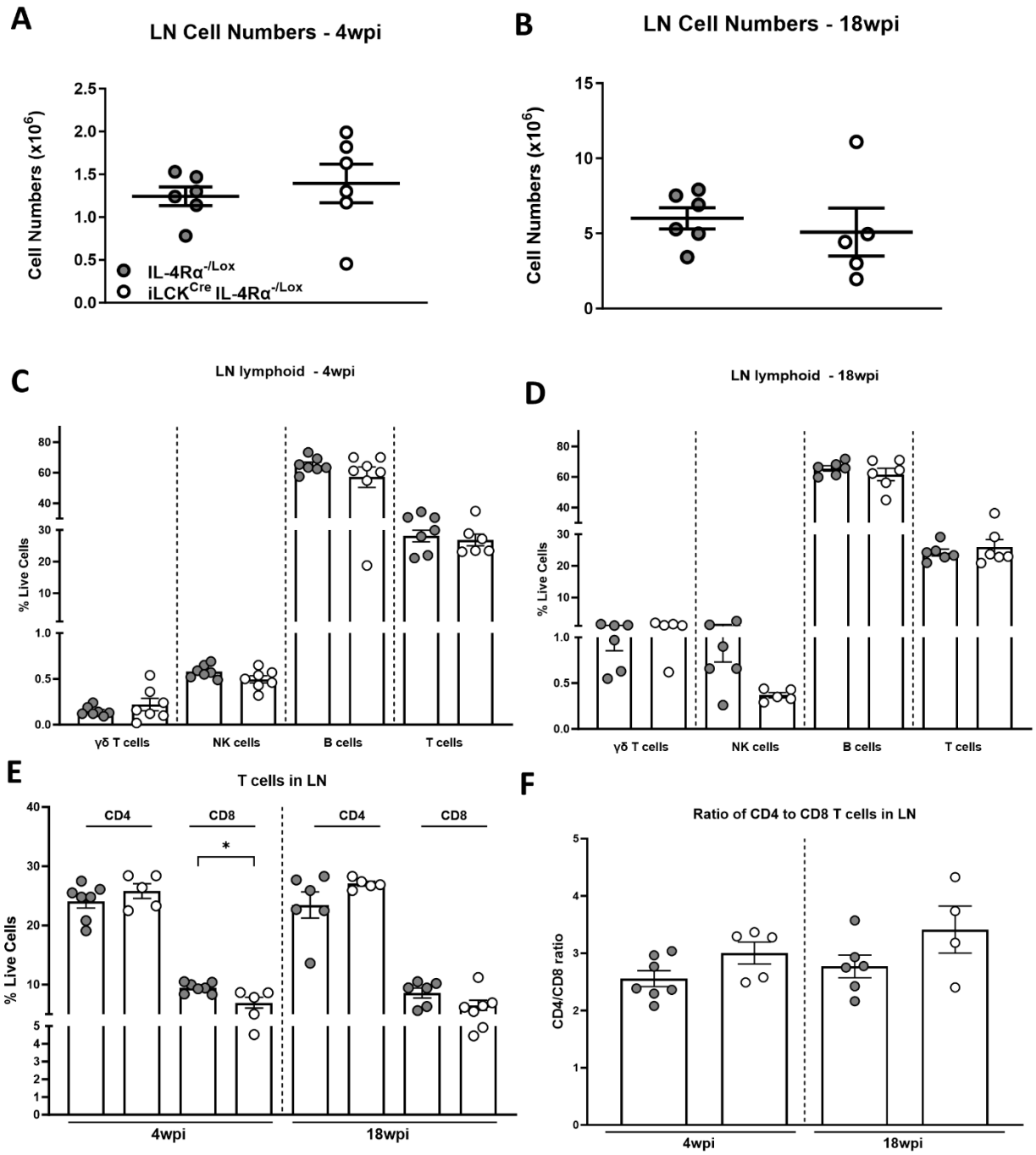

Figure 6: No differences in the cell numbers of iLCK^{Cre}IL-4Rα$^{-/lox}$ mice in the Mediastinal lymph node during *Mtb* HN878 infection. Total MLN cell numbers were enumerated at **(A)** 4 weeks and **(B)** 18 weeks. Single cell suspensions of MLN was analysed by flow cytometry to track lymphoid populations at **(C)** 4 weeks and **(D)** 18 weeks post infection. **(E)** Amounts of CD4 and CD8 T cells are displayed at 4 weeks and 18 weeks post infection. **(F)** Ratio of CD4 to CD8 T cells in the lung at indicated timepoints. Cell populations are displayed as percentage of live cells. Lymphoid populations were determined using the following surface markers. Gamma-delta T cells (γδ T cells): CD3$^+$ γδ TCR$^+$; NK Cells: CD3$^-$NK1.1$^+$; B cells: CD3$^-$CD19$^+$, T cells: γδ TCR$^-$,NK1.1$^-$CD19$^-$CD3$^+$; CD4 T cells: γδ TCR$^-$NK1.1$^-$CD19$^-$CD3$^+$CD4$^+$; CD8 T cells: γδ TCR$^-$NK1.1$^-$CD19$^-$CD3$^+$CD8$^+$. Grey circles indicate IL-4Rα$^{-/lox}$ and white circles indicate iLCK^{Cre}IL-4Rα$^{-/lox}$. Data represented as mean ± SEM of n=5-7 mice/group, and experiments were performed 2-4 times. Statistical significance was analysed by unpaired t-test. *p<0.05 Statistical significance was analysed by student unpaired t-test. *p<0.05

3.5 No major differences in the myeloid populations in the lung and mediastinal lymph node of the iLCK^{Cre}IL-4rα$^{-/lox}$ mice during *Mtb* infection.

The role of myeloid cells in *Mtb* infection is not straight forward, as the large diversity of the myeloid population which may take on different roles. In addition, the myeloid cell populations can act in either restrictive or permissive capacities. Macrophages are the major host for *Mtb*, and are generally considered to be the cells that make first contact with the bacteria and thus are cells that send out danger signals which recruit other macrophages, neutrophils and DCs [186, 187]. Given the increased susceptibility of iLCK^{Cre}IL-4rα$^{-/lox}$, and greater bacterial burden, we assessed the myeloid populations in the lung and MLN during acute and chronic infection of iLCK^{Cre}IL-4rα$^{-/lox}$ and IL-4rα$^{-/lox}$ (Figure 7A-H). We found no differences in the eosinophils, DCs, monocytes and monocyte derived DCs in the lungs of iLCK^{Cre}IL-4rα$^{-/lox}$ during acute and chronic infection. However, we noted in an increase in the amount of neutrophils only during chronic TB infection (Figure 7A-B), indicative of the lung pathology associated with development of alveolitis. A condition where infiltration of neutrophils into the lung cause the filling of the alveolar free spaces, causing damage to the lung parenchyma [188]. Furthermore, necrosis of the lung tissue during *Mtb* infection is associated with increased neutrophils and associated chemokines (CXCL1, CXCL2 and CXCL5) [189]. These observations from other studies could explain that the increased neutrophils during chronic infection could be the underlying cause of the loss of alveolar free space (Figure 4). Surprisingly, no statistically significant differences in number of alveolar macrophages in the lungs at either acute or chronic stages of infection. However, a statistically significant decrease in interstitial macrophages was seen during acute but not chronic infection. We also observed no differences in myeloid populations in the MLN of iLCK^{Cre}IL-4rα$^{-/lox}$ mice during acute or chronic infection (Figure 7C-D). Dendritic cells in the lung can further be divided into CD103+CD11b- and CD103-CD11b+ subsets, known as conventional and plasmacytoid DCs respectively [190]. CD103 DCs are reported to be effective in presenting antigen to CD8 T cells, and as such, fluctuations in the population of CD103 DCs can act as an indicator of the ability of the host to initiate cytotoxic T cell responses [191]. In addition to the role of initiating CD8 responses, there is evidence that CD103+ DCs contribute to the early activation of CD4 T cells [192]. On the other hand, opposing evidence shows that CD11b DCs are the subset that are critical for early Th1 activation [193]. We observed no differences in CD103+CD11b- and CD103-CD11b+ DC subsets in the lung during both acute and chronic *Mtb* infection (Figure 7E-F). Additionally, there were no differences of CD103+CD11b- and CD103-CD11b+ DCs that had migrated to the MLN from the site of disease regardless of the acute/chronic disease

(Figure 7G-H). There were also differences within the resident DCs (CD11c+, MHCII^{hi}) subsets of the MLN, which comprise of CD8 DCs and CD11b DCs (Figure 7I-J). CXCR5 along with Bcl-6 and ICOS is associated with T follicular helper cells. CXCR5+ B cells interact with CXCR5+ T cells in the germinal centre, within secondary lymphoid organs [194]. We found no differences in CXCR5+ T cells and CXCR5+ B cells in the LN during acute and chronic infection (Figure 7K-L), indirectly suggests that disruption of IL-4Rα on T cells has no effect on the formation of germinal centre during *Mtb* infection. Together these data support that the decrease in T cells in iLCK^{Cre}IL-4rα$^{-/lox}$ during acute infection is related to the deletion of IL-4Rα, and recruitment to the lung. Furthermore, this decrease is unlikely to be related to priming of T cell responses.

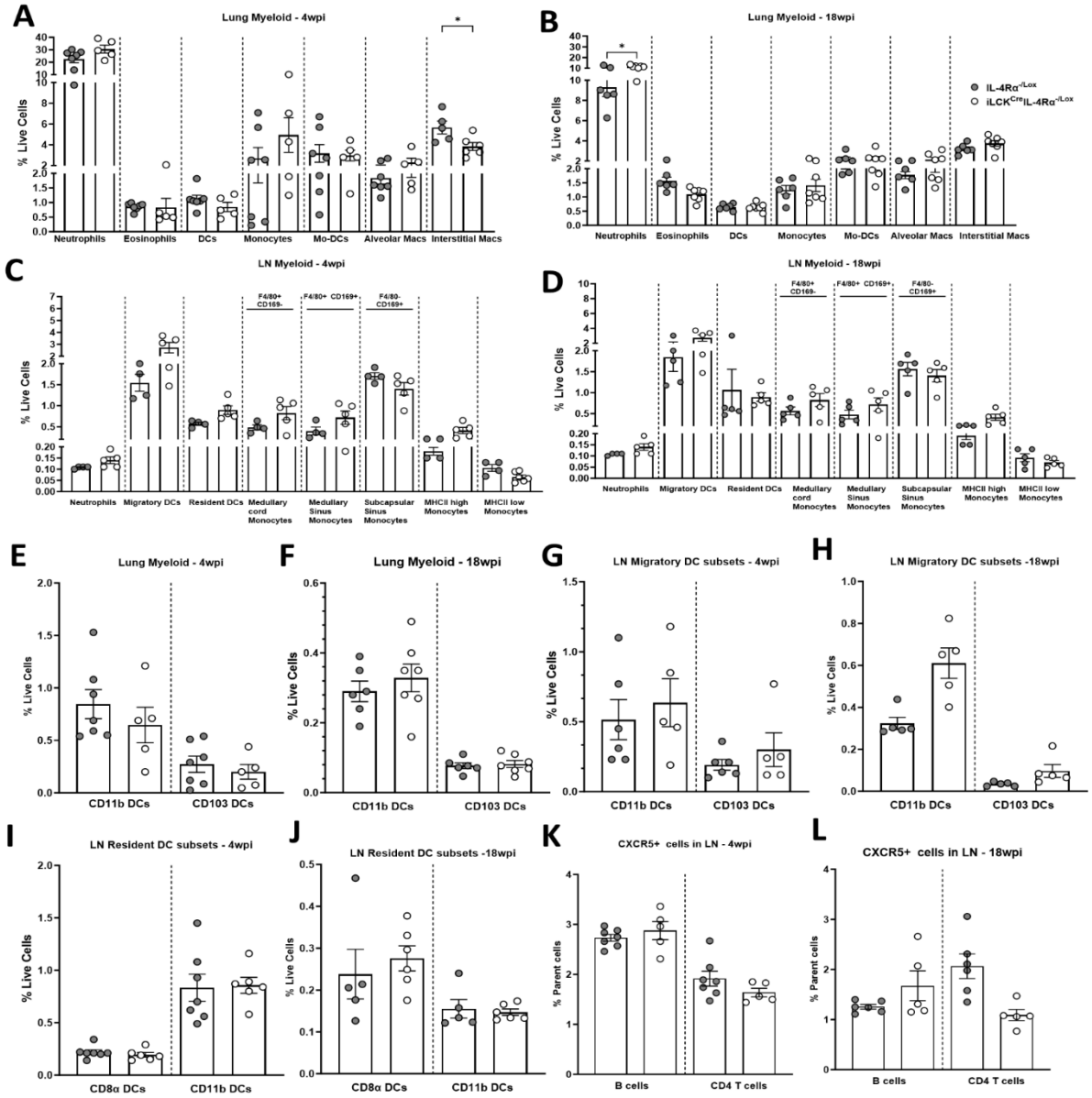

Figure 7: Deletion of IL-4Rα on T cells increased neutrophils in the lung during chronic *Mtb* HN878 infection. Single cell suspensions of lung tissue was analysed by flow cytometry to determine myeloid cell populations at **(A)** 4- and **(B)** 18-wpi and **(C-D)** mediastinal lymph nodes. Various myeloid subsets in the lung and lymph node as indicated **(E-J)**. $CXCR5^+$ B cells and T cells in the LN are shown at **(K)** 4 weeks and **(L)** 18 weeks. Myeloid populations were determined using the following markers. Neutrophils: $Ly6G^+CD11b^+$; Eosinophils: $SiglecF^+CD11b^+CD64^-$; Dendritic cells (DC):$CD11b^+CD11c^+MHCII^+$; Monocytes: $Ly6G^+CD11b^+CD64^-$; Monocyte-derived Dendritic Cells (Mo-DCs): $CD64^+CD11b^+CD11c^+$; Alveolar Macrophages (Alveolar Macs): $CD64^+MerTK^+SiglecF^+CD11c^+$; Interstitial Macrophages (Interstitial Macs): $CD64^+MerTK^+SiglecF^+CD11c^-CD11b^+$. Migratory Dendritic cells (Migratory DCs): $CD11c^+MHCII^{Hi}$. Resident Dendritic cells:$CD11c^+MHCII^{lo}$. Medullary cord Monocytes: $CD11b^+F4/80^+CD169^-$. Medullary Sinus Monocytes: $CD11b^+F4/80^+CD169^+$. Subcapsular Sinus Monocytes: $CD11b^+F4/80^-CD169^+$. $MHCII^+$-monocytes: $CD11b^+Ly6C^+MHCII^{Hi}$. $MHCII^-$-monocytes:$CD11b^+Ly6C^+MHCII^{lo}$. $CD11b^+$ DCs: $CD11c^+MHCII^+CD11b^+CD103^-CD64^-$. $CD103^+$ DCs: $CD11c^+MHCII^+CD11b^-CD103^+CD64^-$. $CD8^+$ Resident DC: $CD11c^+MHCII^{lo}CD8^+CD11b^-$. $CD11b^+$-Resident DC: $CD11c^+MHCII^{lo}CD8^-CD11b^+$. CXCR5+ B cells: $CD3^-CD19^+CXCR5^+$. $CXCR5^+$ T cells: $CD3^+CD19^-CXCR5^+$. Data represented as mean ± SEM of n=5-7 mice/group, and experiments were performed 2-4 times. Statistical significance was analysed by student unpaired t-test. *$p<0.05$

3.6 CD4 T cells from iLCK^{Cre}IL-4rα$^{-/lox}$ mice exhibited increased T-bet and RORγt transcriptional signatures in *Mtb* infection

CD4 T cells adopt helper functions in the immune response. The subclass that the CD4 T cell differentiates into dictates the nature of the immune response. For example, Th1 CD4 T cells secrete large amounts of IFN-γ, prompting macrophages to activate antimicrobial programs, including inducing the production nitrogen intermediates and increasing maturation of phagosome into acidic phagolysosomes to destroy intracellular bacteria [195, 196]. While IL-4 acts as the signal that drives naïve CD4 T cells towards Th2. T helper cells are characterized by the repertoire of cytokines they produce, as well as the transcription factors which act as the master regulators of these programs such as T-bet for Th1, GATA3 for Th2, RORγt for Th17 and FoxP3 for T_{regs}. Given the importance of IL-4Rα in polarizing and maintaining of Th2 cells, we assessed whether deletion of IL-4Rα cause perturbations in the ability of CD4 T cells to commit to various helper functions. Other studies from our laboratory showed iLCK^{Cre}IL-4rα$^{-/lox}$ have stronger Th1 cytokine responses compared to littermate controls in *Schistosoma mansoni* and *Leishmania major* infection [173, 176, 197].

Indeed, we found that deletion of IL-4Rα results in an enhanced expression of T-bet in lung derived CD4 T cells during acute infection as tracked by GMFI and percentage of CD4 T cells (Figure 8A-B). Similarly, RORγt was also increased in CD4 T cells during acute infection. Surprisingly, no alterations in expression of transcription factor GATA3 was observed possibly due to generally low and fewer T cells adopt the Th2 phenotype in *Mtb* infection. Moreover, we also saw no differences in the expression of FoxP3. This is an important observation since it is well recorded that IL-4Rα mediated signalling can be important for the establishment T_{regs} [198-200]. Our observations are consistent during chronic infection, as we see increased T-bet and RORγt expression, and unaltered GATA3 and FoxP3 expression in lung derived CD4 T cells (Figure 8C).

T-bet expression is highly expressed in CD8 T cells, and contributes partly to the production of IFN-γ, perforin, and granzyme B [201]. Certain CD8 effector functions remain intact in the absence of T-bet indicating that there are possible compensatory mechanisms, largely attributed to eomes [202]. Importantly, a study from the Behar group demonstrating the role of helped versus helpless CD8 T cells demonstrated T-bet expression to be a feature of helped CD8 T cells which provide more efficient protection against *Mtb* infection [100]. Thus, knowing the status of T-bet expression in CD8 T cells is an important assessment to make in *Mtb* infection. We did not find any differences in the expression of T-bet in lung derived CD8 T cells during

acute or chronic infection in the absence of IL-4Rα (Figure 8D). Showing that IL-4Rα is not directly, responsible for the reduction of CD8 T cells in the lung. T-bet expression represses the induction of Th2 and Th17 transcriptional programs [75]. Similarly, T cells sourced from NHP granulomas are found to be have either T-bet or RORγt [203]. Since, these helper programs work against each other, it is initially puzzling why elevated T-bet and RORγt are detected. Note that in animal infection models, each granuloma can exhibit unique courses of action with regards to cellular makeup, inflammation, and bacterial load [47]. To demonstrate that both RORγt and T-bet expressing CD4 T cells are detected in the lung, and that they are indeed independent populations we show a representative flow plot captured during chronic infection (Figure 8E-F). These observations confirm that absence of IL-4Rα causes perturbations in transcriptional regulation and causes CD4 T cells to have increased T-bet or RORγt expression.

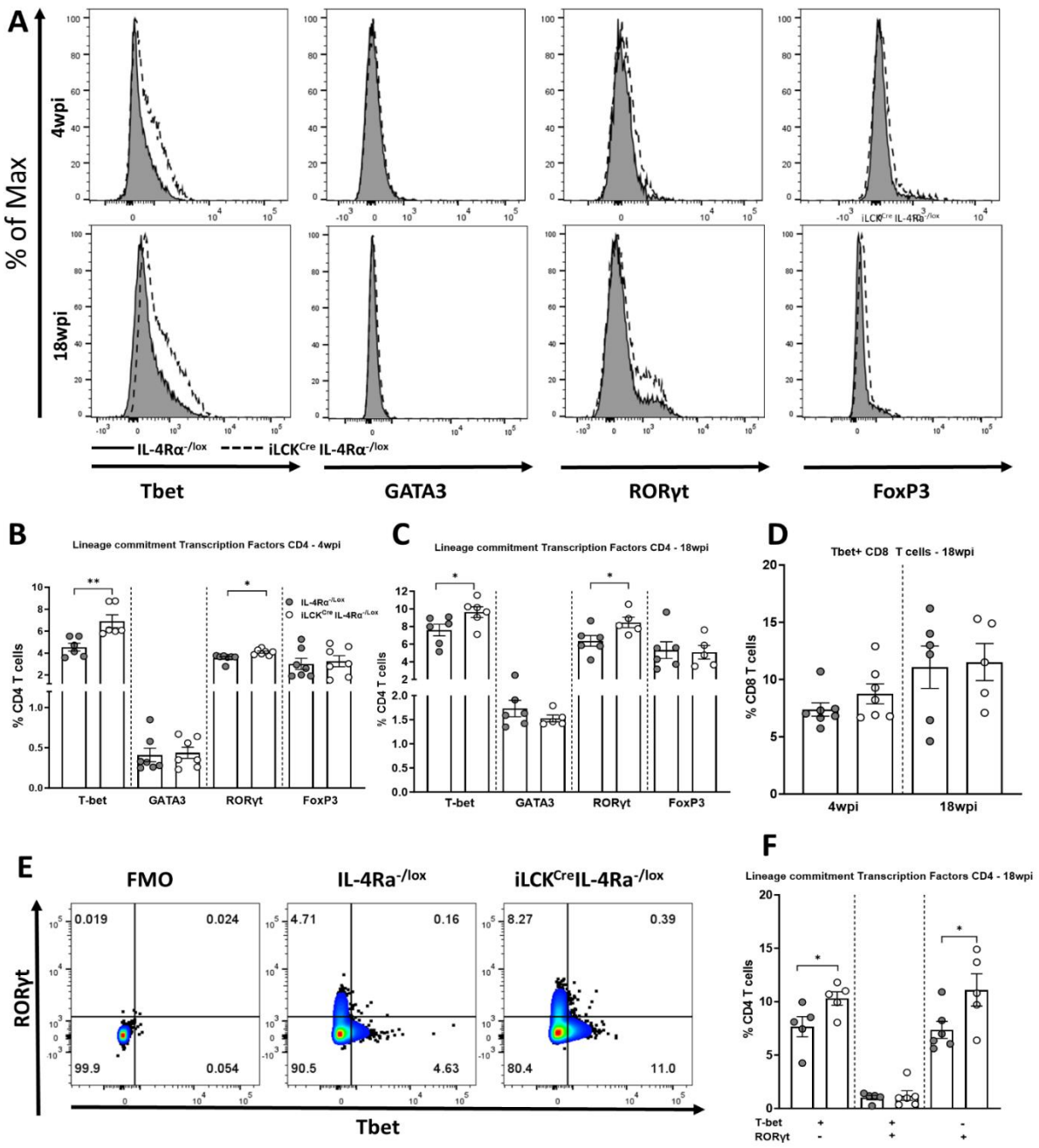

Figure 8: Increased expression of T-bet and RORγt in T cells from *Mtb*-infected iLCK^{Cre}IL-4Rα$^{-/lox}$ mice. iLCK^{Cre}IL-4Rα$^{-/lox}$ and IL-4Rα$^{-/lox}$ littermate controls were intranasally infected with 100 CFU of HN878 at and euthanized at 4 and 18 weeks. Single cell suspensions were prepared from the infected lung tissue were stained for T-bet, RORγt, FoxP3, GATA3 on CD4 and CD8 T cells. These were then analysed by flow cytometry. (A) Representative histograms of indicated lineage markers in CD4 T cells at 4- and 18-weeks post infection. Grey-filled histogram represents IL-4Rα$^{-/lox}$, while the dashed line represents iLCK^{Cre}IL-4Rα$^{-/lox}$. The percentage of CD4 T cells positively stained with various lineage markers at (B) 4 weeks post infection and (C) 18 weeks post infection. (D) Percentage of T-bet^{+} CD8 T cells is displayed at 4 weeks and 18 weeks post infection. Amount of pulmonary CD4 T cells from iLCK^{Cre}IL-4Rα$^{-/lox}$ and IL-4Rα$^{-/lox}$ as shown by (E) representative flow plots and (F) percentage of CD4 T cells. Grey circles indicate IL-4Rα$^{-/lox}$ and white circles indicate iLCK^{Cre}IL-4Rα$^{-/lox}$. Data represented as mean ± SEM of n=5-7 mice/group, and experiments were performed 2-4 times. Statistical significance was analysed by student unpaired t-test. *p<0.05, **p<0.001.

3.7 Effector/effector memory responses are heightened in the lungs of iLCK^{Cre}IL-4rα$^{-/lox}$ mice

Based on our observations which indicated that the deletion of IL-4Rα leads to differences in the early response to *Mtb*, such as reduced T cell recruitment the lung during acute infection and increased expression of T-bet and RORγt, our next objective was to investigate if there any functional differences in the profile of memory T cells. We analysed expression of the of the activation marker CD44 and cell adhesion marker CD62L to distinguish T cell memory subsets. The CD44^{+}CD62L^{-} is also considered to be the antigen experienced, as CD44 is expressed shortly after TCR activation [204]. During the acute *Mtb* infection, we identified an augmented population of effector/effector memory CD4 T cells but not CD8 T cell responses (Figure 9A-C), which remained consistent during chronic *Mtb* infection (Figure 9D-F). Our observations suggest that absence of IL-4Rα on T cells causes an expansion of antigen experienced CD4 T cells (CD44^{+}CD62L^{-}) in the lung but does not have the same effect on CD8 T cells (Figure 9A-F). No discernible variations in the central memory CD4 or CD8 T cells were detected during acute or chronic infections. Since, we observed fewer CD4 T cells during acute infection in the lung but a higher percentages of effector cells, we wished to gain an understanding of the how this translated in terms of raw number. Remarkably, when comparing the numbers of cells acquired, we observed concomitant decrease in CD4 and effector T cells during acute infection of the lung of iLCK^{Cre}IL-4rα$^{-/lox}$ (Figure 10A). Use of this metric during chronic infection confirmed our earlier data that there are no differences in total CD4 T cells, and thus the increased percentage of effector CD4 T cells translate into an increased percentage of effector T cells (Figure 10B). This aligns with the observation that loss of IL-4Rα leads to an increase in the expression of T-bet. Given that the effector population of CD4 T cells predominantly exhibit a Th1 phenotype during *Mtb* infection, we decided to track the IL-4Rα expression across different memory T cells.

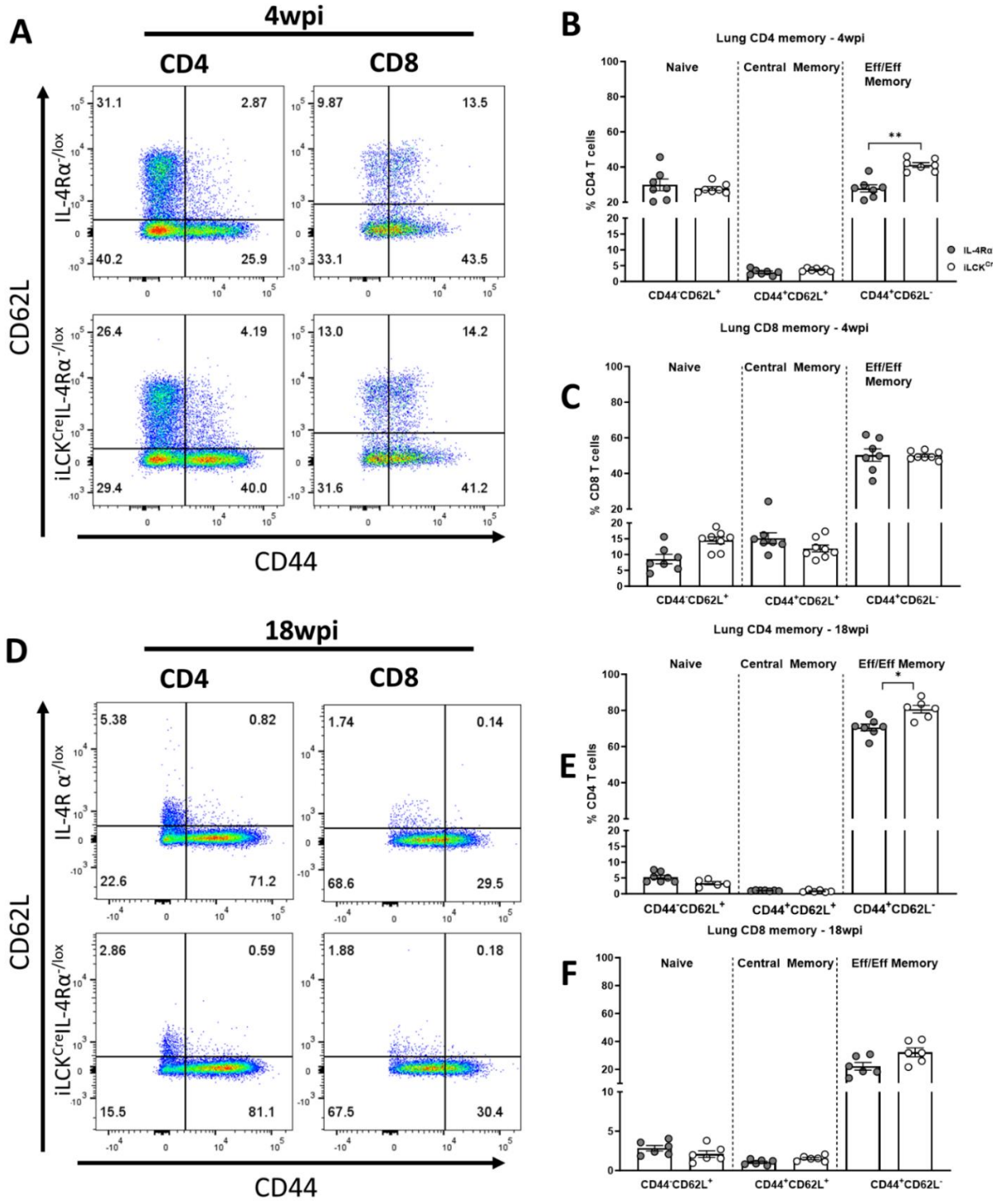

Figure 9: Increased amounts of effector (CD44+CD62L-) T cells in the lungs of *Mtb* infected iLCK^{Cre}IL-4Rα$^{-/lox}$ mice. iLCK^{Cre}IL-4Rα$^{-/lox}$ and IL-4Rα$^{-/lox}$ littermate controls were intranasally infected with 100 CFU of HN878 at and euthanized at 4 and 18 weeks. **(A)** Representative flow plots of pulmonary CD4 and CD8 T cells profiled for CD44 and CD62L at 4 weeks post infection. Quantification of memory markers of **(B)** CD4 and **(C)** CD8 T cells derived from the lungs of *Mtb* infected mice at 4 weeks post infection. **(D)** Representative flow plots of pulmonary CD4 and CD8 T cells profiled for CD44 and CD62L at 18 weeks post infection. Quantification of memory markers of **(E)** CD4 and **(F)** CD8 T cells derived from the lungs of *Mtb* infected mice at 4 weeks post infection. Data represented as mean ± SEM of n=5-7 mice/group, and experiments were performed 2-4 times. Statistical significance was analysed by student unpaired t-test. *p<0.05, **p<0.001.

During acute infection, we observed a significant drop in GMFI of IL-4Rα on the IL-4rα$^{-/lox}$ littermate control, between the naïve to central memory or effector/effector memory phenotype (Figure 10C). Indicating loss of IL-4Rα is associated with differentiation of CD4 T cells from a naïve to central memory or effector phenotype, plausibly due to adoption of a more-Th1 phenotype. No differences in expression of IL-4Rα was seen between naïve, central memory and effector/effector memory subsets of iLCK^{Cre}IL-4rα$^{-/lox}$ during acute infection. Although IL-4Rα remained significantly lower within CD4 subsets of iLCK^{Cre}IL-4rα$^{-/lox}$ compared to controls. Although these observations largely remained consistent during chronic infection, we detected that the effector population showed no discrepancies in IL-4Rα between iLCK^{Cre}IL-4rα$^{-/lox}$ and IL-4rα$^{-/lox}$ (Figure 10D). Suggesting that loss of IL-4Rα, results in an relative increase in antigen specific CD4 T cells over the course of infection. Alternatively, lack of control due to poor early T cell responses leads to an increased bacterial burden, which drives increased inflammation.

The differences in overall CD8 T cell numbers in iLCK^{Cre}IL-4rα$^{-/lox}$ prompted further investigating into memory subsets of CD8 T cells. Two different types of effector subpopulations can be identified by the expression of the terminal differentiation marker, KLRG1 and receptor for IL-7 (CD127). These subpopulations are known as short lived effector cells (SLEC - KLRG1^{+}CD127^{-}) and memory precursor effector cells (MPEC- KLRG1^{-}MPEC^{+}) [205]. Interestingly, during chronic infection with *Mtb* a significant increase in the SLEC population was seen in iLCK^{Cre}IL-4rα$^{-/lox}$ mice when compared to IL-4rα$^{-/lox}$, but no differences were seen in MPECs (Figure 10E-F). We saw no differences in the resident memory CD8 T cell population (T_{RM} – CD103^{+}CD69^{+}) between iLCK^{Cre}IL-4rα$^{-/lox}$ and IL-4rα$^{-/lox}$. This indicates that there is increased amount of highly active CD8 effector cells in the iLCK^{Cre}IL-4rα$^{-/lox}$ during chronic *Mtb* infection.

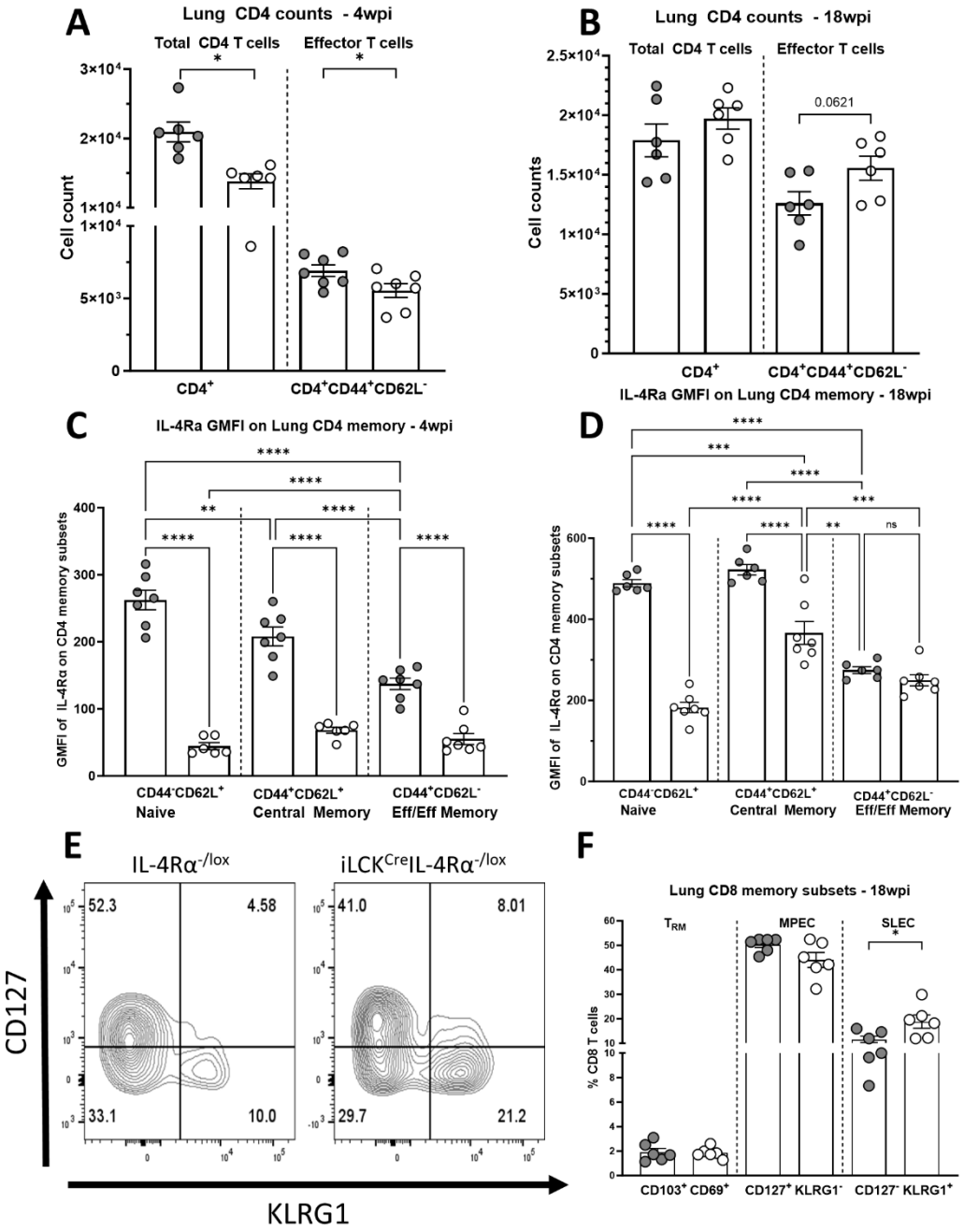

Figure 10: Absence of IL-4R allows for relative expansion of effector T cells in the lungs of *Mtb* infected mice. iLCK^{Cre}IL-4Rα$^{-/lox}$ and IL-4Rα$^{-/lox}$ littermate controls were intranasally infected with 100 CFU of HN878 at and euthanized at 4 and 18 weeks. Total recorded cell counts for CD4 and CD4 effector subsets at **(A)** 4 weeks and **(B)** 18 weeks post infection. Profile of IL-4Rα expression by geometric mean fluorescence intensity (GMFI) on naïve (CD44^{-}CD62L^{-}), Central memory (CD44^{+}CD62L^{+}) and Effector/Effector memory (CD44^{+}CD62L^{-}) at **(C)** 4 weeks and **(D)** 18 weeks post infection. **(E)** Representative flow plot and **(F)** quantification of CD8 T cells derived from the lungs of chronically infected mice, demonstrating expression profile of CD127 and KLRG1. Where CD127^{+}KLRG1^{-} denotes memory precursor effector cells (MPEC) and CD127^{-}KLRG1^{+} denotes short lived effector memory (SLEC) CD8 subsets. Data represented as mean ± SEM of n=5-7 mice/group, and experiments were performed 2-4 times. Statistical significance was analysed by (A-B,F) unpaired student t-test and (C-D)one-way ANOVA with Tukey's post-test. *p<0.05, **p<0.001, ***p<0.0001, ****p<0.00001.

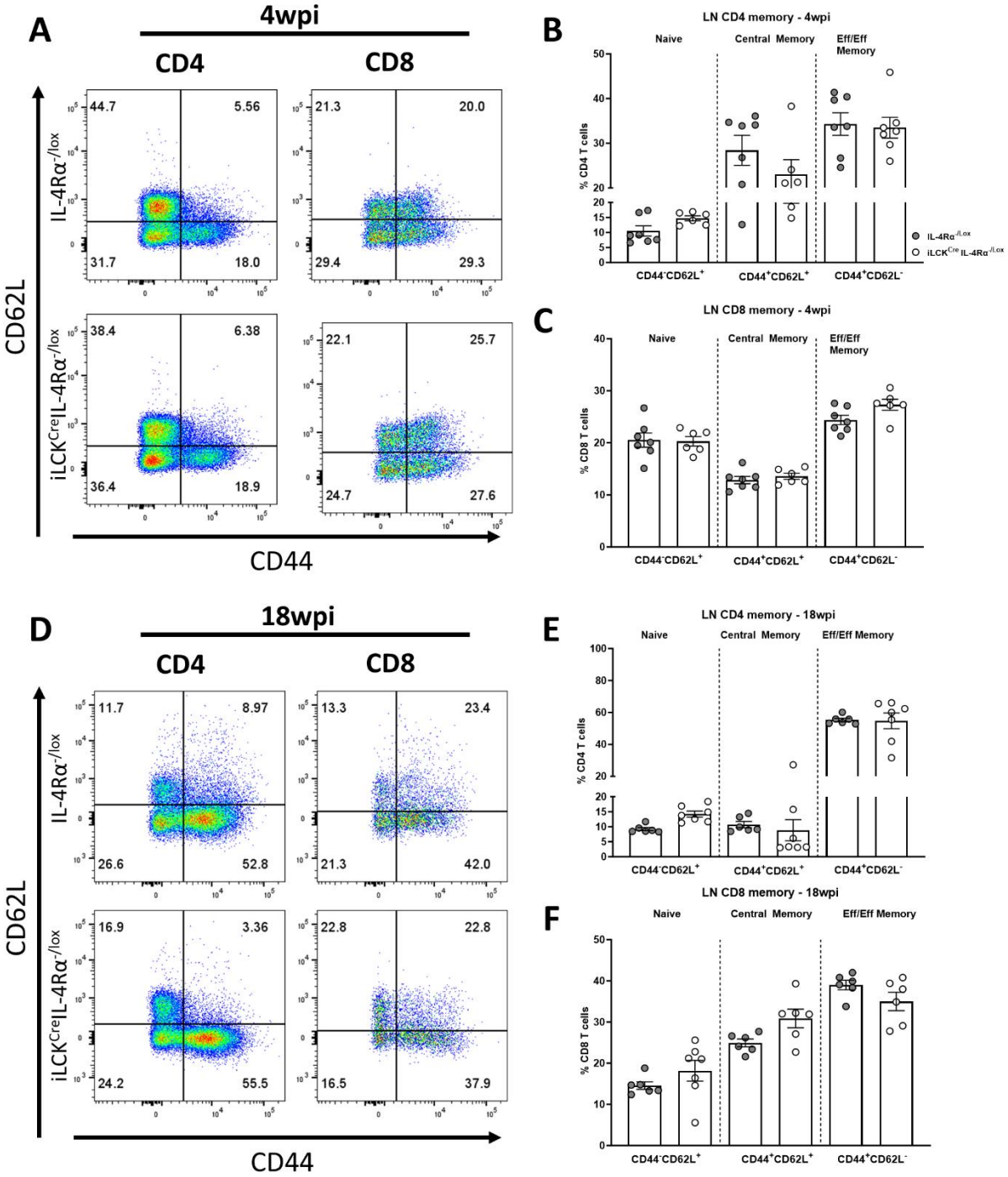

Figure 11: No changes in memory profiles in the lymph nodes of iLCK^{Cre}IL-4Rα$^{-/lox}$ mice during acute or chronic infection. iLCK^{Cre}IL-4Rα$^{-/lox}$ and IL-4Rα$^{-/lox}$ littermate controls were intranasally infected with 100CFU of HN878 at and euthanized at 4 and 18 weeks**(A)** Representative flow plots of CD4 and CD8 T cells from the mediastinal lymph node profiled for CD44 and CD62L at 4 weeks post infection. Quantification of memory markers of **(B)** CD4 and **(C)** CD8 T cells derived from the mediastinal lymph nodes of *Mtb* infected mice at 4 weeks post infection. **(A)** Representative flow plots of CD4 and CD8 T cells from the mediastinal lymph node profiled for CD44 and CD62L at 18 weeks post infection. Quantification of memory markers of **(B)** CD4 and **(C)** CD8 T cells derived from the mediastinal lymph nodes of *Mtb* infected mice at 18 weeks post infection. Grey circles indicate IL-4Rα$^{-/lox}$ and white circles indicate iLCK^{Cre}IL-4Rα$^{-/lox}$. Data represented as mean ± SEM of n=5-7 mice/group, and experiments were performed 2-4 times. Statistical significance was analysed by student unpaired t-test.

Studies investigating the timing of T cell priming and delayed antigen-specific effector response in the lung during low dose *Mtb* infection have shown that CD44 is first expressed by T cells in the MLN before becoming a persistent population in the lung during chronic infection [62, 206]. For this reason, assess if the IL-4Rα associated proportional expansion of the $CD44^{+}CD62L^{-}$ effector population in the lung is reflected in the continued in the MLN. We found no differences in the amount of CD44 expressing CD4 or CD8 T cells in the MLN during acute infection with *Mtb* (Figure 11A-C). Similarly, no differences in the CD4 and CD8 effector populations were identified in the MLN during chronic *Mtb* infection (Figure 11D-E). This supports the idea that decreased amount of T cells recruited to the site of infection in $iLCK^{Cre}IL\text{-}4r\alpha^{-/lox}$ mice is not due to impaired priming in the MLN. It is also suggestive that the relative decreased T-bet signal seen in the littermate controls, $IL\text{-}4r\alpha^{-/lox}$, is sufficient enough to mount a Th1 effector response that traffics to the lung.

3.8 T cells deficient for IL-4rα increased tendency to differentiate into terminal effectors marked by increased KLRG1 expression.

Our observation that T cells lacking IL-4α mediated signalling have a proportional increase in effector population ($CD44^{+}CD62L^{-}$). We investigated the variations in the differentiation markers PD-1 and KLRG1. These markers are commonly associated with exhaustion, however, we now know that they are expressed in different functional subsets of CD4 T cells. PD-1 cells can self-renew and produce relatively little amounts of cytokine. PD-1 expressing cells can then differentiate into KLRG1 expressing T cells, which do not proliferate as readily and produce higher quantities of cytokine. KLRG1 T cells are not able to differentiate into other phenotypes and thus KLRG1 has become a terminal differentiation marker [207]. The absence of IL-4Rα resulted in a relative increase in $KLRG1^{+}PD\text{-}1^{-}$ and $KLRG1^{+}PD\text{-}1^{+}$ lung derived CD4 T cells during acute infection, while no differences in these differentiation markers was observed in lung derived CD8 T cells (Figure 12A-C). Chronic infection in $iLCK^{Cre}IL\text{-}4r\alpha^{-/lox}$ mice is associated with an expanded terminal effector population ($KLRG1^{+}PD\text{-}1^{-}$) in both CD4 and CD8 T cells (Figure 12D-F). The loss of differences in the $KLRG1^{+}PD\text{-}1^{-}$ expressing CD4 population, suggests that the acute phase reflects that CD4 T cells are becoming terminal effectors, and the chronic phase shows a larger portion of both CD4 and CD8 T cells.

Considering greater proportions of active T cells in the lungs of $iLCK^{Cre}IL\text{-}4r\alpha^{-/lox}$, as indicated by higher $CD44^{+}CD62L^{-}$ expression, along with the increased expression of the terminal differentiation marker KLRG1, we sought to determine what fraction of active T cells in the lung exhibit a terminal effector phenotype ($CD44^{+}KLRG1^{+}$) during *Mtb* infection. During

acute *Mtb* infection, we noted slight increase in the $CD44^{+}KLRG1^{+}$ population of CD4 in the lungs of $iLCK^{Cre}IL\text{-}4r\alpha^{-/lox}$ (Figure 13A-C).

No differences in the $CD44^{-}KLRG1^{+}$ population was observed. However, the proportion of $CD44^{+}KLRG1^{+}$ CD4 T cells in the lungs of $iLCK^{Cre}IL\text{-}4r\alpha^{-/lox}$ had a two-fold increase (Mean CD44+KLRG1+ $iLCK^{Cre}IL\text{-}4r\alpha^{-/lox}$: 8.486 vs $IL\text{-}4r\alpha^{-/lox}$: 4.19) when compared to littermate controls (Figure 13D-F). In addition, we found significant increase in $CD44^{+}KLRG1^{+}$ and a concomitant decrease in the double negative $CD44^{-}KLRG1^{-}$ population. Indicating that the proportion of KLRG1 expressing CD4 T cells in the $iLCK^{Cre}IL\text{-}4r\alpha^{-/lox}$ was largely co-expressing CD44. In the case of the littermate controls, this trend was mostly consistent, but in some cases equal amounts of KLRG1 was expressed on active ($CD44^{+}$) and non-active ($CD44^{-}$) CD4 T cells (Figure 13D-E). Interestingly, CD8 T cells in the lungs of $iLCK^{Cre}IL\text{-}4r\alpha^{-/lox}$ during chronic TB, most $KLRG1^{+}$ CD8 T cells expressed CD44, an almost complete reversal in the littermate controls (Figure 13D-F), suggesting that the loss of IL-4Rα leads to a greater proportion of effector CD4 and CD8 T cells being terminally differentiated. The increased expression of KLRG1 on $CD44^{+}$ effector in pulmonary T cells from $iLCK^{Cre}IL\text{-}4r\alpha^{-/lox}$ suggesting that these cells produce large amounts of cytokine and proliferate at a reduced rate.

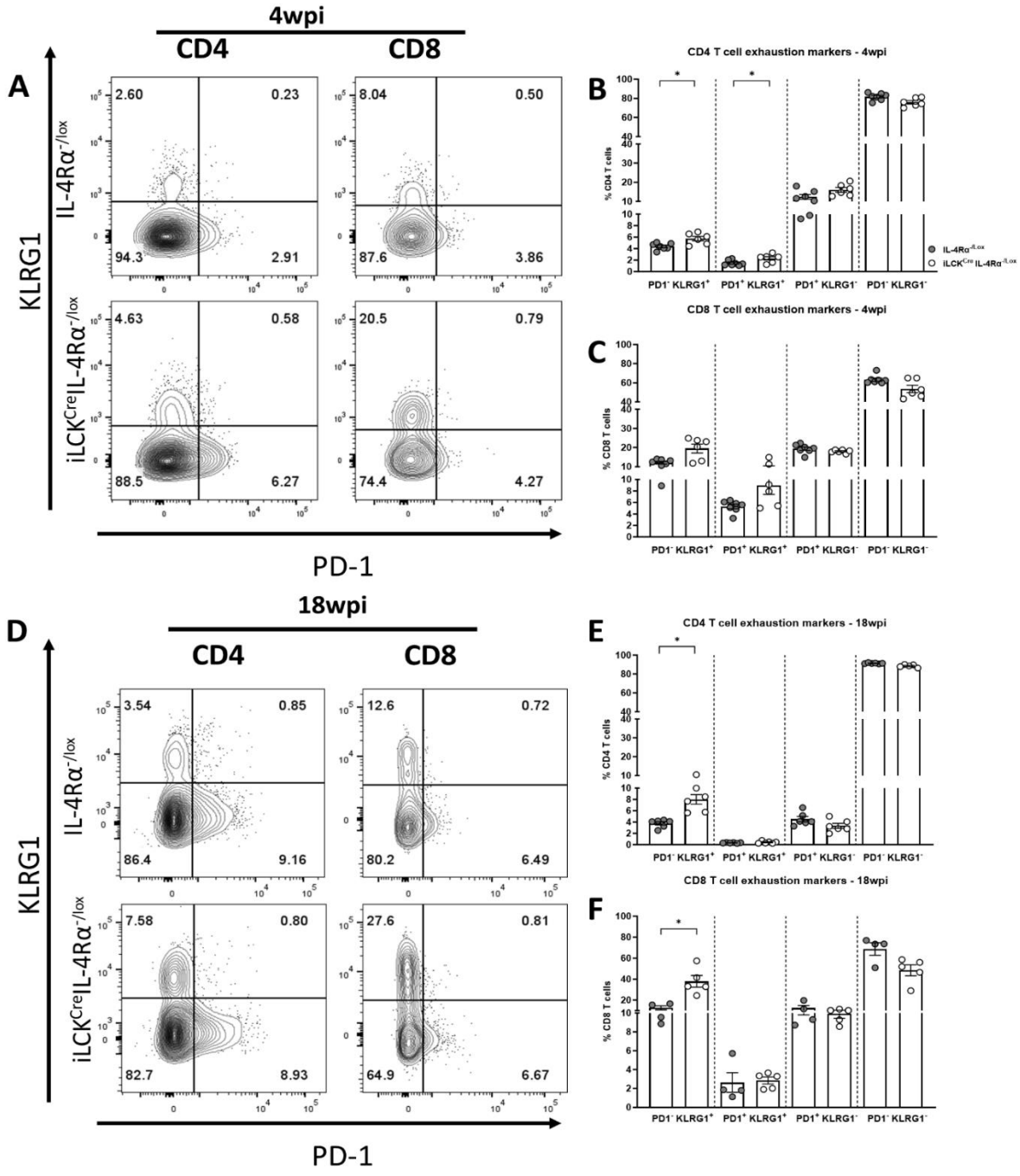

Figure 12: Abrogation of IL-4Rα on T cells leads to increased expression of the terminal differentiation marker KLRG1. iLCK^{Cre}IL-4Rα$^{-/lox}$ and IL-4Rα$^{-/lox}$ littermate controls were intranasally infected with 100CFU of HN878 at and euthanized at 4 and 18 weeks. **(A)** Representative flow plots of pulmonary CD4 and CD8 T cells profiled for expression of KLRG1 and PD-1 at 4 weeks post infection. Quantification of differentiation markers of **(B)** CD4 and **(C)** CD8 T cells derived from the lungs of *Mtb* infected mice at 4 weeks post infection. **(D)** Representative flow plots of pulmonary CD4 and CD8 T cells profiled for expression of KLRG1 and PD-1 at 18 weeks post infection. Quantification of differentiation markers of **(E)** CD4 and **(F)** CD8 T cells derived from the lungs of *Mtb* infected mice at 18 weeks post infection. Grey circles indicate IL-4Rα$^{-/lox}$ and white circles indicate iLCK^{Cre}IL-4Rα$^{-/lox}$. Data represented as mean ± SEM of n=5-7 mice/group, and experiments were performed 2-4 times. Statistical significance was analysed by student unpaired t-test. *p<0.05, **p<0.001.

3.9 Ablation of IL-4rα on T cells is associated with an increased expression of markers associated with poorly protective Th1 T cells.

The large increases in KLRG1 expression on effector T cells in the lung indicated these cells are approaching exhaustion. We decided to further profile these T cells by looking at different markers commonly associated with protection in *Mtb* infection by comparing GMFI on CD4 and CD8 T cells in acute and chronic infection of KRLG1, PD-1, CD69 and CXCR3. In agreement with our previous data, we found higher KLRG1 expression on both CD4 and CD8 T cells across acute and chronic *Mtb* infection (Figure 14A-B). No differences in GMFI of PD-1 was observed in CD4 or CD8 T cells across infection (Figure 14C-D). CD69 is considered an early activation marker in T cells, allowing egress from secondary lymphoid tissue by limiting the expression of SIP1 [208]. A marker also associated with the ability of T cells, especially CD8 T cells, to persist in the lung [208, 209]. We observed a significant decrease in CD69 in CD4 T cells during chronic infection, while a similar decrease in CD69 was seen in CD8 T cells during acute infection (Figure 14E-F). CXCR3 is a chemokine receptor which is strongly associated with the ability of T cells to migrate from the vasculature into the lung parenchyma. It is also associated with increased protection against *Mtb* infection because the T cells are able to infiltrate into the site of disease more effectively [101, 210, 211]. We found that amount of CXCR3 is significantly decreased in CD4 T cells in the lungs iLCK^{Cre}IL-4rα$^{-/lox}$ compared to littermate controls during chronic TB. While a decrease in trend of CXCR3 on T cells in iLCK^{Cre}IL-4rα$^{-/lox}$ during acute infection (Figure 14G). No differences were observed in CXCR3 expression in CD8 T cells during acute or chronic *Mtb* infection (Figure 14H). Given our observations in populations CXCR3 and KLRG1, we sought to do further analysis on the subset of the population, to assess whether there is a relationship between higher KLRG1 and lower CXCR3 expression. To this end, we analysed the percentage of CD4 and CD8 T cells that were either KLRG1^{+}PD^{-} or KLRG1^{-}PD-1^{+}, as these populations are associated with more intravascular-like and more parenchymal-like T cells [101]. We found that while no differences in CXCR3 expression was seen between the more intravascular like (KLRG1^{+}PD-1^{-}) CD4 and CD8 T cells, however, a significant decrease in the expression of CXCR3 in parenchymal-like (KLRG1^{-}PD-1^{+}) CD4 and CD8 T cells during chronic infection (Figure 14K-L).

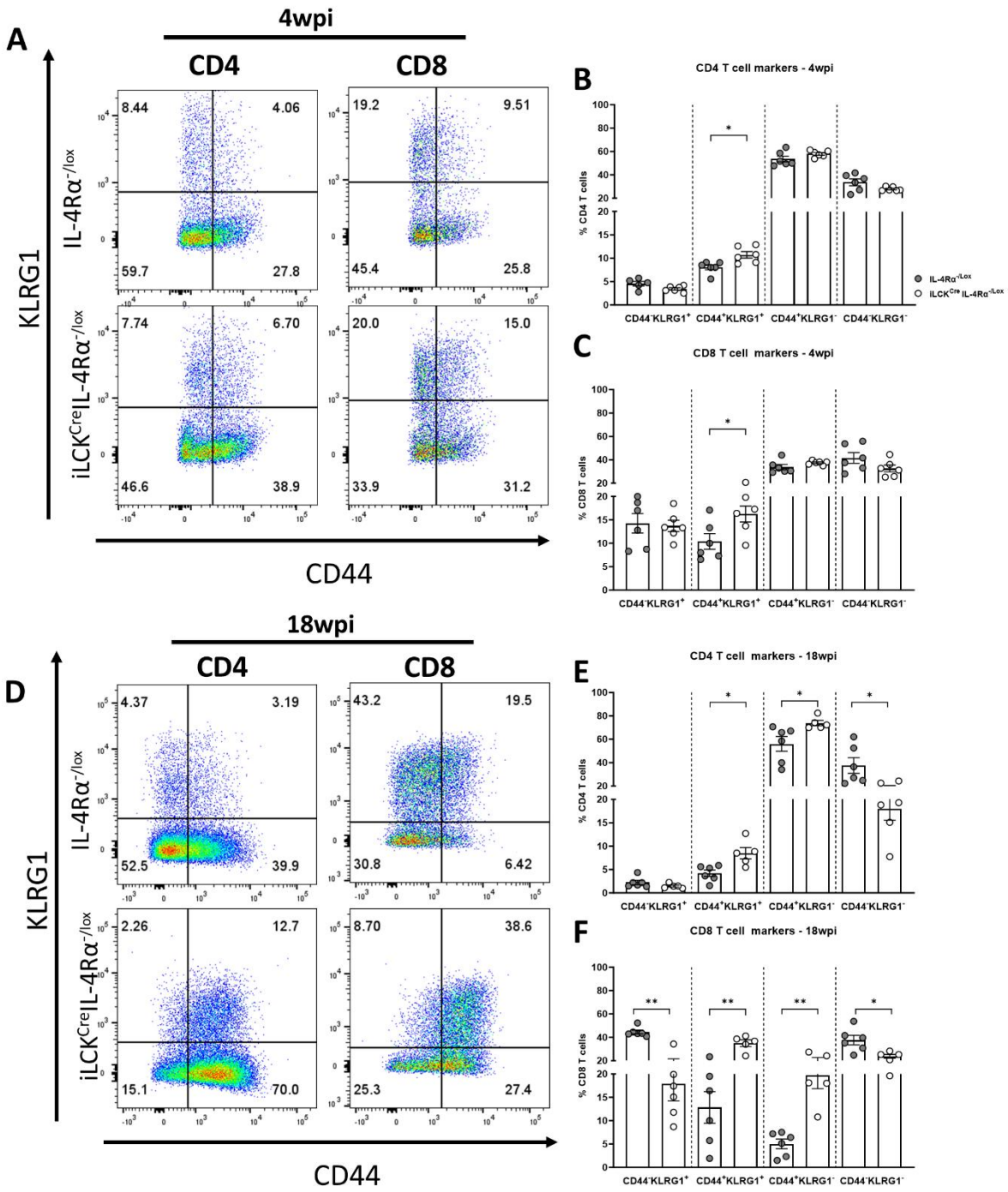

Figure 13: Deletion of IL-4Rα on T cells leads to increased amounts of short-lived antigen-specific T cells. iLCK^{Cre}IL-4Rα$^{-/lox}$ and IL-4Rα$^{-/lox}$ littermate controls were intranasally infected with 100CFU of HN878 at and euthanized at 4 and 18 weeks. **(A)** Representative flow plots of pulmonary CD4 and CD8 T cells profiled for expression of KLRG1 and CD44 at 4 weeks post infection. Quantification of activation and differentiation markers of **(B)** CD4 and **(C)** CD8 T cells derived from the lungs of *Mtb* infected mice at 4 weeks post infection. **(D)** Representative flow plots of pulmonary CD4 and CD8 T cells profiled for expression of KLRG1 and CD44 at 18 weeks post infection. Quantification of activation and differentiation markers of **(E)** CD4 and **(F)** CD8 T cells derived from the lungs of *Mtb* infected mice at 18 weeks post infection. Data represented as mean ± SEM of n=5-7 mice/group, and experiments were performed 2-4 times. Statistical significance was analysed by student unpaired t-test. *p<0.05, **p<0.001.

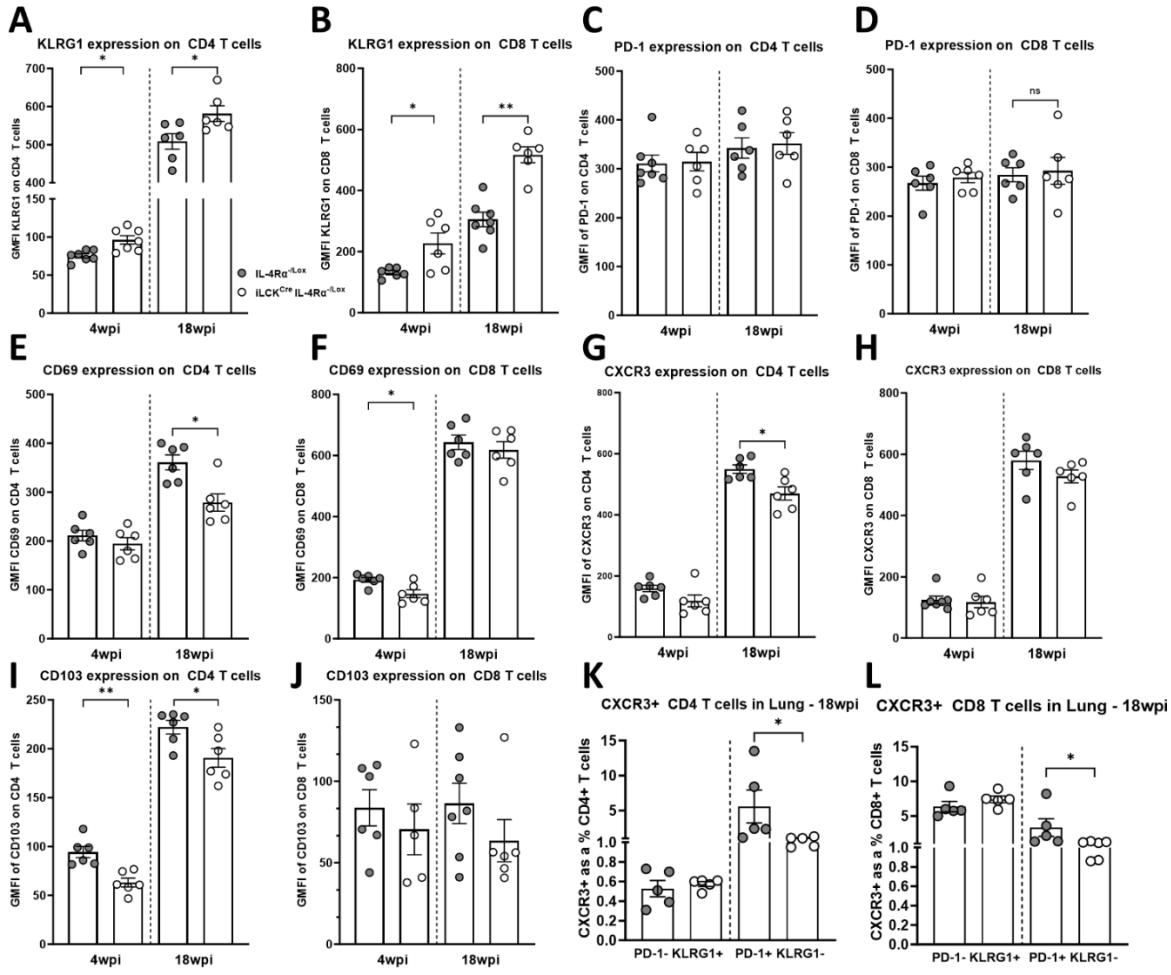

Figure 14: Deletion of IL-4Rα on T cells results in a less-protective, more intravascular phenotype of T cells. iLCK^{Cre}IL-4Rα$^{-/lox}$ and IL-4Rα$^{-/lox}$ littermate controls were intranasally infected with 100 CFU of HN878 at and euthanized at 4 and 18 weeks. **(A-J)** The GMFI of KLRG1, PD-1, CD69, CXCR3 and CD103 on CD4 and CD8 T cells derived from the lungs of infected mice is displayed for both 4 and 18 weeks post infection. The percentage of CXCR3 positive **(K)** CD4 T cells and **(L)** CD8 T cells expressing either PD-1 or KLRG1 is shown at 18 weeks post infection. Data represented as mean ± SEM of n=5-7 mice/group, and experiments were performed 2-4 times. Statistical significance was analysed by student unpaired t-test. *p<0.05, **p<0.001.

It is perhaps expected that the more intravascular like T cells will express a marker associated with entry into the lung, we were intrigued to observe that cells expressing PD-1 also show less CXCR3 expression, indicating that the T cells from iLCK^{Cre}IL-4rα$^{-/lox}$ are possibly less effective at infiltrating the parenchyma in chronic infection. The discrepancies in the numbers of CD4 and CD8 T cells found in the lung could also during acute *Mtb* infection could perhaps be explained by diminished proliferative capacity or increased T cell death. Given that we observed a substantial portion of effector T cells expressing KLRG1, as well as previous findings demonstrating that KLRG1 expression is associated with shorter life span and poor proliferative capacity [207].

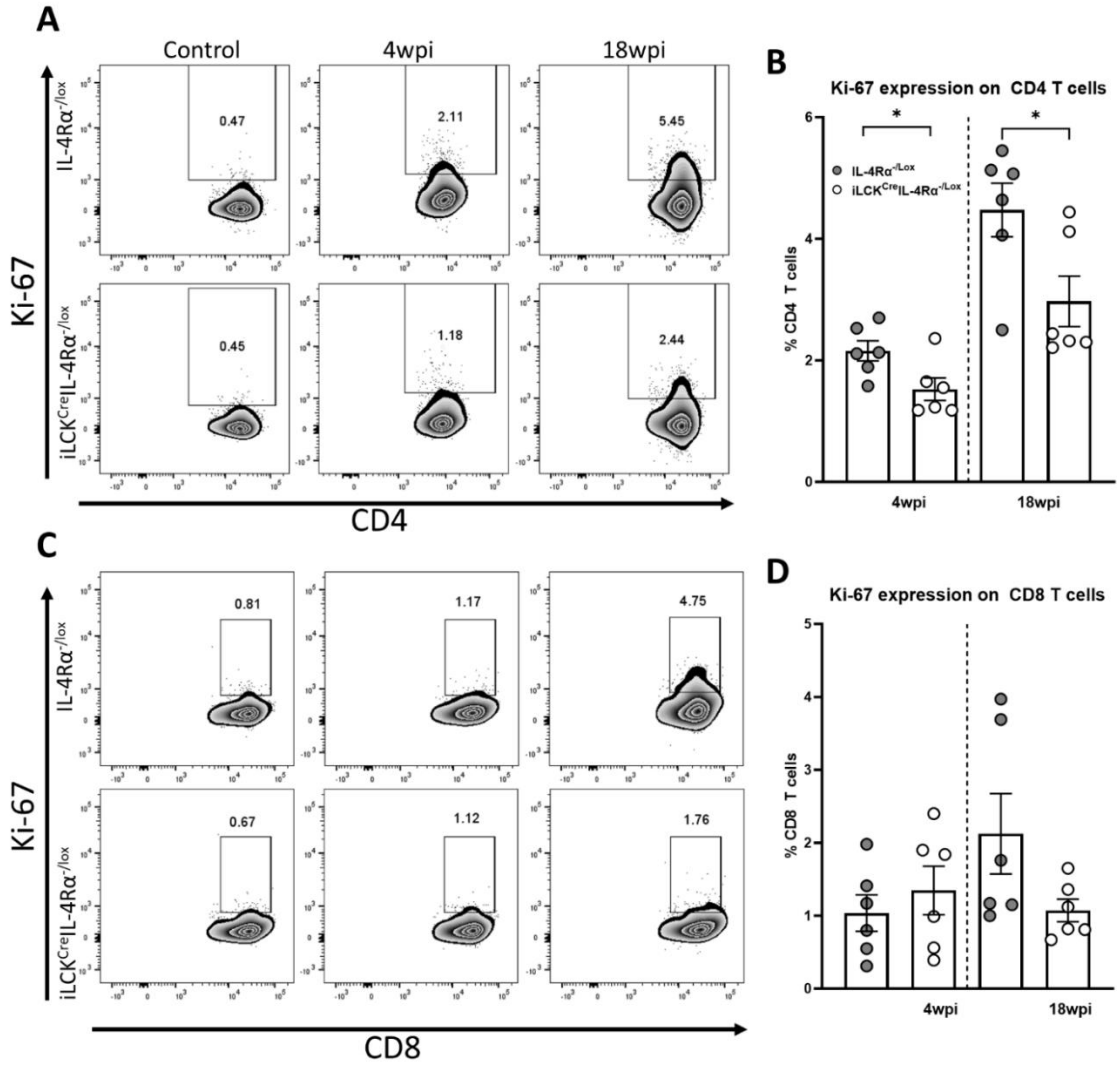

Figure 15: Absence of IL-4Rα on leads to reduced proliferation capacity on on CD4 T cells during *Mtb* infection. iLCK^{Cre}IL-4Rα$^{-/lox}$ and IL-4Rα$^{-/lox}$ littermate controls were intranasally infected with 100 CFU of HN878 at and euthanized at 4 and 18 weeks. **(A)** Representative flow plots and **(B)** quantification of Ki-67^{+}CD4 T cells at both 4- and 18-weeks post infection. **(C)** Representative flow plots and **(D)** quantification of Ki-67^{+}CD8 T cells at both 4 and 18 weeks post infection. Data represented as mean ± SEM of n=5-7 mice/group, and experiments were performed 3 times. Statistical significance was analysed by student unpaired t-test. *p<0.05, **p<0.001.

We decided to evaluate if absence of IL-4Rα could lead to variances in proliferative capacity by measuring Ki-67 expression during acute and chronic *Mtb* infection. We found at both 4wpi and 18wpi there was a decrease in Ki-67 expression in the pulmonary CD4 T cells of iLCK^{Cre}IL-4rα$^{-/lox}$ compared to IL-4rα$^{-/lox}$ (Figure 15A-B). Whereas no significant differences were observed in the CD8 T cells at either time point (Figure 15C-D). Interestingly, we found that there was an increase in Ki-67 expression between acute and chronic time points within the iLCK^{Cre}IL-4rα$^{-/lox}$ and IL-4rα$^{-/lox}$, indicating a slight expansion in *Mtb*-specific CD4 T cells found at the site of disease as the disease progresses. These same differences were only apparent in the CD8 T cells of the littermate controls, while iLCK^{Cre}IL-4rα$^{-/lox}$ CD8 T cells had

no changes in proliferative capacity between acute and chronic timepoints. These data indicate that there are fewer proliferating CD4 T cells from the lungs of infected iLCK^{Cre}IL-4rα$^{-/lox}$ compared to littermate controls.

Another way of visualising differences in flow cytometry involves making use of tSNE projections. Given our differences were mostly on CD4 T cells, we decided to analyse by tSNE. We concatenated groups from a representative experiment performed during acute infection. This type of analysis shows that differences in iLCK^{Cre}IL-4rα$^{-/lox}$ and IL-4rα$^{-/lox}$ comprises variations in rather small population subsets as indicated by minor features allowing populations to be distinguished (Figure 16A). It allows for quantitative differences that we have described thus far, such as differences in percentages of expressing cells or GMFI to be visualized in relation to the entire population, and largely agrees with the data we have already reported. FlowSOM analysis allowed us to cluster different groups within the tSNE (Figure 16B). The approach also enabled us to quantify the amount of CD4 T cells from iLCK^{Cre}IL-4rα$^{-/lox}$ and IL-4rα$^{-/lox}$ present in each cluster (Figure 16C). The tSNE and FlowSOM analysis demonstrated that cluster 5 was made up majorly of iLCK^{Cre}IL-4rα$^{-/lox}$ CD4 T cells and was enriched with KLRG1. However, clusters 3 and 4, which represent an increased expression of CD103 showed no differences. This is in contrast to comparing GMFI, where CD103 expression was found to be significantly decreased in the iLCK^{Cre}IL-4rα$^{-/lox}$ CD4 T cells, and perhaps demonstrates one of the limitations of the tSNE approach. We performed the same analysis from a representative experiment performed during chronic infection (Figure 17A-C). Once again, the cluster that represented high levels of KLRG1 expression, cluster 5, was made of a significant portion of IL-4Rα deficient CD4 T cells. Other interesting observations, included decreased amounts of iLCK^{Cre}IL-4rα$^{-/lox}$ T cells in cluster 4, which represented increased expression of CXCR3 and PD-1. As well as significant enrichment of iLCK^{Cre}IL-4rα$^{-/lox}$ T cells in cluster 1, which represents low expression of PD-1, CXCR3, CD103 and higher expression of CD127 and KLRG1.

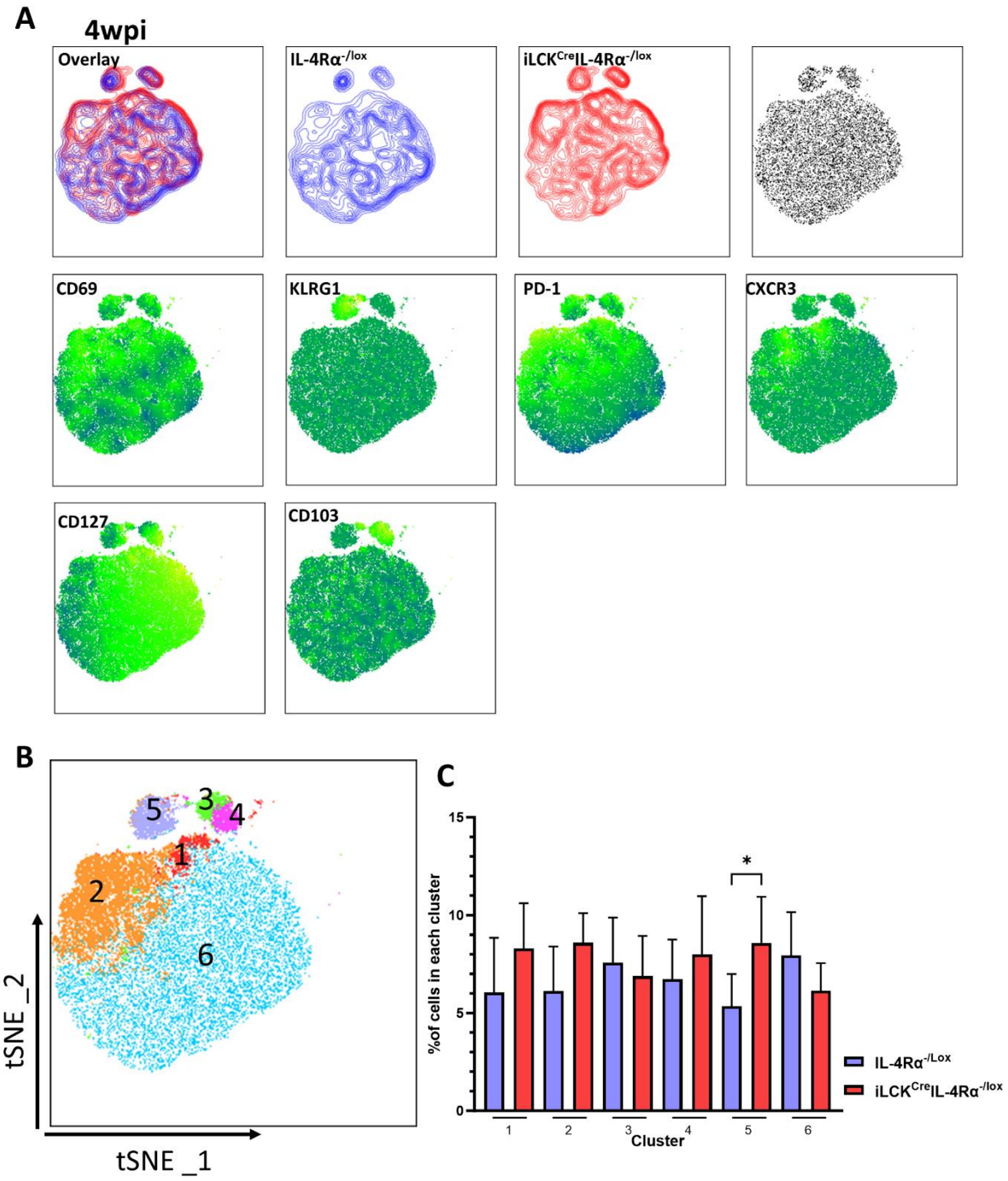

Figure 16: Phenotypic changes in CD4 T cells in the lungs of iLCK^{Cre}IL-4Rα$^{-/lox}$ mice during acute *Mtb* infection represent small variations in proportion to the whole population. iLCK^{Cre}IL-4Rα$^{-/lox}$ and IL-4Rα$^{-/lox}$ littermate controls were intranasally infected with 100 CFU of HN878 at and euthanized at 4 weeks. Single cell suspensions were analysed by flow cytometry and the CD4 population was used for t-SNE projection and FlowSOM clustering. **(A)** iLCK^{Cre}IL-4rα$^{-/lox}$ (red) and IL-4rα$^{-/lox}$(blue) were overlayed with heat-map showing expression of indicated markers. **(B-C)** Six clusters were identified using FlowSOM and the percentage of iLCK^{Cre}IL-4Rα$^{-/lox}$ and IL-4Rα$^{-/lox}$ in each cluster was quantified. Data represented as mean ± SEM of 6 mice/group. Representative data of two experiments. Statistical significance was analysed by student unpaired t-test. *p<0.05

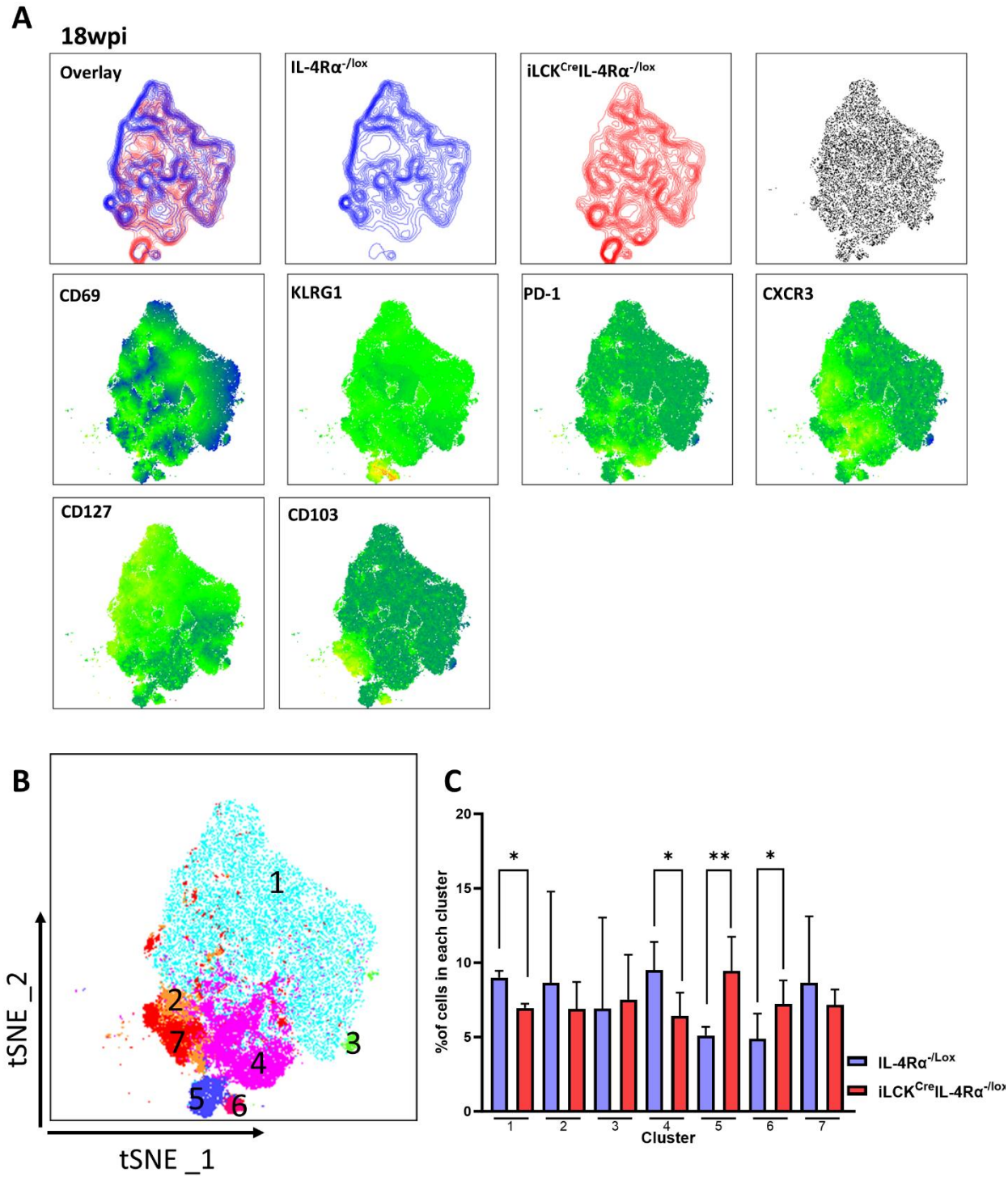

Figure 17: Phenotypic changes in CD4 T cells in the lungs of iLCK^{Cre}IL-4Rα$^{-/lox}$ mice during chronic *Mtb* infection represent small variations in proportion to the whole population. iLCK^{Cre}IL-4Rα$^{-/lox}$ and IL-4Rα$^{-/lox}$ littermate controls were intranasally infected with 100 CFU of HN878 at and euthanized at 18 weeks. Single cell suspensions were analysed by flow cytometry and the CD4 population was used for t-SNE projection and FlowSOM clustering. (A) iLCK^{Cre}IL-4rα$^{-/lox}$ (red) and IL-4rα$^{-/lox}$(blue) were overlayed with heat-map showing expression of indicated markers. (B-C) Six clusters were identified using FlowSOM and the percentage of iLCK^{Cre}IL-4Rα$^{-/lox}$ and IL-4Rα$^{-/lox}$ in each cluster was quantified. Data represented as mean ± SEM of 6 mice/group. Representative data of two experiments. Statistical significance was analysed by unpaired t-test. *p<0.05, **p<0.001.

Moreover, this projection allows us to see the CD4 T cells that express PD-1, CXCR3 and CD69 are clustered in similar population during acute infection. Indicating that these cells are co-expressing these markers (Figure 17A). During chronic infection, there is partial overlap of CXCR3 with PD-1 and CD69 (Figure 17A). These clusters of cells co-expressing these makers likely represent a distinct phenotype. Differences in the proportions of cells co-expressing these markers possibly indicates that this phenotype changes over time.

3.10 The iLCK^{Cre}IL-4rα$^{-/lox}$ mice show minor differences in lung cytokines during *Mtb* infection

The higher proportions of effector pulmonary T cells, and increased expression of terminal differentiation in the iLCK^{Cre}IL-4rα$^{-/lox}$ suggests increased *Mtb*-specific T cells, including heightened inflammatory cytokine responses. To better understand increased percentages of effector responses correlates with decreased survival and increased bacterial burden we performed ELISA using lung homogenates to assess if there are differences in cytokines levels during acute and chronic *Mtb* infection. Despite increased T-bet expression, we found no differences in Th1 associated proinflammatory cytokines, such as IFN-β, IFN-γ, IL-6, IL-12p40, IL-12p70, IL-1α and IL-1β across acute and chronic TB (Figure 18A-B). As expected, the loss of IL-4Rα did not result in major differences in IL-4 and IL-13 production in the lungs. Indicating that *Mtb* infection is a poor driver of Th2 responses, in line with previous findings [62, 207]. Similarly, no differences were observed in IL-10, and TGFβ at either acute or chronic infection, indicating that there is no significant suppressive effect in the absence of IL-4Rα (Figure 18C-D). However, a significant increase was observed in IL-17 production in iLCK^{Cre}IL-4rα$^{-/lox}$ lung homogenates during chronic *Mtb* infection, possibly accounting for increased neutrophilia and loss of alveolar space. This is in line with our observation of increased frequencies of Th17 (RORγt^{+}) CD4 T cells in the lung in iLCK^{Cre}IL-4rα$^{-/lox}$. However, no differences in IL-23 or IL-2 were observed at acute or chronic infections (Figure 18C-D). During chronic infection, the relative decreased CXCL1 and CCL2 remains, but the mean differences in CCL5 are lost. These chemokines are implicated in neutrophil as well as permissive phagocyte recruitment to the lung [212, 213]. This is partly in agreement with the flow myeloid data, in which we demonstrated increased neutrophilia during chronic *Mtb* infection. Additionally, we found reduced GM-CSF in lungs of iLCK^{Cre}IL-4rα$^{-/lox}$ during acute infection, but not in chronic *Mtb* infection (Figure 18E-F). Other chemokines CCL3 and CCL6 were remained unaffected, which also participate in neutrophil recruitment during *Mtb* infection in the lung. Lastly, we also performed the Greiss assay to assess levels of nitrite, allowing us to infer the production of reactive nitrogen species in the lung. We revealed

decreased levels of nitrite in the lungs of iLCK^{Cre}IL-4rα$^{-/lox}$ during acute infection, whereas significantly higher nitrite levels were observed in chronic stage indicating that lungs were more inflamed than littermate controls, a finding corroborated our iNOS analysis by immunohistochemistry (Figure 18G-H).

3.11 Increased *Mtb*-specific T cells in iLCK^{Cre}IL-4rα$^{-/lox}$ is associated with heightened cytokine responses.

We then sought to better understand the cytokine responses from iLCK^{Cre}IL-4rα$^{-/lox}$ and IL-4rα$^{-/lox}$ pulmonary T cells stimulated *ex vivo* with Mtb300. This is a peptide megapool consisting of 300 peptides which are derived of the most immunodominant antigenic sites in *Mtb* as defined by healthy IGRA+ patients [179, 180]. The benefit of using a peptide megapool is for *ex vivo* T cell stimulation is that it by-passes the need for antigen processing and presentation by MHC to TCR. We measured *Mtb*-specific responses by assessing CD44^{+} as an activation marker, versus either IL-2, IFN-γ or TNF. These cytokines have been shown to help promote protection against TB, and CD4 T cells that produce all three constitute a major target for TB vaccine design strategies. During acute infection, we found that there significantly elevated *Mtb*-specific CD4 T cell responses as demonstrated by heightened TNF and IFN-γ responses to the Mtb300 peptide megapool, while IL-2 remained unchanged (Figure 19A-B). The representative flow plots show fewer CD4 T cells, despite proportionately higher effector responses in the IL-4Rα knockout. Interestingly, no differences in CD8 T cells derived from the lungs of mice during acute infection (Figure 19C).

Ex vivo stimulation of T cells derived from mice that are chronically infected with *Mtb* revealed a similar trend as in acute infection. Representative flow plots demonstrate increased secretion of TNF and IFN-γ by the effector CD4 T cells of iLCK^{Cre}IL-4rα$^{-/lox}$ compared to controls in response to Mtb300 stimulation (Figure 19D-E). Whereas IL-2 levels remained similar between iLCK^{Cre}IL-4rα$^{-/lox}$ and IL-4rα$^{-/lox}$ (Figure 19D-E). An interesting observation seeing as IL-2 helps maintain and expand T cell proliferation, while we observed reduced Ki-67 expression. This Indicates that reduced proliferation capacity is not as a result of diminished IL-2 production. Another similarity that was observed between *ex vivo* stimulation of acute and chronically stimulated T cells is that there were no differences in the ability of CD44^{+} CD8 T cells to secrete TNF, IFN-γ and IL-2 (Figure 19F). Indicating that despite the lower numbers of CD8 T cells recruited to the lung, their ability to produce cytokine is not affected. This in turn might possibly suggest that the ability of CD4 T cells to "help" CD8 T cells to become effector cells is not hampered by the absence of IL-4Rα.

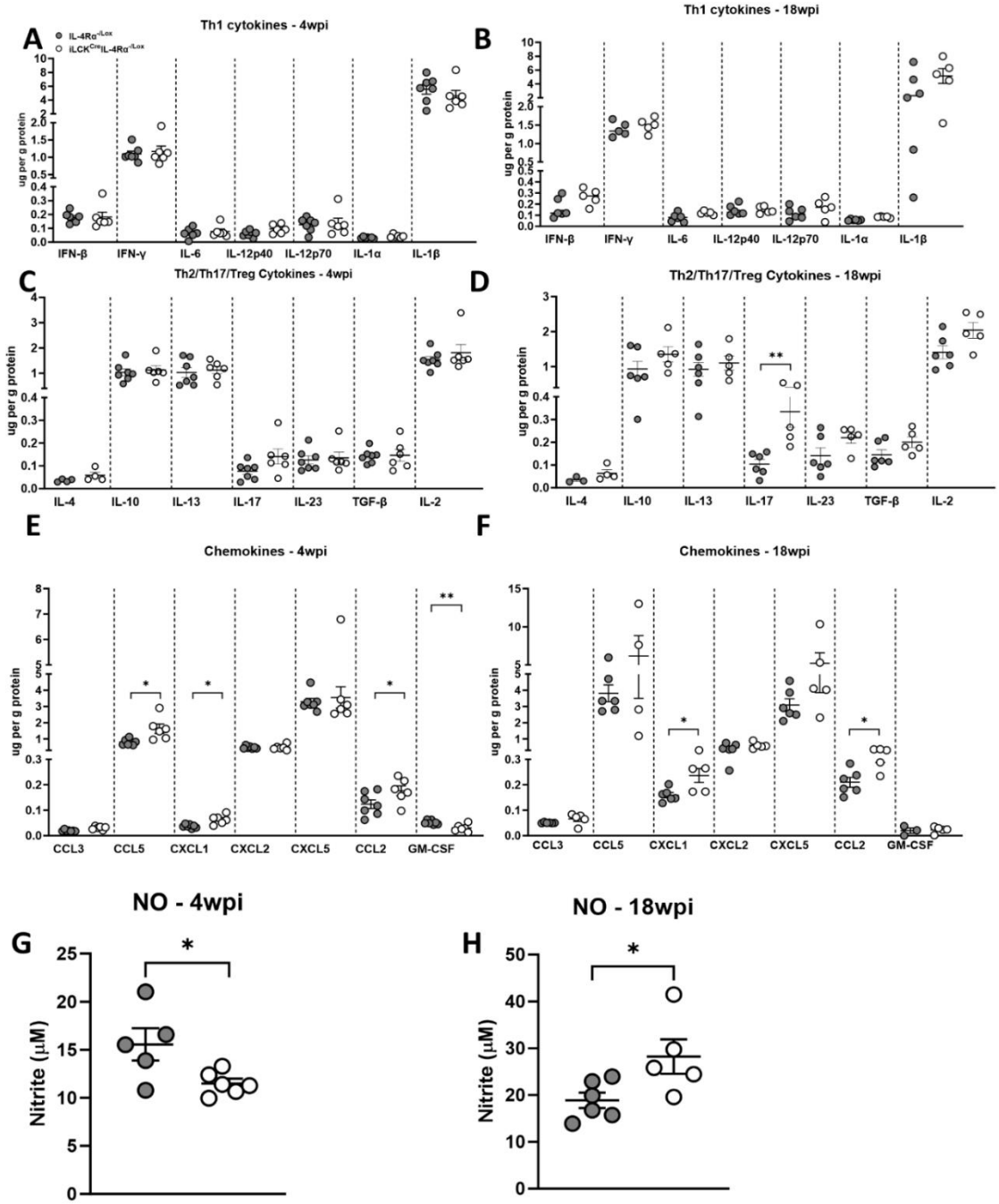

Figure 18: Cytokine and chemokine production in response to *Mtb* infection remains largely the same in the lungs of iLCK^{Cre}IL-4rα$^{-/lox}$ mice. ELISAs performed on the lung homogenate of iLCK^{Cre}IL-4Rα$^{-/lox}$ and IL-4Rα$^{-/lox}$ at either 4 weeks or 18 weeks after intranasal infection with 100CFU of HN878 in order to detect cytokines or chemokines. Th1 cytokines at 4- and 18-weeks post infection **(A-B)**. Th2/Th17/Treg cytokines for 4- and 18-weeks post infection **(C-D)**. Chemokines at 4- and 18-weeks post infection **(E-F)**. Greiss-assay was performed on the lung homogenates of mice euthanised at either **(G-H)** 4 or 18 weeks post infection. Th1 cytokines (IFNβ, IFNγ, IL-6, IL-12p40, IL-12p70, IL-1α and IL-1β). Th2/Th17/Treg (IL-4, IL-10, IL-13, IL-17, IL-23, TGF-β, IL-2). Chemokines (CCL3, CCL5, CXCL1, CXCL2, CXCL5, CCL2, GM-CSF). Data represented as mean ± SEM of n=5-7

mice/group, and experiments were performed 4 times. Statistical significance was analysed by student unpaired t-test. *p<0.05, **p<0.001.

On the other hand, an increased proportion of short-lived effector cells could be an indication that CD8 cells are receiving less "help" from CD4 T cells as they are tending towards exhaustion. To test whether the removal of IL-4Rα an impact on the ability of T cells derived from extra-pulmonary tissue to produce cytokines, we sourced T cells from both the blood and spleen of chronically infected mice. This would tell us if the differences in cytokine production is due to presence of antigen or lack of the IL-4Rα. *Ex* vivo stimulation of whole blood and single cell suspensions of the spleen was performed using Mtb300 as above. We show that numbers of CD4 T cells circulating in the blood or spleen of iLCK^{Cre}IL-4rα$^{-/lox}$ was similar to IL-4rα$^{-/lox}$ (Figure 20A-B). While there the population of CD8 T cells was only affected in the spleen and not the blood, where we found a significant decrease in total CD8 T cells (Figure 20A-B). We also show that that there was no differences in splenic or circulating T cells to produce IFN-γ, IL-17, or IL-2 in response to *ex vivo* stimulation (Figure 20C-D). This suggests that the increased CD4 T cell effector response in the lung is likely due to a combination of an increased Th1 response, as well as antigen load, as the lung would be primary site of disease.

3.12 Increased cytokine production in iLCK^{Cre}IL-4rα$^{-/lox}$ is monofunctional, and represents a poorly protective phenotype

Darrah et al. demonstrated that reduced bacterial burden in *Mtb* infected mice after protective *Mycobacterium bovis* bacillus Calmette-Guerin (BCG) vaccination was correlated with CD4 T cells producing IFN-γ, TNF and IL-2 [214]. These polyfunctional CD4 T cells, as well as CD4 T cells producing IFN-γ and TNF, was highly correlated with increased protection. We observed an increase IFN-γ and TNF but not a corresponding IL-2, warranted whether the IL-4Rα-deficient T cells are polyfunctional in iLCK^{Cre}IL-4rα$^{-/lox}$ mice. Given no differences in CD8 T cells, we performed our analysis on CD4 T cells during acute and chronic *Mtb* infection. *Ex vivo* stimulation of CD4 T cells derived from the lungs of mice during acute *Mtb* infection revealed no differences in the percentage of mono-, bi- or polyfunctionality (Figure 21 A-B). Despite the appearance of larger production of cytokines produced by CD44^{+} CD4 T cells in our previous analysis making use of the same dataset (Figure 19). Thus, demonstrating the importance of extracting polyfunctional data from intracellular cytokine staining experiments. The lack of differences are especially important to note that they are derived from a smaller pool of total CD4 T cells in iLCK^{Cre}IL-4rα$^{-/lox}$ in *Mtb* infection.

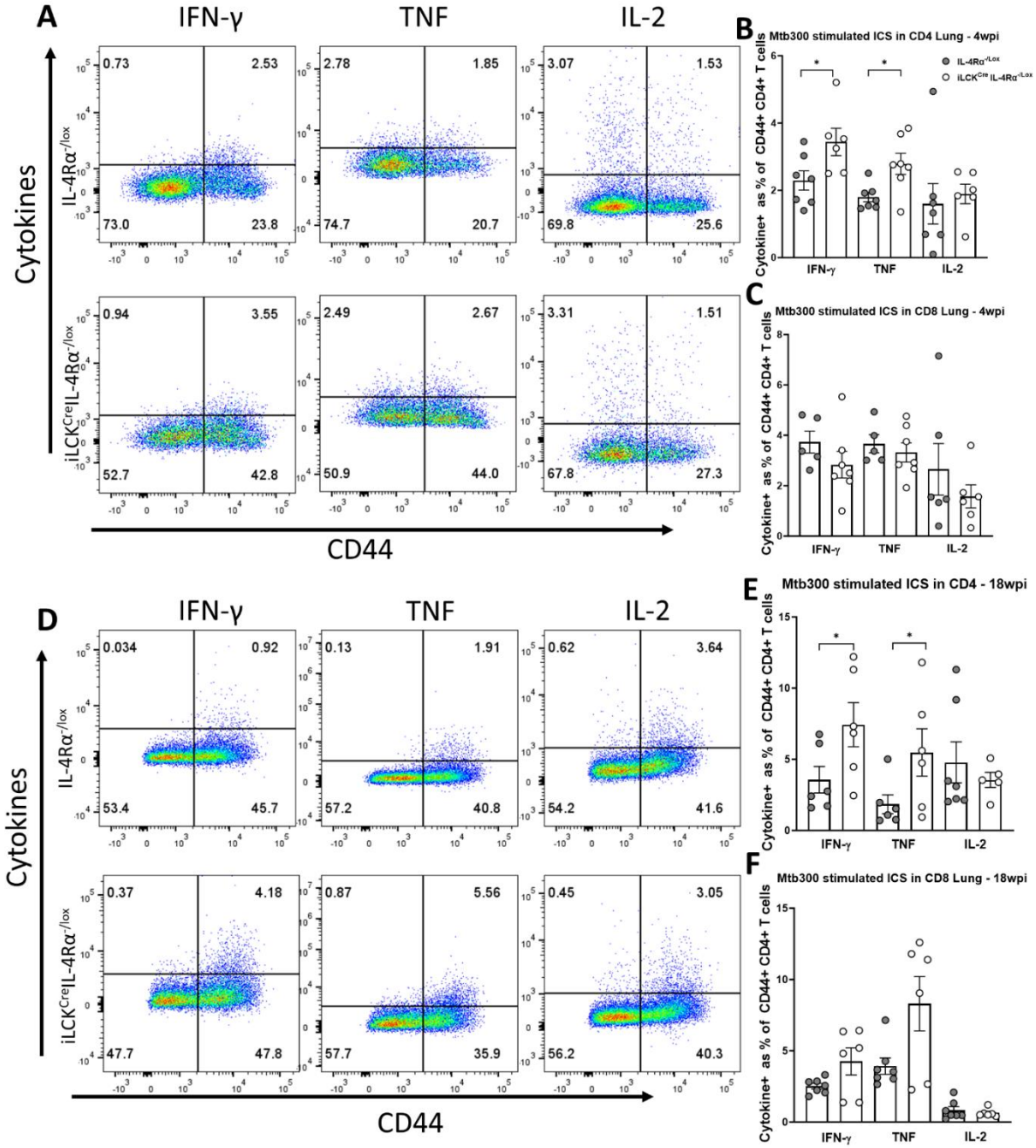

Figure 19: Abrogation of IL-4Rα on lung derived T cells leads heightened production of IFN-γ and TNF after *ex vivo* stimulation. iLCK^{Cre}IL-4Rα$^{-/lox}$ and IL-4Rα$^{-/lox}$ littermate controls were intranasally infected with 100 CFU of HN878 at and euthanized at 4 and 18 weeks. Single cell suspensions were stimulated with the peptide pool, Mtb300 for 5 hours before addition of Golgiplug for another 5 hours. **(A)** Representative flow plots of pulmonary CD44^{+} effector CD4 and CD8 T cells expressing IFN-γ, TNF and IL-2 at 4 weeks post infection. Quantification of cytokine production by **(B)** CD4 and **(C)** CD8 T cells derived from the lungs of *Mtb* infected mice at 4 weeks post infection. **(D)** Representative flow plots of pulmonary CD44^{+} effector CD4 and CD8 T cells expressing IFNγ, TNF and IL-2 at 18 weeks post infection. Quantification of cytokine production by **(E)** CD4 and **(F)** CD8 T cells derived from the lungs of *Mtb* infected mice at 18 weeks post infection. Data represented as mean ± SEM of n=5-7 mice/group, and experiments were performed 3-4 times. Statistical significance was analysed by student unpaired t-test. *p<0.05, **p<0.001.

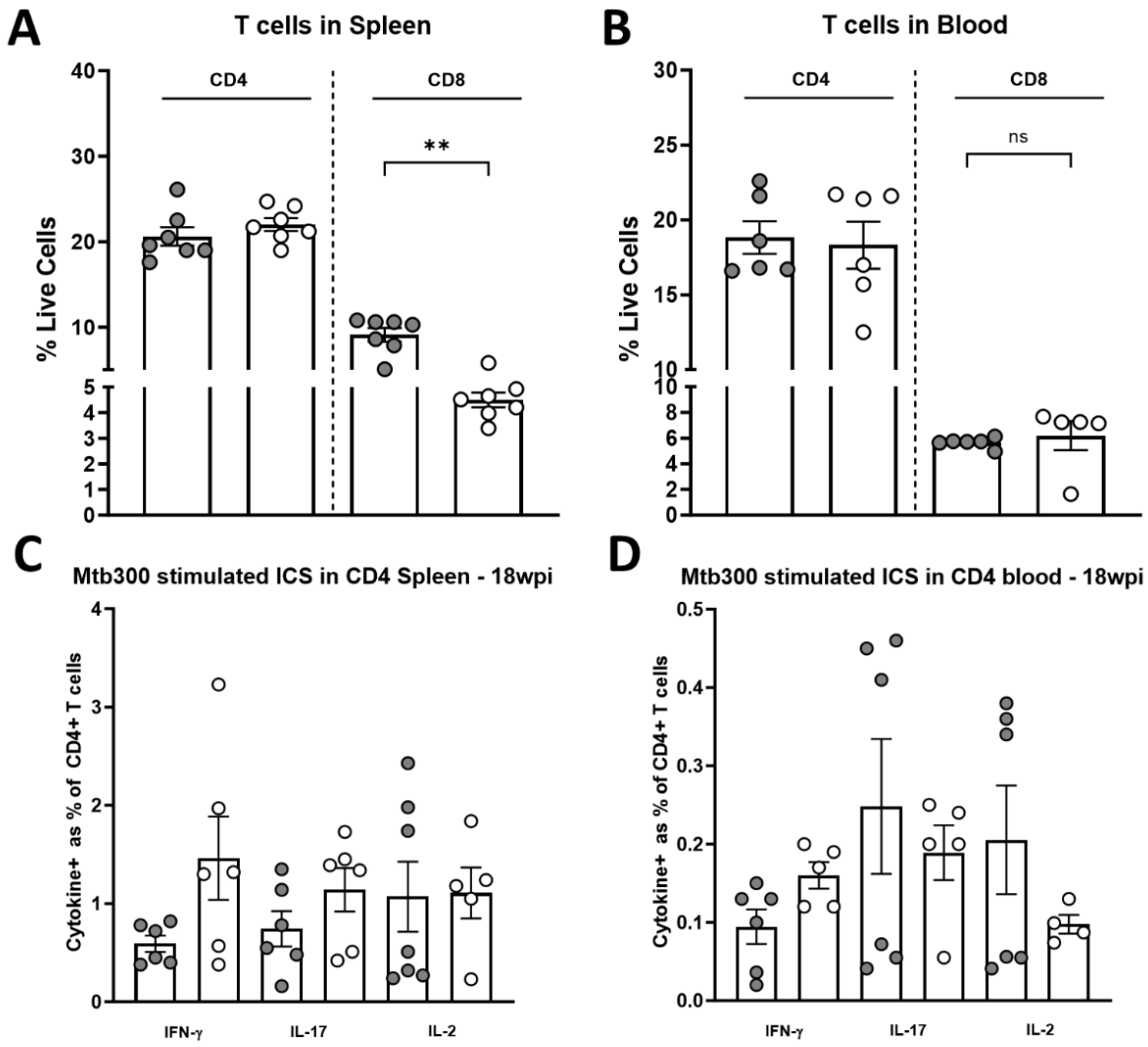

Figure 20: Absence of IL-4Rα on peripheral T cells results in no differences in cytokine production during *Mtb* infection. iLCK^{Cre}IL-4Rα$^{-/lox}$ and IL-4Rα$^{-/lox}$ littermate controls were intranasally infected with 100 CFU of HN878 at and euthanized at 18 weeks. Single cell suspensions were stimulated with the peptide pool, Mtb300 for 5 hours before addition of Golgiplug for another 5 hours. Percentages of live of CD4 and CD8 T cells in the **(A)** spleen and **(B)** blood of iLCK^{Cre}IL-4Rα$^{-/lox}$ and IL-4Rα$^{-/lox}$ during chronic *Mtb* infection. Quantification of intracellular cytokine staining of CD4 T cells in the **(C)** spleen and **(D)** blood of mice during chronic *Mtb* infection. Data represented as mean ± SEM of n=5-7 mice/group, and experiments were performed 3-4 times. Statistical significance was analysed by student unpaired t-test. *p<0.05, **p<0.001.

During chronic *Mtb* infection we observed increased percentages of CD4 T cells producing increased IFN-γ and TNF both, as well as IFN-γ alone in iLCK^{Cre}IL-4rα$^{-/lox}$ (Figure 22A-B). This means the expanded percentages of cytokine producing CD4 effectors (Figure 19)

represent largely a mono- and bi-functional populations. Monofunctional CD4 T cells in *Mtb* disease are a poor correlate of protection and might partially explain why increased cytokine production is present in the population more susceptible to *Mtb* infection.

The Increased population of cytokine producing effector CD4 T cells prompted us to expand our intracellular cytokine staining panel to include IL-4, and IL-17. Additionally, we included a step in which we enrich the T cell population using negative selection magnetic beads (Biolegend). Single cell suspensions were prepared from the of lungs of chronically infected iLCK^{Cre}IL-4rα$^{-/lox}$ and IL-4rα$^{-/lox}$ mice (12wpi) and stimulated *ex vivo* with *Mtb* lysate. In our experience *Mtb* lysate is better at inducing Th17 responses than peptide stimulation. Th removal of undesired cell populations through the use of magnetic beads have the added benefit of reducing the background in our analysis. IL-4Rα-deficient pulmonary CD4 T cells were found to have increased percentages of IFN-γ, IL-17 and TNF (Figure 23A-D). The increased levels of IL-17 corroborates with the ELISA of lung homogenate. No differences were observed in IL-2, while decreased IL-4 secretion was observed in iLCK^{Cre}IL-4rα$^{-/lox}$. While IL-4 levels are considerably lower compared to other cytokines, one must bear in mind that that IL-4 is not typically produced by T cell in response to recognizing *Mtb* antigen. Especially, seeing as the T cell response in TB is largely considered to primarily comprise of Th1 and Th17 effectors [215]. That being said, the lower levels of IL-4 in IL-4Rα-deficient T cells although statistically significant are likely not biologically significant to have an effect on the outcome of disease. Boolean gating revealed that the CD4 T cells of iLCK^{Cre}IL-4rα$^{-/lox}$ consist of substantial portions of monofunctional IL-17 and IFN-γ effectors (Figure 23G). While no differences were seen polyfunctional, or other cytokine producing subsets. We performed the same analysis on CD8 T cells and found heightened production of IFN-γ and TNF, while no differences were observed in IL-17 production in iLCK^{Cre}IL-4rα$^{-/lox}$ mice (Figure 24A-D). Additionally, we also observed decreased IL-2 and IL-4 production in IL-4Rα deficient CD8 T cells (Figure 24E-F). Moreover, the cytokine producing CD8 T cells comprised largely of a monofunctional IFN-γ producing subset. These data are indicative that increased effector response seen in iLCK^{Cre}IL-4rα$^{-/lox}$ consists of a large portion of monofunctional production of either IFN-γ, TNF or IL-17 during chronic infection, which is considered to be poorly protective against *Mtb* infection.

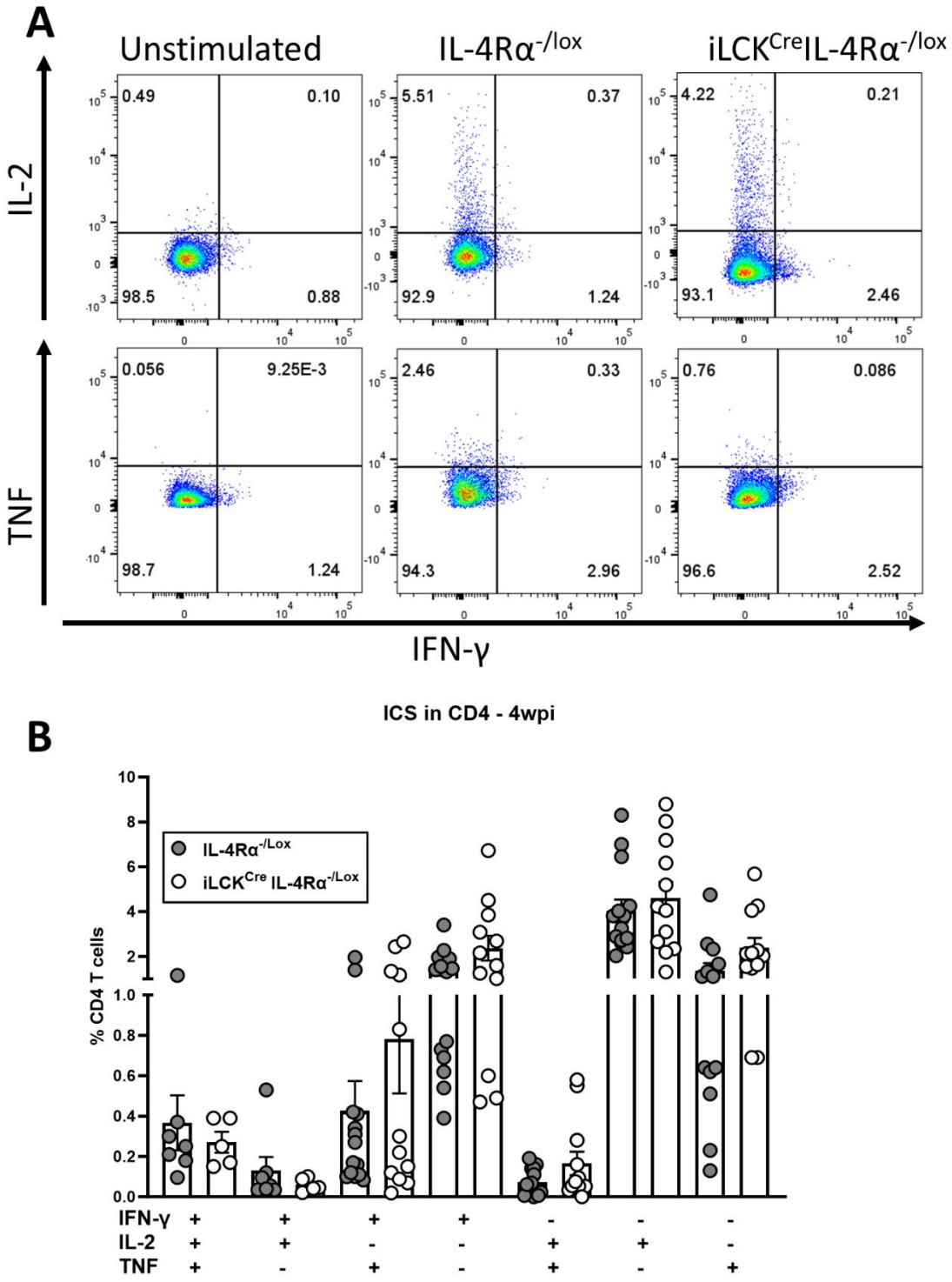

Figure 21: No differences in polyfunctional profiles of T cells in the lungs of iLCK^{Cre}IL-4rα$^{-/lox}$ mice during acute infection. iLCK^{Cre}IL-4Rα$^{-/lox}$ and IL-4Rα$^{-/lox}$ littermate controls were intranasally infected with 100 CFU of HN878 at and euthanized at 4. Single cell suspensions were stimulated with the peptide pool, Mtb300 for 5hours before addition of Golgiplug for another 5 hours. (A) Representative flow plots showcasing cytokine production of CD4 T cells derived from infected lungs after 4 weeks and stimulated ex vivo. (B) Quantification of mono-, bi- and polyfunctional CD4 T cells after 4 weeks of *Mtb* infection.

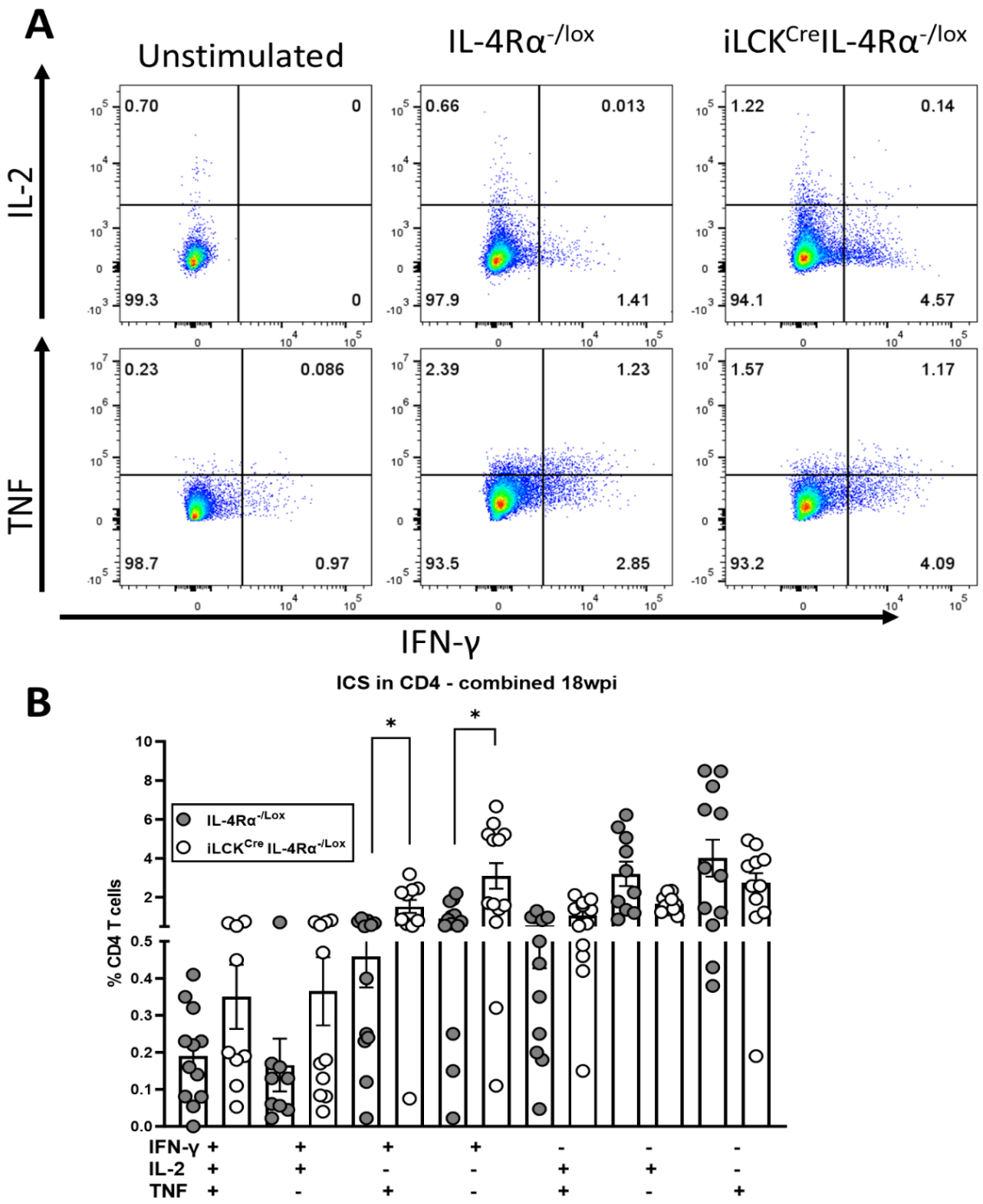

Figure 22: Increases in cytokine producing T cells in the lungs of iLCK^{Cre}IL-4rα$^{-/lox}$ mice chronic infection are largely monofunctional. iLCK^{Cre}IL-4Rα$^{-/lox}$ and IL-4Rα$^{-/lox}$ littermate controls were intranasally infected with 100 CFU of HN878 at and euthanized at 18 weeks. Single cell suspensions were stimulated with the peptide pool, Mtb300 for 5hours before addition of Golgiplug for another 5 hours. **(A)** Representative flow plots showcasing cytokine production of CD4 T cells derived from infected lungs after 18 weeks and stimulated ex vivo. **(B)** Quantification of mono-, bi- and polyfunctional CD4 T cells after 18 weeks of *Mtb* infection. Data represented as mean ± SEM of n=5-7 mice/group, and experiments were performed 2-4 times. Statistical significance was analysed by student unpaired t-test. *p<0.05, **p<0.001.

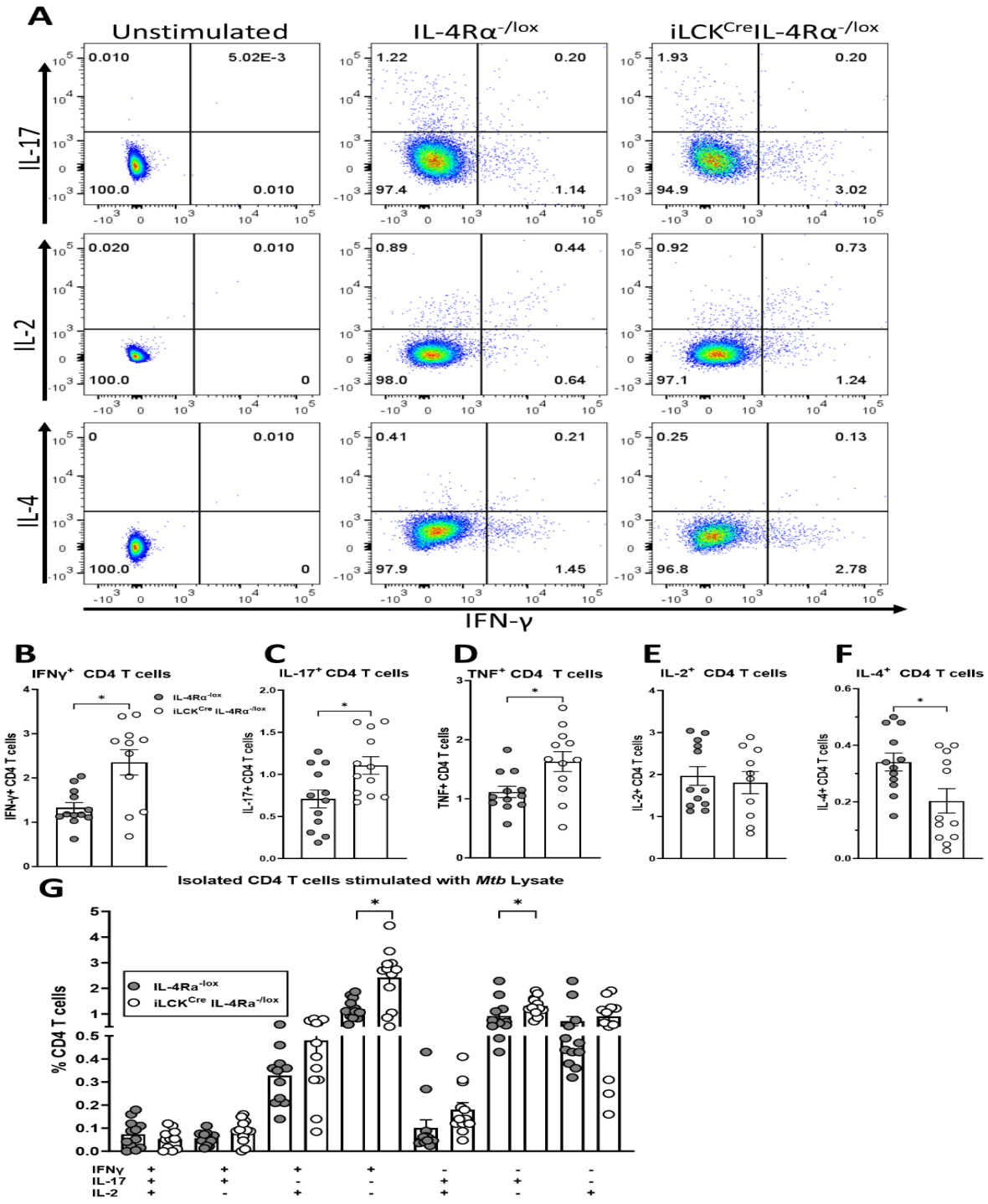

Figure 23: CD4 T cells in iLCK^{Cre}IL-4Rα$^{-/lox}$ mice exhibit increased production of IFN-γ and IL-17 after 12 weeks infection. iLCK^{Cre}IL-4Rα$^{-/lox}$ and IL-4Rα$^{-/lox}$ littermate controls were intranasally infected with 100CFU of HN878 and euthanized at 12 weeks post infection. Single cell suspensions prepared from the infected lungs of these mice was stimulated for 5 hours with *Mtb* lysate before adding Golgi plug for another 5 hours. A T cell enriched population was generated using negative CD3 magnetic isolation (Miltenyi). **(A-F)** Intracellular cytokine staining was performed to reveal amounts of IFN-γ,IL-17, TNF, IL-2 and IL-4 produced by isolated T cells after ex vivo stimulation. **(G)** Boolean gating of cytokine positive CD4 T cells used to show extent of mono-, bi- and polyfunctional CD4 T cells. Data represented as mean ± SEM of n=12 mice/group. Statistical significance was analysed by student unpaired t-test *p<0.05.

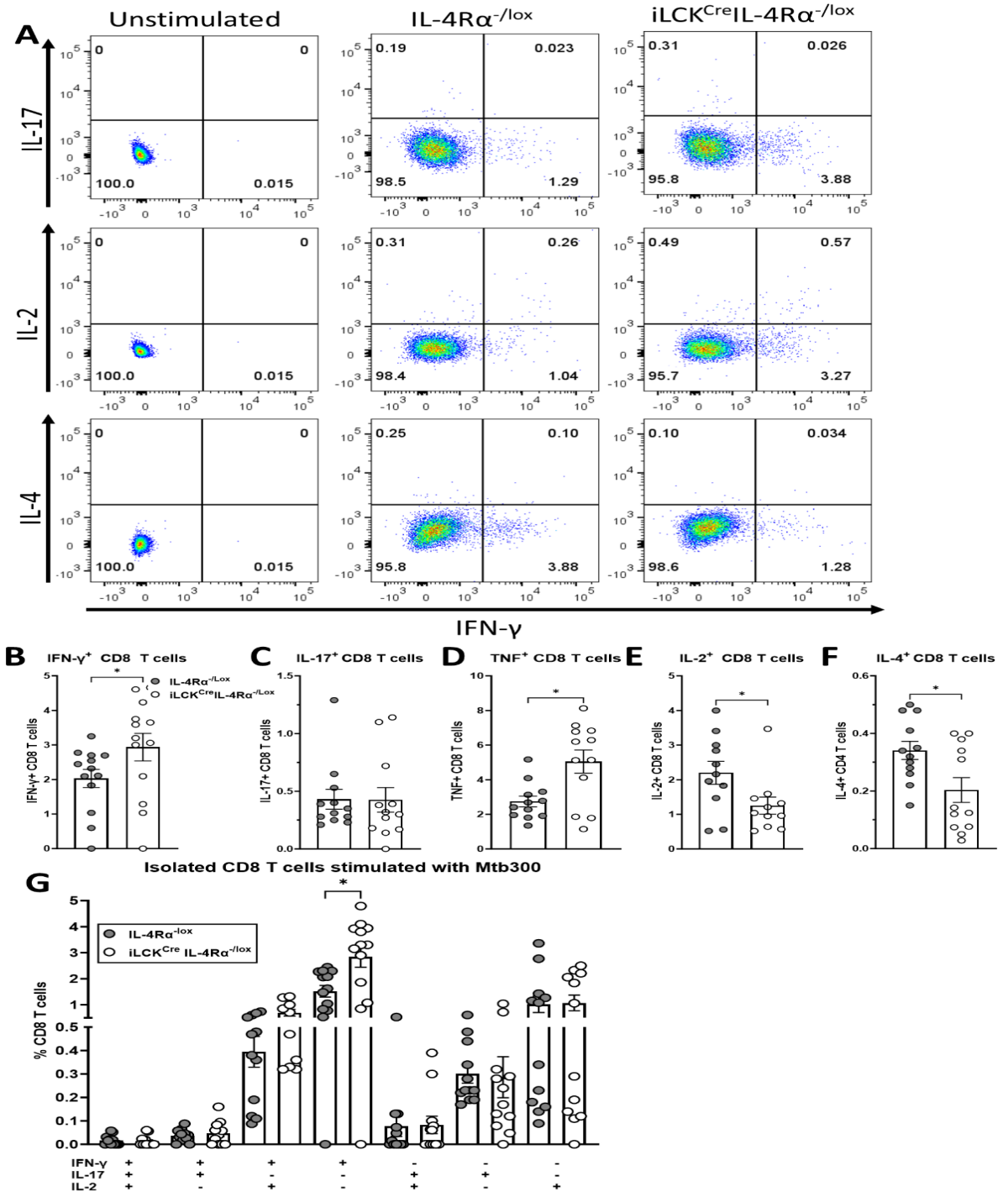

Figure 24: CD8 T cells in iLCK^{Cre}IL-4rα$^{-/lox}$ mice exhibit increased production of IFN-γ after 12 weeks infection. iLCK^{Cre}IL-4Rα$^{-/lox}$ and IL-4Rα$^{-/lox}$ littermate controls were intranasally infected with 100CFU of HN878 at and euthanized at 12 weeks post infection. Single cell suspensions prepared from the infected lungs of these mice was stimulated for 5 hours with *Mtb* lysate before adding Golgi plug for another 5 hours. A T cell enriched population was generated using negative CD3 magnetic isolation (Miltenyi). **(A-F)** Intracellular cytokine staining was performed to reveal amounts of IFNγ, IL-17, TNF, IL-2 and IL-4 produced by isolated T cells after ex vivo stimulation. **(G)** Boolean gating of cytokine positive CD8 T cells used to show extent of mono-, bi- and polyfunctional CD8 T cells. Grey circles indicate IL-4Rα$^{-/lox}$ and white circles indicate iLCK^{Cre}IL-4Rα$^{-/lox}$. Data represented as mean ± SEM of n=12 mice/group. Statistical significance was analysed by student unpaired t-test. *p<0.05

3.13 Absence of IL-4Rα on T cells does not affect ability to control *Mtb* growth *in vitro*

In effort to gain insight into the functional aspects of the increased susceptibility of iLCK^{Cre}IL-4rα$^{-/lox}$ to *Mtb* infection, we cultured pulmonary T cells from iLCK^{Cre}IL-4rα$^{-/lox}$ and IL-4rα$^{-/lox}$ with either *Mtb* infected or uninfected bone marrow derived macrophages (BMDM) from IL-4rα$^{-/lox}$. Flow cytometry was used to measure the production of IFN-γ and TNF after 48 hours of being co-cultured with infected BMDMs. We found there was no difference in the levels of TNF produced by CD44^{+}CD4 T cells (Figure 25A). We observed an increase the amount of IFN-γ producing CD44^{+} CD4 T cells after 48 hours of co-culture with infected macrophages (Figure 25A-B). When making use of the co-culture system, we did not see differences in the amount of CD44 expression. Suggesting that that activation of the antigen-specific T cells is tied to the ability to recognize infected macrophages. At 48 hours after co-culture, a representative sample of cells were spun down, rinsed with PBS, lysed and plated on 7H11 plates in order to allow us to enumerate CFU. We found co-culturing of T cells from either background of mice, lead to increased control of mycobacteria compared to macrophages alone. The ability of T cells to control *Mtb* growth is shown by decreased CFU in co-cultured samples when compared to macrophages alone (Figure 25C). Remarkably, no differences in the ability to control bacterial burden was observed regardless whether IL-4Rα was present or absent on T cells. This observation is in direct contrast to what was observed *in* vivo. Supernatants of co-cocultured cells was collected and levels of IFN-γ and GM-CSF was assessed by ELISA. We assessed that were no differences between IFN-γ and GM-CSF in the supernatants of T cells co-cultured with infected macrophages, albeit that it is higher than T cells co-cultured with uninfected macrophages (Figure 25D-E). Demonstrating that T cells produce cytokines in response to recognizing *Mtb*-infected macrophages, but the levels seen in uninfected macrophages, is possibly due to the continuing response that was present in the site of infection. We sought to find differences in proliferation capacity as well as accumulation of apoptosis in T cells co-cultured with infected macrophages as measured by Ki-67 and Caspase-3 respectively. We observed significantly reduced levels of Ki-67 in IL-4Rα deficient T cells after both one and two days after being cultured with infected macrophages (Figure 25F). This observation corroborates our findings *in vivo*. After 48 hours of co-culture we measured the levels of Caspase-3^{+} CD4 and CD8 T cells. Despite the mean level of Caspase-3 being higher in IL-4Rα deficient T cells, this was not statistically significant (Figure 25G-H). In order to reconcile the disparity between the *in vivo* and *in vitro* we speculated that iLCK^{Cre}IL-4rα$^{-/lox}$ have a reduced ability to recognize infected T cells. A study in the Behar group [216] show that the majority of T cells that recognize infected macrophages *in vitro* express the early activation

CD69. Since we saw differences in CD69 expression *in vitro,* we considered it prudent to assess it. While few differences were observed in the outright levels of CD69 on CD4 T cells cultured with infected macrophages, we did note a similar observation seen in the Behar study [216]. In that a substantial portion of IFN-γ producing CD4 T cells, were $CD69^-$ (Figure 25I). Moreover, these CD4 T cells were sourced from $iLCK^{Cre}IL\text{-}4r\alpha^{-/lox}$. This observation, combined with the lack of differences in the ELISA results, indicates that although IL-4Rα deficient T cells have the ability to produce increased cytokines when stimulated *ex vivo*, the ability to recognize infected macrophages is potentially dampened, or the peptides presented by infected macrophages are not as immunogenic as peptides used in re-stimulation.

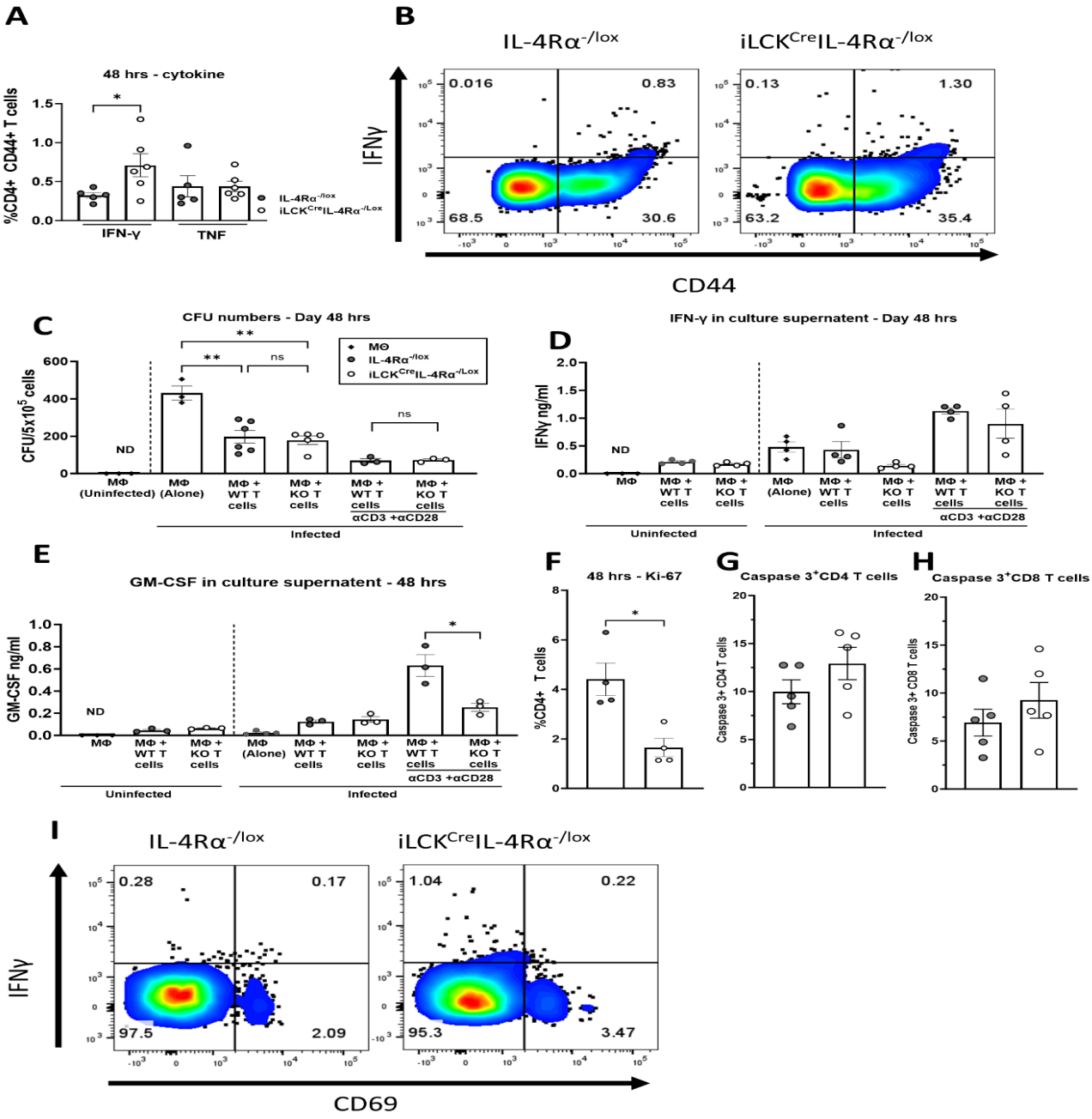

Figure 25: Loss of IL-4Rα on T cells had no effect on mycobacterial growth, despite increased effector responses after ex vivo stimulation. BMDMs were derived from IL-4Rα$^{-/lox}$ mice and co-cultured with isolated T cells derived from *Mtb* infected mice after 12 weeks of infection. Isolated T cells were added to either infected or uninfected BMDMs (MOI =1) at a ratio of 4:1 and cultured for 48 hours. **(A-B)** Cells were collected after 48 hours of co-culture and the ability to produce IFNγ and TNF was assessed by ICS after Mtb300 stimulation for 5 hours. **(C)** After 48 hours of co-culture the cells were lysed and plated on 7H11 to determine bacterial burden. **(D-E)** The collected supernatant was used to measure the amount of **(D)** IFNγ and **(E)** and GM-CSF secreted into the media, in the presence of infected or uninfected macrophages. **(F)** Proliferation of CD4 T cells was determined by the expression of Ki-67 by flow cytometry after 48 hours of co-culture with infected macrophages. **(G-H)** Apoptosis of CD4 and CD8 T cells was measured by Caspase-3 on flow cytometry after 48 hours. **(I)** Representative flow plot of CD4 T cell expressing IFN-γ and CD69. Grey circles indicate IL-4Rα$^{-/lox}$ and white circles indicate iLCK^{Cre}IL-4Rα$^{-/lox}$. Data represented as mean ± SEM of n=5-7 mice/group,

and experiments were performed 3 times. Statistical significance was analysed by student unpaired t-test. *p<0.05, **p<0.001.

3.14 iLCK^{Cre}IL-4rα$^{-/lox}$ mice remains susceptible to the H37Rv laboratory strain

Genetic variation of *Mtb* results in differences in virulence, disease progression, rate of mortality and transmissibility[217-219]. This difference in genetic makeup also influences immunopathological events related to factors including rate of growth and phenotypic make up [220]. Reports include differential activation of Toll-like-receptors (TLRs) by different strains. Differences in immune sensing events result in distinct cytokine profiles leading to protective or pathogenic events, with *HN878* eliciting an early and intense Th1 response, including production of IFN-γ by CD4 and CD8 T cells, before substantially downregulating T cell responses. This substantial contraction in T cell responses is linked to increased mortality of mice infected with *HN878* [221, 222]. The popular lab strain, H37Rv is less virulent than HN878, and induced different immune responses. Infection of C57BL/6 with H37Rv causes the formation of disorganized granulomas in the lung, while HN878 produces a lesion with a visible lymphocyte cuff surrounding a core of macrophages, more closely resembling TB granulomas observed in humans [223]. For this reason, we asked whether the susceptibility of iLCK^{Cre}IL-4rα$^{-/lox}$ mice with HN878 is also present during H37Rv infection. iLCK^{Cre}IL-4rα$^{-/lox}$ and IL-4rα$^{-/lox}$ were infected with 100 CFU of H37Rv intranasally, and euthanized at 24wpi (chronic). The uptake of *Mtb* CFU in the lungs was verified in uptake mice one day after infection and counted 21 days later. The iLCK^{Cre}IL-4rα$^{-/lox}$ mice significantly reduced body weight, as measured by change in body weight percentage over time (Figure 26A). This was confirmed by significantly increased bacterial burden in the lungs, although no such differences were observed in the spleen of iLCK^{Cre}IL-4rα$^{-/lox}$ (Figure 26B). No differences in the weights of the lung or spleen were observed between the littermate control and iLCK^{Cre}IL-4rα$^{-/lox}$ (Figure 26C). Furthermore, there were no discernible differences in the total cell numbers in either the lung or MLN between iLCK^{Cre}IL-4rα$^{-/lox}$ and the IL-4rα$^{-/lox}$ mice during chronic infection with H37Rv (Figure 26D-E). Flow cytometry was used to assess levels of various immune cell populations in the lung. We found no differences in the amount of γδ T cells, and B cells seen in the lung (Figure 26F). Nevertheless, a significant decrease in T cells in the lung was observed of the iLCK^{Cre}IL-4rα$^{-/lox}$, and is primarily attributed to a decline in CD4 T cells present in the lung as CD8 T cells were not affected (Figure 26F-G). Histological analysis reveals a decrease in alveolar free space in iLCK^{Cre}IL-4rα$^{-/lox}$ mice compared to littermate controls, however, it is not statistically significant (Figure 26H-I). Analysis of the myeloid populations revealed significantly elevated neutrophils and interstitial macrophages (Figure

26J). Interstitial macrophages are typically associated as being restrictive during the acute stage of *Mtb* infection [224]. This observation is owed to interstitial macrophages typically differentiating into the M1 phenotype which bear more bactericidal properties than the M2 phenotype, due to the production of IL-1α, IL-1β, and IL-12 [225]. An important caveat to consider, is that *Mtb* protein ESAT-6, can drive differentiation of restrictive M1 macrophages into the more permissive M2 over time [226]. M2 macrophages are found in necrotic as well as non-necrotic granulomas of patients [225], and have altered metabolic activity which results in a favourable environment for the mycobacteria [227]. Thus it is possible that during chronic infection with *Mtb*, an increased interstitial macrophage population may not necessarily control, but could instead consist of the more permissive M2 macrophages [227] which in turn results in a larger niche of for *Mtb* to infect and proliferate, possibly explaining the increased mycobacterial burden. This assertion would have to confirmed with further testing to see if this is indeed the case.

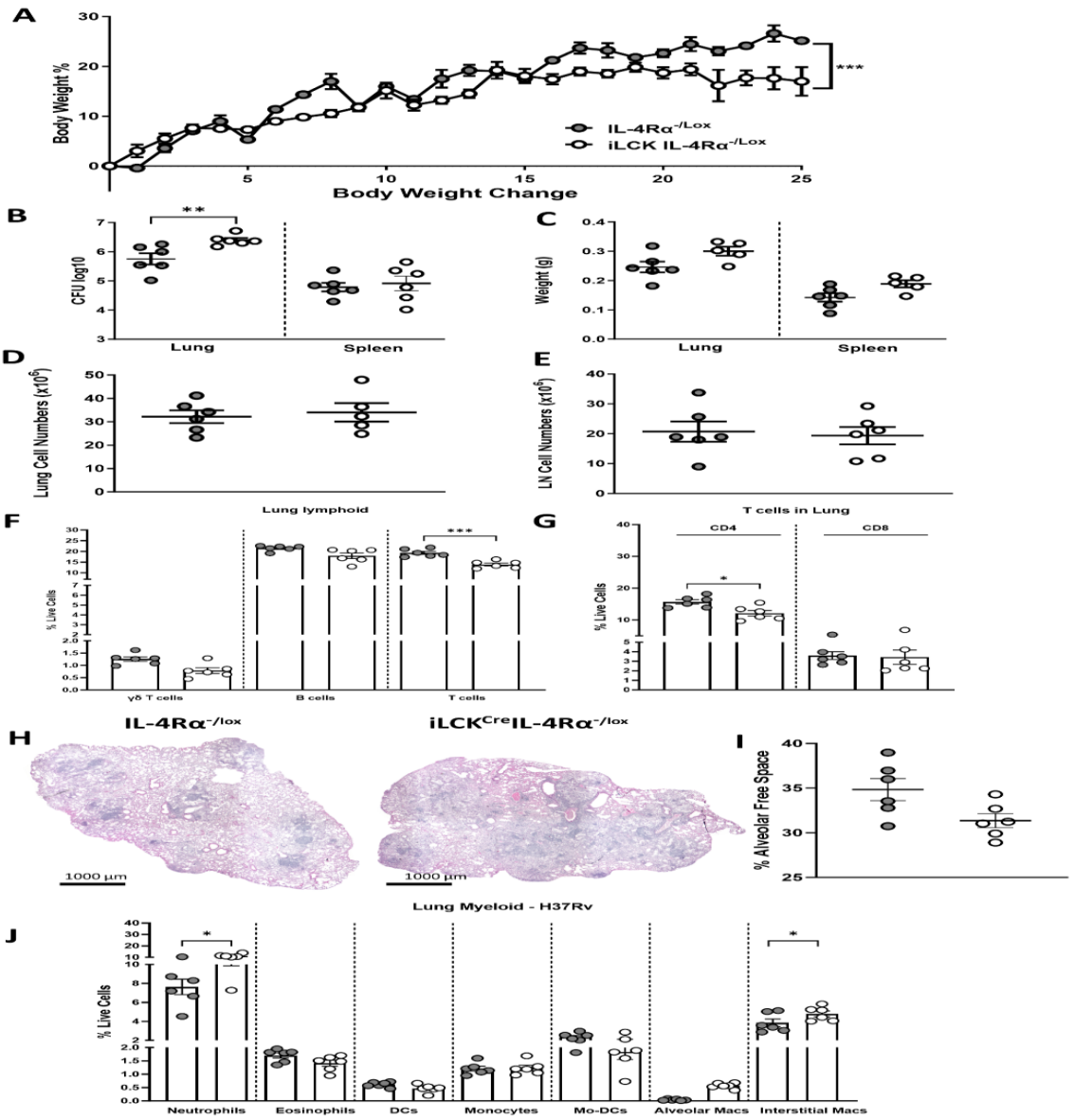

Figure 26:The outcome of *Mtb* infected iLCK^{Cre}IL-4Rα$^{-/lox}$ mice is comparable between HN878 and H37Rv. iLCK^{Cre}IL-4Rα$^{-/lox}$ and IL-4Rα$^{-/lox}$ littermate controls were intranasally infected with 100CFU of H37Rv at and euthanized at 25 weeks. (A) Change in body weight percentage during the course of infection. (B) Lung and spleen mycobacterial burdens. (C) lung and spleen weights. (D) lung andI) lymph node cell numbers were determined. (F) Single cell suspensions of lung was analysed by flow cytometry. (G) The amount of CD4 and CD8 T cells displayed as percentage of live cells. Lymphoid populations were determined using the following surface markers. Gamma-delta T cells (γδ T cells): CD3$^+$ γδ TCR$^+$; B cells: CD3$^-$CD19$^+$, T cells: γδ TCR$^-$,NK1.1$^-$CD19$^-$CD3$^+$; CD4 T cells: γδ TCR$^-$NK1.1$^-$CD19$^-$CD3$^+$CD4$^+$; CD8 T cells: γδ TCR$^-$NK1.1$^-$CD19$^-$CD3$^+$CD8$^+$. (H) Representative H&E histopathology of lung sections (40x) scale bar indicates 1000 µm (I) quantification of alveolar free space. (J) Myeloid population in the lungs as determined by flow cytometry. Myeloid populations were determined using the following markers. Neutrophils: Ly6G$^+$CD11b$^+$; Eosinophils: SiglecF$^+$CD11b$^+$CD64$^-$; Dendritic cells (DC):CD11b$^+$CD11c$^+$MHCII$^+$; Monocytes: Ly6G$^+$CD11b$^+$CD64$^-$; Monocyte-derived Dendritic Cells (Mo-DCs): CD64$^+$CD11b$^+$CD11c$^+$; Alveolar Macrophages (Alveolar Macs): CD64$^+$MerTK$^+$SiglecF$^+$CD11c$^+$; Interstitial Macrophages (Interstitial Macs): CD64$^+$MerTK$^+$SiglecF$^+$CD11c$^-$CD11b$^+$. Grey circles indicate IL-4Rα$^{-/lox}$ and white circles indicate iLCK^{Cre}IL-4Rα$^{-/lox}$. Data represented as mean ± SEM of n=5-7 mice/group. Statistical significance was analysed by student unpaired t-test. *p<0.05, **p<0.001.

Chapter 4:
Discussion

The 2022 WHO tuberculosis report indicates that an estimated 1.6 million people died as a result of TB. This highlights the extent of the global burden of TB, and highlights the challenge that lies ahead in reaching the WHO End TB strategy. Moreover, the rise in multi-drug resistant TB incidence amplifies the urgency in the efforts to mitigate and ultimately eliminate TB through innovations in novel therapeutics.

The advancement towards the development of better therapeutics and vaccines could partly be achieved by gaining a better understanding of the host-pathogen interactions and host's immune response to Mtb that can potentially be exploited to combat the disease. The core question of this study aims to describe the role of IL-4Rα signalling on T cells in *Mtb* infection, pathogenesis and control, which often-overlooked receptor in TB. To address this question, we made use of T cell specific knockout mouse model iLCK^{Cre}IL4Ra$^{-/lox}$, and assessed immune response to *Mtb* infection with the hypervirulent strain, HN878, during acute and chronic infection. In this study, we show that deletion of IL-4Rα on T cells causes perturbations in the immune response to *Mtb* infection which ultimately result in detrimental effects to the host. We demonstrated that in the absence of the IL-4Rα the T cell response is sufficiently disrupted, resulting increased and sub-optimal control of *Mtb* replication. This study shows that disruption of IL-4Rα on T cells, results in decreased recruitment of T cells to the lung during acute *Mtb* infection, while having no effect on T cell priming in the mediastinal lymph node. Although, the recruitment of T cells to the site of infection seems to stabilize during chronic infection, where similar numbers of CD4 and CD8 T cells are seen in the lungs of both iLCK^{Cre}IL4Ra$^{-/lox}$ and IL4Ra$^{-/lox}$. The increased effector responses (CD44^{+}CD62L^{-}) were observed in both CD4 and CD8 T cells in the lungs of iLCK^{Cre}IL4Ra$^{-/lox}$ at both acute and chronic timepoints. We show in the following sections that disruption of IL-4Rα seemingly skews the response of T cells towards a predominant Th1 and Th17 response. This dysregulated T cell response is associated with an increase in TB susceptibility that could be partly due to: 1) A reduced migration into lung parenchyma resulting in a delay in the T cell response at the site of disease, 2) The establishment of disease leads higher bacterial burden, and increased tissue pathology which result in higher mortality. In the following sections, the impact of IL-4Rα removal is discussed in greater detail. Lastly, we look at clinical data to explore the translational aspects of our observations in the murine system.

We found that expression of IL-4Rα increased particularly in the CD4 T cells of both iLCK^{Cre}IL4Rα$^{-/lox}$ and IL4Rα$^{-/lox}$ during acute infection compared to naïve mice (Figure 1). Interestingly, the amount of IL-4Rα expressed was not altered when looking at chronic infection. Similarly, the amount of IL-4Rα expressed on splenic T cells, does not change during infection in the littermate controls, but does increase in the iLCK^{Cre}IL4Rα$^{-/lox}$ (Figure 2). This possibly indicates the role of antigenic load of *Mtb* in driving IL-4Rα expression, seeing as the lung has greater amounts of *Mtb* bacilli compared to the spleen. In our experience from other studies making use of cell-specific knockouts, residual expression of IL-4Rα in the iLCK^{Cre}IL4Ra$^{-/lox}$ model is likely due to inefficiencies in the Cre recombinase enzyme, which results in the significant knockdown of the receptor. The iLCK^{Cre}IL4Ra$^{-/lox}$ is a well characterized mouse model from our laboratory. There is published evidence which demonstrates that IL-4Rα is deleted on CD4, CD8, γδ T cells and NK T cells [197]. Furthermore, expression of IL-4Rα is preserved on non-T cell types such as B cells, dendritic cells, NK cells and macrophages. We are able to show that IL-4Rα expression is significantly lower in γδ T cells and NK T cells at both 4- and 18 weeks in iLCK^{Cre}IL4Ra$^{-/lox}$ mice. A previous study from our group made use of the LysM^{Cre}IL4Ra$^{-/lox}$ model in which IL-4Rα is deleted on macrophages and neutrophils[165] and found that there were no major differences in LysM^{Cre}IL4Ra$^{-/lox}$ mice during TB [163].

The IL-4Rα KO is the most common mouse model to study the IL-4/IL-13 signalling. However, since IL-4Rα is component of both Type 1 and Type 2 receptors it is not useful to assigning specific functions to either signalling pathway [228]. Genetic disruption of the other component of the type 1 receptor, γC, results in a phenotype that resembles X-linked severe combined immunodeficiency (X-SCID) in humans, including a substantial reduction in T cells, and B cells [229]. As such, the only feasible alternative to study differences between these receptor systems is through making use of a mouse in which IL-13Rα1 is knockout, which effectively disrupts Type 2 signalling. Studies which make use of IL-13Rα1 KO mice in *S. mansoni, N. brasiliensis* and asthma had some interesting findings. For example, IL-4Rα is required for Alternatively activated macrophage (AAMφ) development but not IL-13Rα. Thus, demonstrating that the Type 2 receptor does not play a role in AAMφ development.

In *S. mansoni* infections, IL-13Rα$^{-/-}$ mice develop similar antibody responses as control mice during chronic infection. Type II IL-4R signalling is minimally involved in development of humoral responses in *S. mansoni*. However, IL-4R global KO mice succumb to infection by 8 weeks. IL-13 receptors are not expressed on T cells, but IL-13 KO mice seem to imply that it

plays an indirect role in TH2 development. However, these observations might be due to the fact that IL-13 disruption might affect the expression of IL-4 which is found on the same locus. IL-13Ra KO develop greater TH2 responses in *S. mansoni* infection as demonstrated by greater amounts of IL-4, IL-5 and IL-13 in the liver at 9 weeks. However, greater amounts of IFN-y also found in addition to these cytokines at 12 weeks, demonstrating that there is no inhibitory effect on Th1 counter-regulatory response. Type II IL-4R seems to function as a negative regulator of Th2 responses *in vivo*.

IL-13Rα1 deficiency impairs expulsion of *N. brasiliensis*. The host immunity to *N. brasiliensis* depends on IL-4Rα and STAT6. Despite stronger Th2 responses, IL-13Rα KO mice fail to expel parasites, emphasising the importance of type 2 receptors in this disease.

There are studies which explore whether *Mtb* drives IL-4Rα expression. Some researchers explore the link between IL-4 and IL-13 expression in *Mtb* infection, although there are conflicting reports in the literature. We have previously shown that IL-4Rα expression increases on B cells in response to *Mtb* infection in WT mice [178]. It has been demonstrated in C57BL/6 mice, that there were no significant alterations in the expression of IL-4 and IL-13 in response to *Mtb* infection compared to IL-4Rα global KO mice, and both do not develop centrally necrotizing granulomas [146]. However, *Mtb* infected mice which overexpress IL-13 develop centrally necrotizing granulomas, indicating that IL-4Rα mediated signally might play a role in granuloma formation [146]. Levels of the cognate cytokines, IL-4 and IL-13 are strongly associated with IL-4Rα activity. It is important to bare in mind that IL-4 is physiologically active at low concentrations [230], and as such a minor change in levels might indicate a profound change in signaling activity. High dose *Mtb* infection studies have demonstrated that increased IL-4 levels are associated with lung fibrosis and focal necrosis [156, 157]. Both the Heitman and the Hernandez studies made use of the *Mtb* strain, H37Rv, whereas our study predominantly made use of HN878. At this stage, it is not clear whether the extent to which IL-4Rα expression on T cells is strain specific. Increased secretion of IL-4 by CD4 and CD8 T cells in response to *Mtb*, correlates significantly with pulmonary cavitation in human patients [158, 230, 231]. Additionally, an increased IL-4 to IFN-γ ratio is observed in the blood but not BAL of active TB patients [161]. This observation, that expression of IL-4 differs at the site of disease compared to peripheral blood is in line with our findings of IL-4Rα. It is important to bear in mind that the increase in T cells expressing IL-4Rα do not seem to fall into the effector T cell subset (Figure 10 C-D), and as such are likely to minimally contribute towards controlling infection. Plausibly, the IL-4Rα expressing T cells during

infection represents only a small fraction of the *Mtb*-specific, antigen experienced T cells. Ours is the first study that describes how IL-4Rα expression increases on T cells after *Mtb* infection.

The deletion of IL-4Rα on T cells resulted in increased morality of iLCK^{Cre}IL-4Rα $^{-/lox}$ in our survival experiments (Figure 3). Similarly, we saw increased severity of disease in iLCK^{Cre}IL-4Rα $^{-/lox}$ mice at both the acute and chronic stages, with increased bacterial burden in the lungs at both stages (Figure 3). However, it is also important to note that no differences in bacterial burden were seen in the spleen, indicating that IL-4Rα absence does not affect dissemination of disease.

The major difference in the iLCK^{Cre}IL-4Rα $^{-/lox}$ mice was seen during acute infection, where IL-4Rα KO on T cells led to a reduction of T cells recruited to the lung by approximately 40% (Figure 5). However, no differences in either CD4 or CD8 T cell numbers were observed in the mediastinal lymph node, indicating that the reduced number of T cells detected in the lung cannot be ascribed to the organism having less T cells but rather, is suggestive of reduced recruitment, or infiltration into the infected tissue. As the T cell response is considered instrumental for *Mtb* control [232-234], impaired T cell recruitment to the disease site may substantially impact the ability of the host to limit bacterial replication. Moreover, the delayed onset of the adaptive response to *Mtb* compared to other respiratory pathogens is considered to be one of the major reasons that the pathogen is able to establish and persist in the lung [64, 67, 68]. Some researchers argue that the most reliable correlate of protection against TB is the ability to rapidly mount a T cell response in the lung [235, 236]. We believe the delay in T cell recruitment into the lungs of iLCK^{Cre}IL-4Rα $^{-/lox}$ mice is plausibly the primary reason for increased bacterial burden. Indeed, a study investigating the host factors which contribute to dissemination of *Mtb* by making use of C57BL/6 and C3H/HeJ mice made some interesting findings. The core findings were that *Mtb* needed to disseminate to the lymph node in order to activate *Mtb*-specific T cell responses [60]. The authors also found that dissemination occurred earlier in the more resistant C57BL/6 mice compared to the more susceptible CH3/HeJ mice, and the resultant earlier T cell response contributes the resistance in the C57BL/6 mice. Moreover, the detection of T cell responses in these models only differed by 3 days, but the amount of IFN-γ differed by 10-fold 21 days after infection. This study really highlights the importance in the kinetics of the T cell response in TB disease. While our study indicates that absence of IL-4Rα on T cells does not affect the dissemination of disease, earlier timepoints would allow us to dissect the kinetics of the T cell response.

The difference in T cell numbers was lost by the time we assessed chronic infection. It is tempting to speculate that CD4 T cell infiltration into the lung could be normalized with time. Again, this is suggestive that IL-4Rα expression partially influences the migration of T cells into the lung tissue. However, when we investigated chronic infection of iLCK^{Cre}IL-4Rα $^{-/lox}$ mice using H37Rv, we found that there was a reduction in the amount of T cells at 25 weeks. Altered responses to infection by different *Mtb* strains is well documented. Different strains of *Mtb* have the potential to be detected by different innate pathways. For example, H37Rv is preferentially detected by TLR2 while the 02-171 strain is preferentially detected by TLR4 [237]. These result in distinct cytokine profiles in both an *in vitro* and *in vivo* settings. Additionally, BMDMs infected with H37Rv produce more TNF and IL-6 compared to HN878 infected BMDMs [237]. Infection of BALB/c mice with various strains reported differences in time taken for certain immune cell populations to migrate in the lung including B cells, and FoxP3^{+} T_{reg} cells [238]. This study showed that infection of BALB/c mice with Beijing-1585 or EAI-1627 strain resulted in early B cells recruitment to the lung 14 days after infection, while B cell infiltration was delayed (14 to 28 days) when infection was performed using the H37Rv strain. C57BL/6 mice infected with a mutant strain of H37Rv encoding a disrupted mycobacteria membrane protein large 7 gene (MmpL7), which results in a lack of phthiocerol dimycocerosate (PDIM) residues on the surface of membrane surface, resulted in increased inducible Bronchus-associated Lymphoid Tissue (iBALT) [239]. Another study demonstrated differences in myeloid cell recruitment to the lung, with increased neutrophils, DCs, and monocyte derived DCs being observed up to day 60 when infected with M299 compared to the H37Rv strain [188]. The evidence that different strains induce different immune responses, including distinct rates of cell recruitment is similar to what we observed in our experiments. However, no strain specific differences in lymphoid recruitment have thoroughly been investigated during chronic infection. Other studies making use of an IL-4Rα knockout models in other respiratory diseases have described similar observations, with 1) reduced infiltration of IL-4Rα deficient T_{reg} in the liver of *S. mansoni* infected FoxP3^{Cre}IL-4Rα$^{-/lox}$ [198], 2) Reduced numbers of T_{reg} cells were observed in the lungs of FoxP3^{Cre}IL-4Rα$^{-/lox}$ mice in the response to allergens in an allergic asthma model., in which IL-4Rα has been removed in T_{reg} cells [240] and 3) reduced lymphocytes were observed in the lungs of CD4^{Cre}IL-4Rα$^{-/lox}$ during *N. brasiliensis* infection [241, 242]. These data suggest that IL-4Rα may play a role in B and T cell infiltration to the sites of disease. These observations are largely consistent with our own findings, where the knockout of IL-4Rα resulted in diminished levels of lymphocytes in the lung during acute *Mtb* infection.

Although our study was focused on the role of IL-4Rα on T cells, we also investigated myeloid cells, given their significance as they comprise of the primary host cells for *Mtb*. Two main macrophage populations present are alveolar macrophages and interstitial macrophages in the lung over the course of *Mtb* infection. Alveolar macrophages reside in the alveoli and are generally considered to be the first responders to respiratory infections. While interstitial macrophages represent a population that is recruited to the lung during infection, and are derived from bone marrow monocytes [243]. These two populations have different underlying metabolic programming, with alveolar macrophages relying on fatty acid oxidation, while interstitial macrophages are more glycolytic at least in the early stages of infection [224, 244]. These metabolic profiles in interstitial macrophages during early infection and alveolar macrophages represent profiles seen in M1 and M2 macrophages, respectively. *Mtb* benefits from increased levels lipids, and this exploitation of the host microenvironment means that alveolar macrophages (that rely on fatty acid oxidation for energy generation) are seen as more permissive to *Mtb* growth than the M1-like interstitial macrophages [224, 243, 244]. In our study, we found that absence of IL-4Rα associated with similar number of alveolar macrophages in the lung, but interestingly fewer recruited interstitial macrophages (Figure 7A). The decreased amount of restrictive interstitial macrophages, likely contribute to the increased bacterial burden. It is unclear what drives these differences, since the recruitment of interstitial macrophages has been shown to occur ~ 2 weeks after infection, while T cell responses are only detected in the lung at 3 weeks [23, 207]. Thus, it is unlikely that the decreased numbers of interstitial macrophages are linked to delayed T cell recruitment. In fact, it is the interstitial macrophages which help recruit both effector and regulatory T cells into lung during infection [245].

Infected interstitial macrophages begin to accumulate more lipid bodies over-time, and differentiate into foamy macrophages [36]. These foamy macrophages represent a shift from M1 to M2 macrophages, and are more permissive to mycobacteria, modulate granuloma formation and facilitate dissemination of disease [246, 247]. Although, we did not investigate how differences in cellular composition of the granuloma in either iLCK^{Cre}IL-4Rα $^{-/lox}$ mice. We saw slight differences in lesion size during acute infection (Figure 4C). Moreover, BALB/c mice do not form necrotizing granulomas and are perhaps not the best strain to investigate *Mtb*-induced granuloma [248]. There were no differences in interstitial macrophages observed in the lungs of chronically infected mice infected with HN878, but heightened numbers of interstitial macrophages were observed during chronic H37Rv infection. Perhaps during

chronic H37Rv chronic infection, the increased levels of interstitial macrophages represent the more permissive, M2-like macrophages [227]. However, without deeper investigation of the subsets of the interstitial macrophages, we cannot say anything with certainty. The secretion of IFN-γ by Th1 CD4 T cells in the lung induce the production of iNOS in *Mtb* infected macrophages. This in turn will drive the production of NO, resulting in a more restrictive environment for *Mtb* bacilli [182]. Thus, during the acute time point the reduced amounts of T cells trafficking to the lung, means reduced helper function for infected macrophages, which in turn leads to lower amounts of bactericidal function, leading to increased bacterial growth. IFN-y induced signalling leads to increase in NO production by macrophages which in turn leads to enhanced microbiocidal potential [182], however, we did not see that in our study. The likely reason for this is that it is the heightened bacterial burden which leads an enhanced inflammatory phenotype. It is certainly possible that this increased NO is actually contributing to killing the *Mtb*, however, also contributing in lung pathology. Consequently, this enhanced inflammatory phenotype which ultimately results in the decreased survival of these mice.

The role of neutrophils in TB immunity is complex. Neutrophils have been shown to be protective during acute infection as the responding cells are able to mop up and destroy invading bacilli [249]. While increased neutrophilia in chronic TB is a driver of immunopathology, where dysfunctional neutrophils recruit more pro-inflammatory macrophages resulting in uncontrolled inflammation [250]. Moreover, neutrophils with impaired killing function can contribute to dissemination of disease [251]. Interestingly we observed no differences in the number of neutrophils during acute infection (Figure 7A), however heightened amounts of neutrophils in both HN878 and H37Rv chronic infection in the lungs of iLCK^{Cre}IL-4Rα $^{-/lox}$ mice (Figure 7A and Figure 22J). The increased neutrophilia in chronically infected iLCK^{Cre}IL-4Rα $^{-/lox}$ mice is plausibly the major contributor to lower alveolar space, immunopathology and subsequent death. The reduction in the T cell response, observed during acute infection allows for *Mtb* to gain a better foothold in the lung. The increased bacterial burden leads to an increased inflammatory state, which causes increased recruitment of neutrophils during chronic *Mtb* infection. The increased levels of neutrophils could interfere with the ability of T cells interact with infected cells, further hindering the adaptive response and protective immunity [252].

In this study, we demonstrated that IL-4Rα deletion results in an increase in T cells expressing either high levels of T-bet or RORγt (Figure 8). Th1 and Th17, which correspond with T-bet or RORγt expression, respectively, are normally considered protective responses in TB [253].

However, they can also contribute towards immunopathology [253, 254]. These discrepancies between described roles of certain helper subsets are a reminder of the importance of a finely tuned response, and how quickly it can unravel. It is well documented how different transcriptional programming responsible for driving T helper responses actively inhibit each other. For example, IFNγ induced T-bet expression prevents Th2 or Th17 differentiation [75, 98, 255]. Similarly, IL-4 induced Th2 differentiation restricts IFN-γ production in CD4 T cells, thereby inhibiting Th1 responses [117, 126]. Interestingly the use of T-bet deficient mouse model showed that CD4 T cells defaulted to Th2 programming [75].

We believe a similar explanation could be used when IL-4Rα is removed allowing progression to Th1 and Th17 programming. This phenomenon of increased Th1 responses in the absence of IL-4Rα on T cells has been reported before, but not for Th17 responses [176, 197]. It is questionable why the increased Th1 and Th17 responses do not lead to increased protection [256]. To further explore this, we looked at the effector populations and the cytokines they produced. The increases in T-bet or RORγt contribute to the substantial proportional expansions of effector T cells ($CD44^{+}CD62L^{-}$) in the lungs of $iLCK^{Cre}$IL-4Rα $^{-/lox}$ mice (Figure 10). However, the greater percentages of CD4 T cells are not indicative of a larger total response, as the numbers of effector CD4 T cells are still lower during acute infection (Figure 10G). Moreover, this expansion is not seen in the mediastinal lymph nodes (Figure 11). This is evidenced by similar T cell numbers observed in the MLN. We did not assess the levels of transcription factors in T cells in the MLN, this would answer with greater degree of certainty if the increased percentages in effector population is related to increased T-bet expression, enhanced recruitment or a combination of both. Interestingly, we saw an increase in T-bet expression in CD4 T cells without an alteration of GATA3 expression, such changes could be sufficient to skew the Th1/Th2 balance. We also observed no differences in FoxP3 expression, suggesting that T_{reg} is unaffected by IL-4Rα during TB. This suggests that the increased inflammation in the lungs of $iLCK^{Cre}$IL-4Rα $^{-/lox}$ mice is not due to a decreased ability in the modulating effect of T_{reg} cells. We found this interesting as IL-4Rα mediated signaling, through the actions of IL-4 and IL-13 have been shown to be important in generating FoxP3+ T_{reg} cells [257]. However, T_{regs} obtained from IL-4 KO mice have poorer suppressive ability compared to controls, despite having similar frequencies [258]. Moreover IL-4Rα has been shown to be important for T_{reg} cell function during helminth infections [198]. Specifically, absence of IL-4Rα lead to a reduction in the expression of FoxP3 and consequently lead to a reduction in T_{reg} in inflamed tissues [198]. The findings of the aforementioned study [258] shows that disruption

of IL-4Rα signaling might affect the ability of T_{reg} cells to modulate inflammation, and might possibly indicate that the increases in inflammation was due to impaired function of T_{reg} cells. However, we found no differences in IL-10 and TGF-β in lung homogenates of either KO or control mice, meaning that T_{reg} function is preserved despite IL-4Rα KO. These studies highlight how our observation that FoxP3 expression is unaffected by IL-4Rα removal contrasts with previous observations.

High T-bet expression correlates to high expression of KLRG1 in CD4 T cells during *Mtb* infection of the murine model [207, 211, 259]. These T cells are characterized as being short-lived, highly active and proliferating at a reduced rate [207]. Moreover, KLRG1 expressing T cells are considered to be less protective against *Mtb* infection, while another differentiation marker, PD-1, is associated with greater protection [210, 260]. In our study, we found that that IL-4Rα deficiency leads to increase KLRG1 expression but had no effect on PD-1 expression on both CD4 and CD8 T cells. Moreover, we found that a larger proportion of active $CD44^+$ CD4 and CD8 IL-4Rα KO T cells also expressed larger amounts of KLRG1 compared to littermate controls, these differences were most prominent during chronic infection (Figure 13). The association between KLRG1 expression and reduced capacity to migrate into the lung and protect against *Mtb* protection has been demonstrated [101, 260, 261] and provides explanation for our own observations. Overall, increased KLRG1 expression suggests that the protective ability of IL-4Rα-deficient CD4 and CD8 T cells is impaired.

The pulmonary T cells isolated from $iLCK^{Cre}$IL-4Rα $^{-/lox}$ mice partially fit the profile of intravascular, poorly protective T cells. This includes expression or reduction of various chemokine and tissue residency markers. Poorly protective, lung intravascular CD4 T cells are characterized by the expression of KLRG1, CX3CR1, CXCR4, VLA-4, and Ly6C, as well as expressing elevated T-bet and IFNγ [43, 101-103, 210]. On the other hand, lung parenchymal cells, which are associated with increased protection to *Mtb* infection express relatively higher levels of CXCR3, CD69, VLA-1, CD103, ICOS, CTLA4, and CD28, while expressing relatively lower amounts of T-bet and IFNγ. We demonstrated that $iLCK^{Cre}$IL-4Rα$^{-/lox}$ mice, KLRG1 expression is increased on both CD4 and CD8 T cells during acute and chronic timepoints (Figure 13A-B). Reduced CD69, CXCR3 and CD103 on pulmonary CD4 T cells during chronic infection (Figure 13E, G, I). While no differences in PD-1 was detected on CD4 or CD8 T cells, we found increased CXCR3 expression on PD-$1^+$$KLRG1^-$ subsets. The differential expression of these markers which describe intravascular T cells, partially correlate with what has been described in the studies carried out by the Barber group [101-103, 210,

260]. In addition to this, we also observed that the expression of Ki-67 was reduced in CD4 and CD8 T cells derived from the lungs of infected iLCK^{Cre}IL4Ra$^{-/lox}$ mice (Figure 15 and Figure 25F). However, no differences were observed in Caspase 3 (Figure 25G-H). Indicating that although deletion of IL-4Rα results in decreased proliferation, it does not result in increased apoptosis.

The Barber group made use of a mathematical modelling approach to conduct kinetic studies investigating entry of *Mtb*-specific effector CD4 T cells into the lung parenchyma. Their findings revealed that migration of CD4 T cells from the vasculature into the lung parenchyma is a relatively long process, taking on average 8.6 hours [210]. Furthermore, T cell responses in the lungs of *Mtb* infected mice peak at about 20 days after *Mtb* exposure [262]. Reduced T cell numbers in the lung are possibly as a result of reduced entry into the parenchyma, or as a result of short-lived T cells.

We measured levels of cytokines in the lung homogenates of infected mice at acute and chronic time points. We demonstrated that no observable differences in IFNβ, IFNγ, IL-6, IL-12p40, IL-12p70, IL-1α and IL-1β are apparent in mice with IL-4Rα-deficient T cells. The lack of differences in TGFβ and IL-10 further support our assertion that T_{reg} cells are unaffected by IL-4Rα removal during TB. In fact, the only major differences in cytokine levels that we observed was in IL-17 in chronic infection. This observation corresponds with our previous observations of increased neutrophilia and reduced alveolar space. Increases in CCL5, CXCL1, and CCL2 were observed in iLCK^{Cre}IL4Ra$^{-/lox}$ mice during acute infection, while reduced GM-CSF was observed. GM-CSF has been shown to drive Hif1α activation in infected macrophages, allowing for increased *Mtb* control [108]. The decreased levels of GM-CSF could perhaps contribute to decreased control, although the levels are too low for any conclusive evidence. During chronic TB, the heightened levels of CXCL1 and CCL2 remained. These chemokines are associated with increased neutrophil recruitment to the lung, while also allowing for the recruitment of phagocytes that are permissive for *Mtb* growth [212, 213].

IL-17 is particularly important for neutrophil recruitment to the lungs. Mice with IL-17R KO show a significant delay in neutrophil recruitment to the lungs [263]. While neutrophils are among some of the first phagocytes recruited into the lung from the pulmonary vasculature during *Mtb* infection, we do not see differences in IL-17, or bulk frequencies of neutrophils in iLCK^{Cre}IL4Ra$^{-/lox}$ mice in acute infection. There are several studies that show how neutrophils positively contribute to the control of *Mtb* infection during acute timepoints. For example,

depletion of neutrophils during the first week of infection, exacerbates the bacterial burden in lung, liver and spleen [264]. There are suggestions that the positive contributions of neutrophils at early timepoints is mediated by non-phagocytic, possibly immunomodulatory mechanism that enhances IFN-γ production [264].

We see a significant upregulation of the frequencies of IL-17 producing RORγt CD4 T cells in iLCK^{Cre}IL4Ra$^{-/lox}$ mice and a corresponding increase in the amount of neutrophils in the lung in chronic infection We believe it is the IL-17 producing CD4 T cells that are responsible for recruiting the increased neutrophils during chronic infection. An important caveat to our findings is that we only analysed bulk frequencies of neutrophils, and thus do not have exact insight into the kind of environment that they are generating. For example, if they are necrotic, or non-phagocytic, will have different effects on how permissive the environment is to mycobacterial growth.

Neutrophils in late states of *Mtb* infection has a host-detrimental effect. IL-17 induced neutrophil recruitment has been implicated with stress-induced granulopoiesis [265]. Additionally, the response of neutrophils to hypoxic environments in granulomas results in their secretion of MMP-8, MMP-9 and elastase which contribute destruction of lung tissue [266].

Re-stimulation of T cells using antigen is an alternative method for assessing cytokine responses in the lung. By assessing cytokine responses in CD44^{+} T cells, we are able to specifically asses the functional profile of *Mtb*-specific CD4 T cells [267]. In both acute and chronic infection, we saw increased production of IFN-γ and TNF. Increased levels of TNF and IFN-γ is often cited as source of increased protection against *Mtb* infection [93, 94]. However, there is an increasing body of evidence that suggests that these are poor correlates of protection. For example, adoptive transfer of IFN-γ deficient T cells provided the same level of protection as IFN-γ suficient CD4 T cells in *Mtb* infection [106]. Moreover, increased IFN-γ production by CD4 T cells may in some cases correlate with less protection. Murine studies show that Th1 CD4 KLRG1^{+} produce more interferon than KLRG1^{-} CD4 T cells, poorly migrate into lung parenchyma and are short lived [43, 101-103, 260]. Despite increased IFN-γ production the KLRG1^{+} are less protective, than the long-lived, parenchymal CD4 KLRG1^{-} T cells. Finally, adoptive transfer of IFN-γ TNF double knockout T cells had no differences in protective capacity compared to WT T cells [106]. Moreover, infants who have receive MVA85A heterologous boost after BCG vaccination saw no protective benefit despite having 1-2 logs

more IFN-γ+ *Mtb*-specific T cells in the blood compared to BCG alone [107]. Showing that presence of IFN-γ producing CD4 T cells does not necessarily correlate with protection. Overall, these data indicate that there are IFN-γ independent mechanisms responsible for protection. One of these mechanisms involves the secretion of GM-CSF from T cells, which activates HIF-1α specific bactericidal programs in infected macrophages [108].

To try to ascertain how the removal of IL-4Rα on T cells could lead to increased TB susceptibility, we opted to co-culture T cells from the lungs of either infected iLCK^{Cre}IL-4Rα $^{-/lox}$ or control mice with bone marrow infected macrophages. We found that there were no differences in intracellular bacterial growth or cytokine production in BMDMs cultured with T cells derived from either iLCK^{Cre}IL-4Rα $^{-/lox}$ or IL-4Rα $^{-/lox}$ mice. However, we found increased IFN-γ production in T cells derived from iLCK^{Cre}IL-4Rα $^{-/lox}$ after *ex vivo* stimulation with Mtb300 peptides. The increased frequency of IFN-γ producing T cells was not associated with either the cytokine levels or control of *Mtb* replication. There are several studies in mice demonstrating that *Mtb*-specific T cells do not necessarily recognize infected cells. For example, one study found that TB10.44-1-specific CD8 T cells, do not efficiently recognize infected macrophages in culture [216]. Possible explanations for this phenomenon include *Mtb* induced downregulation of certain antigens, impairment of MHC-II-antigen presentation, and hindering co-stimulatory receptor expression [66-68, 71, 268]. Another explanation is simply that some immunodominant *Mtb*-antigens are not presented on the surface of the infected macrophage [216]. This discrepancy in being able to secrete IFN-γ in response to *Mtb*-derived peptide but not recognizing infected macrophages corroborates our own observations.

Despite seeing lower amounts of CD4 T cells in the lungs, we found no differences in blood or spleen of iLCK^{Cre}IL-4Rα $^{-/lox}$ mice (Figure 20). One can hypothesize that reduced T cell infiltration in the lung could result in an increase in *Mtb*-specific T cells in the blood, as cells are “trapped” in the vasculature. However, we did not observe this in our study. The frequency of *Mtb*-specific Th1 effector cells in the blood or peripheral lymphoid tissue do not correlate with protection [235, 269]. Once again, in mice models, it is not the magnitude of T cell response but rather the rate at which the T cell response reaches the lung that provides protection against *Mtb* infection [235, 270-272].

Although our study describes how the absence of IL-4Rα on T cells contributes to heighten susceptibility to TB disease in a mice model, there are several avenues that could be pursued to further describe this finding. Such as a detailed kinetics approach, including looking at

multiple timepoints (Particularly during the early stages of acute infection) would be necessary to understand the precise dynamic of cell recruitment to the lung. In addition to this, we wish to make use of an intravascular marker in order to accurately distinguish T cells that are in the parenchyma of the lung and those that are in the vasculature. These combined approaches will allow us to describe how absence of IL-4Rα leads to decreased T cell recruitment into the lung in greater detail.

The iLCK^{Cre}IL-4Rα$^{-/lox}$ mouse model is on the BALB/c background, and it is important to consider the extent to which the genetic background might influence our findings. Typically, in C57BL/6, Th1 responses play a key role, and they produce relatively larger amounts of IFN-y [150]. In contrast, BALB/c mice induce a stronger Th2 response [150]. Intracellular parasitic infection such as *Leishmania major* induce severe pathology in BALB/c mice whereas C57BL/6 control infection [273]. Interestingly, a study that use of a CD4 T cell-specific IL-4Rα KO on the BALB/c background (LCK^{Cre}IL-4Rα$^{-/lox}$), were found to be more resistant during *L. major* infection [173]. The LCK^{Cre}IL-4Rα$^{-/lox}$ develop a healing disease phenotype which closely resembles resistant C57BL/6 mice. This disruption of the IL-4Rα-mediated signalling axis, impairs the Th2 response, and consequently strengthens the Th1 response, evidenced by increased levels of IFN-γ, IL-12, iNOS and decreased IL-10 [173].

In *Mtb* infections, the two different backgrounds show differences in cellular responses. C57BL/6 are able to control *Mtb* infection more efficiently than BALB/c. Part this could be attributed to the differences in cellular make up of the lung in these two different strains. For example, the C57BL/6 mice have higher levels of alveolar macrophages, and their pulmonary epithelial cells express higher levels of the antimicrobial peptide, cathelicidin [274]. This contributes to differences in early control, with C57BL/6 mice having lower CFU than BALB/c mice 3 days after infection [274]. The same study also found that BALB/c mice have higher levels of infiltrating neutrophils and inflammatory CD11b^{+} APCs in days 1-3 post infection. Thus, showing differences in the underlying innate responses between these strains. It is also worth noting that while the BALB/c mice fail to mount an adaptive response in comparison with C57BL/6 mice, as evidenced by significantly reduced T cell numbers in the lung at 27dpi, the BALB/c mice still have higher levels of TNF, MCP-1 and IFN-γ in lung homogenates [275, 276].

Other studies have shown using higher doses of *Mtb* that there are fewer differences in bacterial burden until day 43. This likely indicates that the differences in the adaptive immune response

is also at play. It is also very important to note that C57BL/6 mice are more likely to exhibit lymphocytic granulomas which consist of large numbers of macrophages, epithelioid cells and heavily infiltrating lymphocytes [275]. While BALB/c have been observed to have atypical granulomas during *Mtb* infection, marked by small collections of macrophages and clear separation between the macrophages and a dense surrounding lymphocytic accumulation [275]. It is largely thought that the relatively increased susceptibility of BALB/c mice, is due to decreased Th1 responses. It is also suggested that BALB/c mice might need additional signals for Th1 differentiation, as observed by both Shibuya and Wakeham in which BALB/c mice have more robust cytokine responses at the earlier timepoints but apparently do not facilitate Th1 differentiation [275, 277]. Importantly, we tend to see very low induction of Th2 responses in both BALB/c and C57BL/6 mice [275].

Thus, T cell-specific IL-4Rα KO mice on C57BL/6 mice likely to show similar disease outcome. This based on the; Firstly, increased Th1 responses in the BALB/c KO mice does not correlate with increased control of *Mtb* infection. We are likely to see an even stronger shift to Th1 responses in C57BL/6 background. It is also important to remember that the initial IL-4Rα, STAT6, and IL-4 global KO studies performed by North were on BL/6 background, in which he concluded that the Th1 response was not being held back by the Th2 response in TB.

The co-culture experiment can be expanded to include conditions such as IL-4 and IFN-γ stimulation. This will demonstrate whether IL-4 stimulation has a detrimental effect of bacterial containment, similar to what has been described with human PBMCs and infected MDMs [161]. The focus in this case would be on the IL-4Rα$^{-/lox}$ T cells, as IL-4 stimulation has no effect on the IL-4Rα KO. Since IFN-γ and IL-4 have antagonistic effects in T cell biology, the inclusion of IFN-γ will act as an experimental control. Additionally, specific analysis of Th1 or Th2 associated cytokine signalling pathway (Measuring STATs phosphorylation) could improve our understanding of regulatory mechanism involved in *Mtb* control and/or progression. it would certainly be interesting to perform a vaccination experiment in these animals. Critically, our study found that iLCK^{Cre}IL4Ra$^{-/lox}$ had a significant reduction of T cells recruited to the lung during acute infection. It would be interesting to see if subcutaneous vaccination with BCG made any differences to this observation, and if there would be any different in protection. Lastly, investigating both the expression and activity IL-4Rα on T cells, using PBMCs from human participants with LTBI or aTB will inform us if our findings in mice, translate into the human setting.

Conclusion

While the data from the mouse study showed that lack of IL-4Rα on T cells resulted in increased susceptibility. We observed that *Mtb* infection in mice leads to an increase in the expression of IL-4Rα on T cells compared to naïve mice. Demonstrating that progression of disease correlates with increased IL-4Rα expression on T cells on mice (Figure 4.1A). We believe that our KO mouse model study demonstrates the importance of IL-4Rα on T cells during TB, by leading to perturbations in fundamental immunological function. Namely, that absence of IL-4Rα on T cells results in a biased Th1 response, characterised by an increased expression of T-bet, and decreased expression of markers associated with efficient infiltration of lung tissue (CXCR3, CD69 and CD103). The decreased rate of infiltration results in a delay in the accumulation of T cells in the lung parenchyma, allowing the mycobacteria a chance to proliferate and establish disease (Figure 4.1B). The decreased recruitment of T cells to the site occurs despite no apparent differences in T cell frequencies in the MLN in the iLCK^{Cre}IL-4Rα$^{-/lox}$ or control mice. The consequence of the delayed recruitment is increased bacterial burden. Although, the rate of recruitment stabilizes during chronic infection (Figure 4.1B), the proverbial damage has been done, and the T cells are unable to efficiently clear the bacteria. Furthermore, absence of IL-4Rα results in increased frequencies of KLRG1^{+} CD44^{+} T cells, and which express lower levels of Ki-67. This is especially apparent during chronic TB infection. This indicates that these cells resemble terminally differentiated effectors, proliferate poorly, and are thus poorly protective against *Mtb*. The increased bacterial burdens drive increased immunopathology during chronic infection as evidenced by increased IL-17 levels and consequently induce neutrophilia during chronic infection resulting in decreased alveolar free spaces which eventually result in the mice succumbing to disease. Our co-culture results indicate that although IL-4Rα deficient T cells secrete more IFN-γ in response to *ex vivo* stimulation, they deliver the same degree of protection to infected BMDMs as WT T cells. Similarly, there were no differences in IFN-γ levels in the supernatants. Likely indicating that they do no efficiently recognize infected macrophages. While the absence of IL-4Rα on T cells results in increased susceptibility to *Mtb*, IL-4Rα mediated signalling is a poor target for inhibition approach in host-directed therapy. This was demonstrated by Pooran and colleagues, in which PBMCs pre-primed with PPD and IL-4, conferred a lower degree of protection to infected MDMs, compared to PBMCs pre-primed with PPD alone [161].

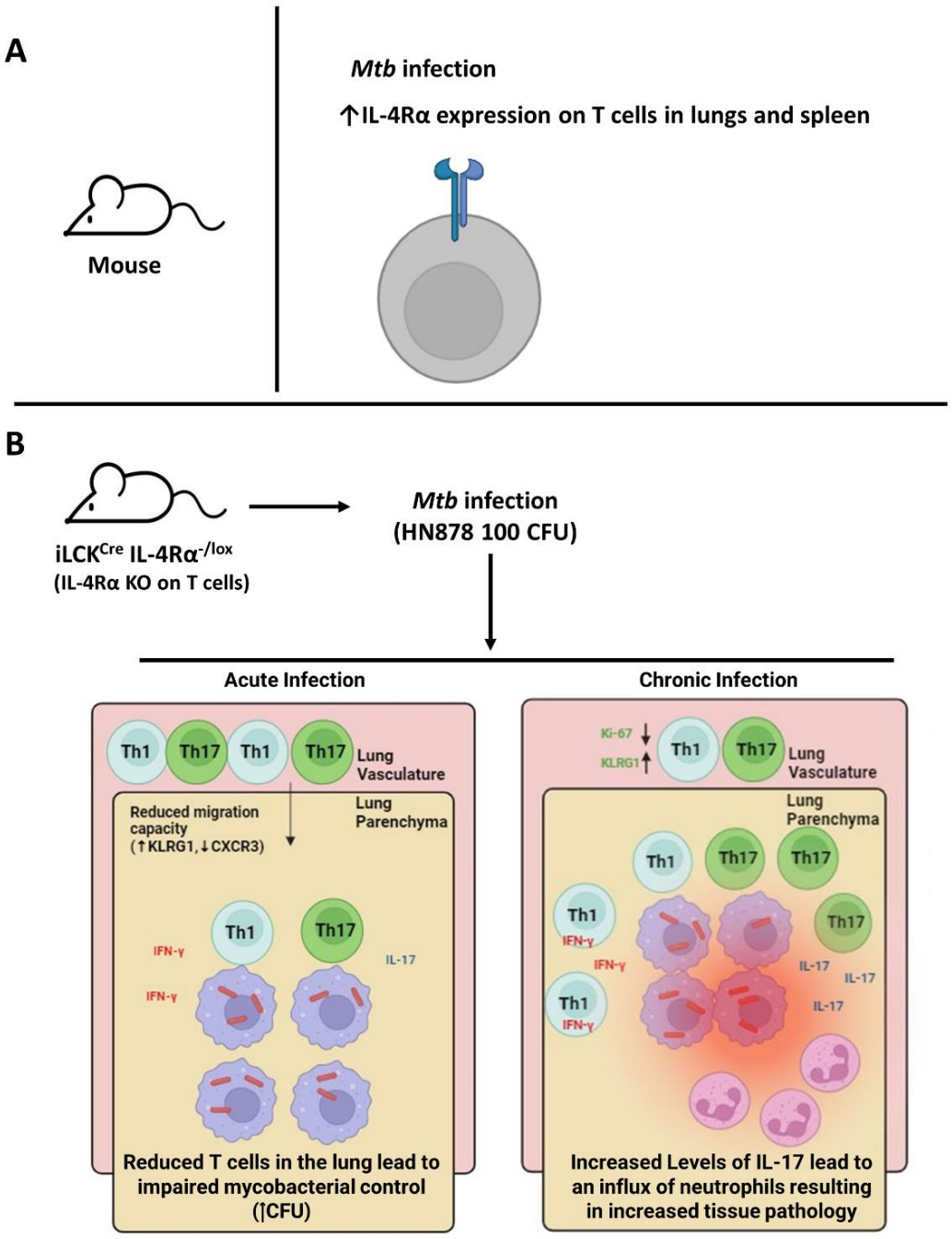

Figure 4.1: Proposed model on the effect of IL-4Rα loss on T cells has during Mtb infection. **(A)** Infection with Mtb, or progression to active disease causes an increase in IL-4Rα expression on T cells. **(B)** Our study in the mouse model showed that loss of IL-4Rα on T cells leads to a dysregulated immune response, marked by a significant increase in terminal effectors which poorly infiltrate into the lung tissue. The lower levels of T cells in the lungs, during **acute** infection leads to impaired mycobacterial control and subsequent increased bacterial burden. During **chronic** *Mtb* infection, the levels of T cells in the lungs of both WT and KO are similar. However, a combination of short-lived, terminally differentiated CD4 effectors (↑KLRG1 and ↓Ki-67) and high bacterial burden results in greater IL-17 secretion compared to controls. The IL-17 recruits substantial amounts of neutrophils which cause tissue damage instead of bacterial control (↑NO and ↓alveolar free-space). Ultimately resulting in increased mortality (Image generated in Biorender).

It is important to remember that there are also limitations in animal models used to study TB disease. The observations made by the Barber group that describes how in mice terminally differentiated Th1 effectors cells do not readily migrate into the lung, an observation we see in our own study, is not observed in macaques [43]. These type of discrepancies in important model systems are a reminder that there limitations to the conclusions we can make, and more importantly, that they may not necessarily translate into what we see in humans. An optimal immune response requires a finely tuned balance between pro- and anti-inflammatory signals, to efficiently curb Mtb replication while limiting tissue destruction [185, 252, 278]. We showed that loss of IL-4Rα on T cells did not lead to any differences in T_{regs} which would mitigate inflammation. Conversely, we show that decreased infiltration into the lung tissue during acute infection allows *Mtb* to establish. Although this stabilizes during chronic infection, the increased secretion of IL-17 in the IL-4Rα KO mice leads to neutrophilia, resulting in enhanced tissue destruction and consequently increased mortality (Figure 4.1B). In conclusion, our study demonstrates that absence of IL-4Rα on T cells promotes a predominant Th1/Th17 response, that results in delayed recruitment into the lung tissue, which ultimately proves detrimental for the host. This is the first study to describe the T cell specific role of IL-4Rα in TB.

Appendix

Lymphoid population gating strategy

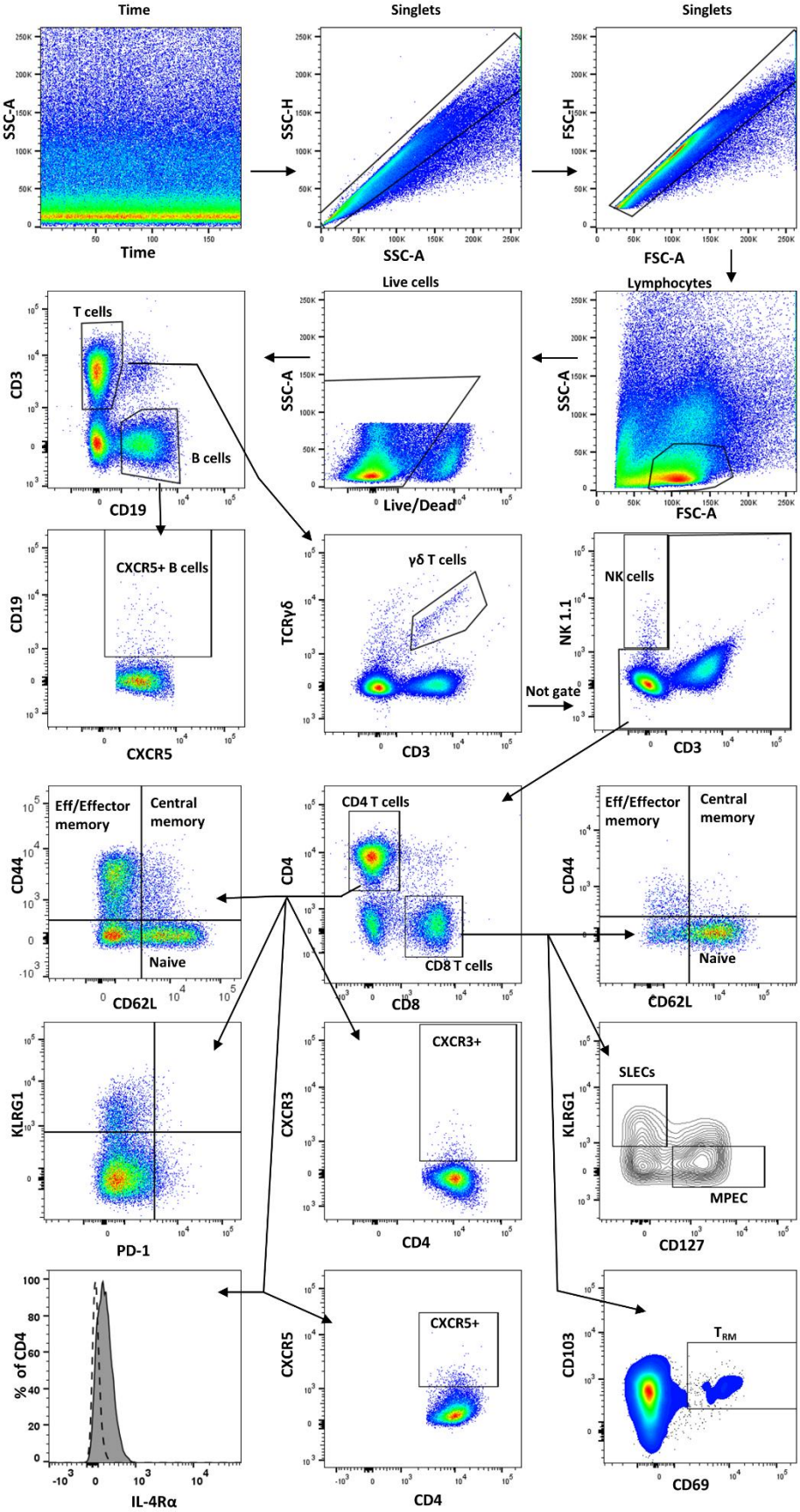

Myeloid population gating strategy

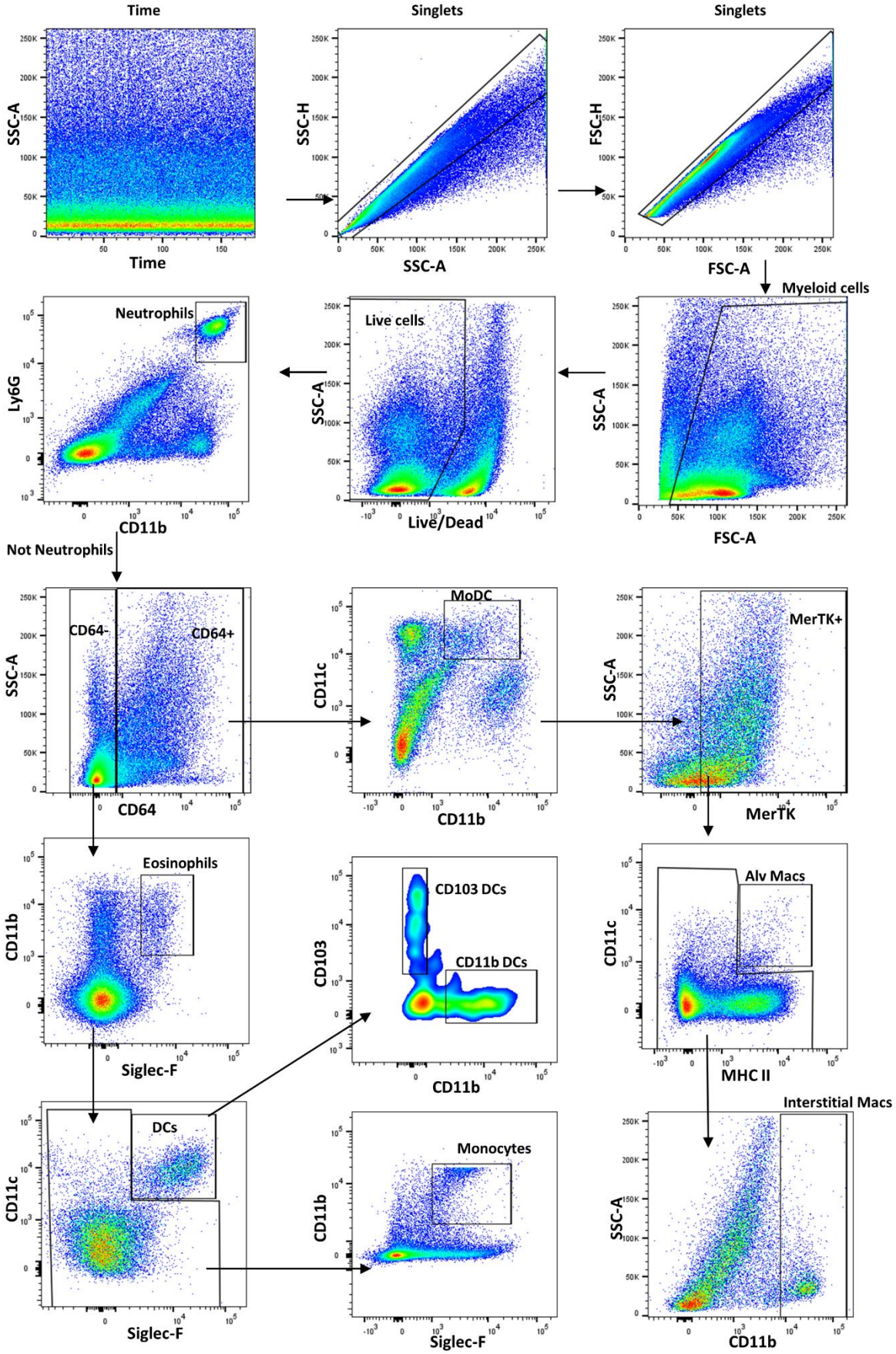

Flow Cytometry panels

Panel 1: Lymphoid 1

CD3-A700, CD4-Bv421, CD8-Bv510, CD19-PerCP, CD44-FITC, CD62L-APC, CXCR5-PeCy7, IL-4Rα-PE, TCRγδ-biotin (PE-Dazzle), NK1.1-APCcy7

Panel 2: Lymphoid 2

CD3-A700, CD4-Bv421, CD8-APC, PD-1-FITC, CD103-PerCP, KLRG1-Bv786, CD69-Bv510, CD127-PeCy7,CXCR3-PE

Panel 3: Myeloid 1 (Lung)

Ly6G-FITC, Ly6C-PerCP, MerTK-Bv786, CD11b-Bv421, CD64-PeCy7, CD103-PE, MHCII-A700, CD11c-APC, SiglecF-APCcy7

Panel 4: Meyeloid 2 (LN)

Ly6G-FITC, Ly6C-PerCP, CD8a-Bv510, CD11b-Bv421, F4/80-PeCy7, CD103-PE, MHCII-A700, CD11c-APC, CD169-APCcy7

Panel 5: Lymphoid Transcription Factors

CD3-A700, CD4-Bv421, CD8-Bv510, RORγt-PerCp, GATA3-PeCY7, T-bet-PE, FoxP3-APC

Panel 6: Lymphoid Proliferation

CD3-A700, CD4-Bv421, CD8-Bv510, Ki-67-PE

Panel 7:Lymphoid Cytokines

CD3-PE-Dazzle, CD4-Bv421, CD8-APC, IFNγ-A700, TNF-APCcy7, IL-17-Bv650, IL-2-PE, and IL-4-APC

Reagent List

1. **General Lab Solutions**

Saline [0.9% (w/v) NaCl]
4.5 g NaCl in 500 ml ddH_2O

Tissue homogenisation solution [0.04% (v/v) Tween 80 in Saline]
200 µl Tween-80 in 500 ml Saline

1X PBS, pH 7.4
purchased from Thermo Fisher Scientific (Massachusetts, United States) [10010023]

Neutral buffered tissue storage solution [10% (v/v) formaldehyde in 1X PBS]
100 ml of 38-40% Formaldehyde solution in 900 ml of 1X PBS, adust pH to 7.0

Cell Lysis solution
100 µl Triton-X100 (0.1% [v/v]) added to 100 ml of 1X PBS, pH 7.4

FACS buffer
0.1% (w/v) of BSA in 1X PBS, pH 7.4

1g of BSA

Lung Digestion buffer (5X)
0.0018 g Collagenase Type I
0.0002 g DNAse I
Dissolve in 20 ml DMEM (no FCS) and filter sterilize (0.22 um). Dilute 1:5 in DMEM to obtain working concentration.

2. ELISA Buffers

ELISA Coating buffer, pH 9.5
1.6g Na_2CO_3
2.9g $NaHCO_3$
4.2g NaCl

In 1000 ml ddH_2O

ELISA Blocking buffer
2% (w/v) BSA in PBS

ELISA Dilution buffer
1% (w/v) BSA in PBS

ELISA Washing buffer (20X)
20g KCL
20g $KH_2PO_4.2H_2O$
800g NaCl
50ml Tween-20

Dissolve in 5 L ddH_2O in a volumetric flask. Dilute 1:20 with ddH_2O to obtain working concentration as needed.

ELISA AP substrate buffer
0.2g NaN_3
97ml diethanolamine
0.8g $MgCl_2.6H_2O$

Adjust to pH 9.8 and adjust volume to 1 L using ddH_2O.

3. Greiss assay reagents (NO detection)
Greiss Reagent Standard (1mM $NaNO_2$)

6.899mg $NaNO_2$ dissolved in 100 ml of ddH_2O.

Greiss Reagent 1

1 g sulfanilamide dissolved in 100 ml of 2.5% of phosphoric acid.

Greiss Reagent 2

0.1 g napthyl-ethylene-diamine dissolved in 100 ml of 2.5 % phosphoric acid

References

1. WHO, *Global Tuberculosis Report 2022*. 2022.
2. Diana, M.C.-H. and J.R.-M. Alfonso, *Epidemiological Burden of Tuberculosis in Developing Countries*, in *Current Topics in Public Health*, J.R.-M. Alfonso, Editor. 2013, IntechOpen: Rijeka. p. Ch. 15.
3. Mekonnen, H.S. and A.W. Azagew, *Non-adherence to anti-tuberculosis treatment, reasons and associated factors among TB patients attending at Gondar town health centers, Northwest Ethiopia.* BMC Res Notes, 2018. **11**(1): p. 691.
4. Nidoi, J., et al., *Impact of socio-economic factors on Tuberculosis treatment outcomes in north-eastern Uganda: a mixed methods study.* BMC Public Health, 2021. **21**(1): p. 2167.
5. Tesfahuneygn, G., G. Medhin, and M. Legesse, *Adherence to Anti-tuberculosis treatment and treatment outcomes among tuberculosis patients in Alamata District, northeast Ethiopia.* BMC Res Notes, 2015. **8**: p. 503.
6. Tola, H.H., et al., *Tuberculosis Treatment Non-Adherence and Lost to Follow Up among TB Patients with or without HIV in Developing Countries: A Systematic Review.* Iran J Public Health, 2015. **44**(1): p. 1-11.
7. Koomen, L.E.M., R. Burger, and E.K.A. van Doorslaer, *Effects and determinants of tuberculosis drug stockouts in South Africa.* BMC Health Services Research, 2019. **19**(1): p. 213.
8. Connolly, L.E., P.H. Edelstein, and L. Ramakrishnan, *Why is long-term therapy required to cure tuberculosis?* PLoS Med, 2007. **4**(3): p. e120.
9. Chakraborty, P., et al., *Biofilm formation in the lung contributes to virulence and drug tolerance of Mycobacterium tuberculosis.* Nat Commun, 2021. **12**(1): p. 1606.
10. Dartois, V.A. and E.J. Rubin, *Anti-tuberculosis treatment strategies and drug development: challenges and priorities.* Nature Reviews Microbiology, 2022. **20**(11): p. 685-701.
11. Verma, A., et al., *Tuberculosis: The success tale of less explored dormant Mycobacterium tuberculosis.* Front Cell Infect Microbiol, 2022. **12**: p. 1079569.
12. Sotgiu, G., et al., *Tuberculosis treatment and drug regimens.* Cold Spring Harb Perspect Med, 2015. **5**(5): p. a017822.
13. Dorman, S.E., et al., *Four-Month Rifapentine Regimens with or without Moxifloxacin for Tuberculosis.* New England Journal of Medicine, 2021. **384**(18): p. 1705-1718.
14. Allué-Guardia, A., J.I. García, and J.B. Torrelles, *Evolution of Drug-Resistant Mycobacterium tuberculosis Strains and Their Adaptation to the Human Lung Environment.* Frontiers in Microbiology, 2021. **12**.
15. Dulberger, C.L., E.J. Rubin, and C.C. Boutte, *The mycobacterial cell envelope — a moving target.* Nature Reviews Microbiology, 2020. **18**(1): p. 47-59.
16. Han, S.J., et al., *Complete genome sequence of Mycobacterium tuberculosis K from a Korean high school outbreak, belonging to the Beijing family.* Stand Genomic Sci, 2015. **10**: p. 78.
17. Jarlier, V. and H. Nikaido, *Permeability barrier to hydrophilic solutes in Mycobacterium chelonei.* J Bacteriol, 1990. **172**(3): p. 1418-23.
18. Patterson, B. and R. Wood, *Is cough really necessary for TB transmission?* Tuberculosis (Edinb), 2019. **117**: p. 31-35.
19. Dinkele, R., et al., *Aerosolization of Mycobacterium tuberculosis by Tidal Breathing.* Am J Respir Crit Care Med, 2022. **206**(2): p. 206-216.
20. Duguid, J.P., *The size and the duration of air-carriage of respiratory droplets and droplet-nuclei.* J Hyg (Lond), 1946. **44**(6): p. 471-9.
21. Riley, R.L., et al., *Aerial dissemination of pulmonary tuberculosis. A two-year study of contagion in a tuberculosis ward. 1959.* Am J Epidemiol, 1995. **142**(1): p. 3-14.
22. Xu, G., et al., *Insights into battles between Mycobacterium tuberculosis and macrophages.* Protein & cell, 2014. **5**(10): p. 728-736.
23. Cohen, S.B., et al., *Alveolar Macrophages Provide an Early Mycobacterium tuberculosis Niche and Initiate Dissemination.* Cell Host Microbe, 2018. **24**(3): p. 439-446.e4.

24. Pai, M., et al., *Tuberculosis.* Nature Reviews Disease Primers, 2016. **2**(1): p. 16076.
25. Ehrt, S. and D. Schnappinger, *Mycobacterial survival strategies in the phagosome: defence against host stresses.* Cellular Microbiology, 2009. **11**(8): p. 1170-1178.
26. Clemens, D.L. and M.A. Horwitz, *Characterization of the Mycobacterium tuberculosis phagosome and evidence that phagosomal maturation is inhibited.* J Exp Med, 1995. **181**(1): p. 257-70.
27. Flynn, J.L. and J. Chan, *Immune evasion by Mycobacterium tuberculosis: living with the enemy.* Curr Opin Immunol, 2003. **15**(4): p. 450-5.
28. Fratti, R.A., et al., *Mycobacterium tuberculosis glycosylated phosphatidylinositol causes phagosome maturation arrest.* Proc Natl Acad Sci U S A, 2003. **100**(9): p. 5437-42.
29. Fulton, S.A., et al., *Inhibition of major histocompatibility complex II expression and antigen processing in murine alveolar macrophages by Mycobacterium bovis BCG and the 19-kilodalton mycobacterial lipoprotein.* Infect Immun, 2004. **72**(4): p. 2101-10.
30. Hanekom, W.A., et al., *Mycobacterium tuberculosis inhibits maturation of human monocyte-derived dendritic cells in vitro.* J Infect Dis, 2003. **188**(2): p. 257-66.
31. Sturgill-Koszycki, S., et al., *Lack of acidification in Mycobacterium phagosomes produced by exclusion of the vesicular proton-ATPase.* Science, 1994. **263**(5147): p. 678-81.
32. Bhavanam, S., et al., *Understanding the pathophysiology of the human TB lung granuloma using in vitro granuloma models.* Future Microbiol, 2016. **11**: p. 1073-89.
33. Chai, Q., Y. Zhang, and C.H. Liu, *Mycobacterium tuberculosis: An Adaptable Pathogen Associated With Multiple Human Diseases.* Frontiers in Cellular and Infection Microbiology, 2018. **8**(158).
34. Soldevilla, P., C. Vilaplana, and P.-J. Cardona, *Mouse Models for Mycobacterium tuberculosis Pathogenesis: Show and Do Not Tell.* Pathogens, 2023. **12**(1): p. 49.
35. Cronan, M.R., *In the Thick of It: Formation of the Tuberculous Granuloma and Its Effects on Host and Therapeutic Responses.* Frontiers in Immunology, 2022. **13**.
36. Ramakrishnan, L., *Revisiting the role of the granuloma in tuberculosis.* Nature Reviews Immunology, 2012. **12**(5): p. 352-366.
37. Cronan, M.R., et al., *A non-canonical type 2 immune response coordinates tuberculous granuloma formation and epithelialization.* Cell, 2021. **184**(7): p. 1757-1774.e14.
38. Gern, B.H., et al., *TGFβ restricts expansion, survival, and function of T cells within the tuberculous granuloma.* Cell Host Microbe, 2021. **29**(4): p. 594-606.e6.
39. Marin, N.D., et al., *Friend or Foe: The Protective and Pathological Roles of Inducible Bronchus-Associated Lymphoid Tissue in Pulmonary Diseases.* J Immunol, 2019. **202**(9): p. 2519-2526.
40. Das, S., et al., *Lung Epithelial Signaling Mediates Early Vaccine-Induced CD4(+) T Cell Activation and Mycobacterium tuberculosis Control.* mBio, 2021. **12**(4): p. e0146821.
41. Kruh, N.A., et al., *Portrait of a pathogen: the Mycobacterium tuberculosis proteome in vivo.* PLoS One, 2010. **5**(11): p. e13938.
42. Rahman, S., et al., *Compartmentalization of immune responses in human tuberculosis: few CD8+ effector T cells but elevated levels of FoxP3+ regulatory t cells in the granulomatous lesions.* Am J Pathol, 2009. **174**(6): p. 2211-24.
43. Kauffman, K.D., et al., *Defective positioning in granulomas but not lung-homing limits CD4 T-cell interactions with Mycobacterium tuberculosis-infected macrophages in rhesus macaques.* Mucosal Immunol, 2018. **11**(2): p. 462-473.
44. Esaulova, E., et al., *The immune landscape in tuberculosis reveals populations linked to disease and latency.* Cell Host Microbe, 2021. **29**(2): p. 165-178.e8.
45. Lin, P.L., et al., *Sterilization of granulomas is common in active and latent tuberculosis despite within-host variability in bacterial killing.* Nature Medicine, 2014. **20**(1): p. 75-79.
46. Gideon, H.P., et al., *Variability in Tuberculosis Granuloma T Cell Responses Exists, but a Balance of Pro- and Anti-inflammatory Cytokines Is Associated with Sterilization.* PLOS Pathogens, 2015. **11**(1): p. e1004603.

47. Gideon, H.P., et al., *Multimodal profiling of lung granulomas in macaques reveals cellular correlates of tuberculosis control.* Immunity, 2022. **55**(5): p. 827-846.e10.
48. Grant, N.L., et al., *T cell transcription factor expression evolves over time in granulomas from Mycobacterium tuberculosis-infected cynomolgus macaques.* Cell Rep, 2022. **39**(7): p. 110826.
49. Ashenafi, S. and S. Brighenti, *Reinventing the human tuberculosis (TB) granuloma: Learning from the cancer field.* Frontiers in Immunology, 2022. **13**.
50. Cooper, A.M., K.D. Mayer-Barber, and A. Sher, *Role of innate cytokines in mycobacterial infection.* Mucosal Immunol, 2011. **4**(3): p. 252-60.
51. Khader, S.A., et al., *In a murine tuberculosis model, the absence of homeostatic chemokines delays granuloma formation and protective immunity.* J Immunol, 2009. **183**(12): p. 8004-14.
52. Pagán, A.J. and L. Ramakrishnan, *The Formation and Function of Granulomas.* Annu Rev Immunol, 2018. **36**: p. 639-665.
53. Cadena, A.M., S.M. Fortune, and J.L. Flynn, *Heterogeneity in tuberculosis.* Nat Rev Immunol, 2017. **17**(11): p. 691-702.
54. Chandra, P., S.J. Grigsby, and J.A. Philips, *Immune evasion and provocation by Mycobacterium tuberculosis.* Nature Reviews Microbiology, 2022. **20**(12): p. 750-766.
55. Tian, T., et al., *In vivo depletion of CD11c+ cells delays the CD4+ T cell response to Mycobacterium tuberculosis and exacerbates the outcome of infection.* J Immunol, 2005. **175**(5): p. 3268-72.
56. Wolf, A.J., et al., *Mycobacterium tuberculosis infects dendritic cells with high frequency and impairs their function in vivo.* J Immunol, 2007. **179**(4): p. 2509-19.
57. Flynn, J.L., et al., *IL-12 increases resistance of BALB/c mice to Mycobacterium tuberculosis infection.* J Immunol, 1995. **155**(5): p. 2515-24.
58. Hölscher, C., et al., *A protective and agonistic function of IL-12p40 in mycobacterial infection.* J Immunol, 2001. **167**(12): p. 6957-66.
59. Khader, S.A., et al., *Interleukin 12p40 is required for dendritic cell migration and T cell priming after Mycobacterium tuberculosis infection.* J Exp Med, 2006. **203**(7): p. 1805-15.
60. Chackerian, A.A., et al., *Dissemination of Mycobacterium tuberculosis is influenced by host factors and precedes the initiation of T-cell immunity.* Infect Immun, 2002. **70**(8): p. 4501-9.
61. Wolf, A.J., et al., *Initiation of the adaptive immune response to Mycobacterium tuberculosis depends on antigen production in the local lymph node, not the lungs.* J Exp Med, 2008. **205**(1): p. 105-15.
62. Reiley, W.W., et al., *ESAT-6-specific CD4 T cell responses to aerosol Mycobacterium tuberculosis infection are initiated in the mediastinal lymph nodes.* Proc Natl Acad Sci U S A, 2008. **105**(31): p. 10961-6.
63. Khader, S.A., et al., *IL-23 and IL-17 in the establishment of protective pulmonary CD4+ T cell responses after vaccination and during Mycobacterium tuberculosis challenge.* Nat Immunol, 2007. **8**(4): p. 369-77.
64. Knudson, C.J., et al., *The pulmonary localization of virus-specific T lymphocytes is governed by the tissue tropism of infection.* J Virol, 2014. **88**(16): p. 9010-6.
65. Lawrence, C.W. and T.J. Braciale, *Activation, differentiation, and migration of naive virus-specific CD8+ T cells during pulmonary influenza virus infection.* J Immunol, 2004. **173**(2): p. 1209-18.
66. Mehra, A., et al., *Mycobacterium tuberculosis type VII secreted effector EsxH targets host ESCRT to impair trafficking.* PLoS Pathog, 2013. **9**(10): p. e1003734.
67. Armstrong, J.A. and P.D. Hart, *Phagosome-lysosome interactions in cultured macrophages infected with virulent tubercle bacilli. Reversal of the usual nonfusion pattern and observations on bacterial survival.* J Exp Med, 1975. **142**(1): p. 1-16.
68. Portal-Celhay, C., et al., *Mycobacterium tuberculosis EsxH inhibits ESCRT-dependent CD4(+) T-cell activation.* Nat Microbiol, 2016. **2**: p. 16232.

69. Tobian, A.A., et al., *Alternate class I MHC antigen processing is inhibited by Toll-like receptor signaling pathogen-associated molecular patterns: Mycobacterium tuberculosis 19-kDa lipoprotein, CpG DNA, and lipopolysaccharide.* J Immunol, 2003. **171**(3): p. 1413-22.
70. Fortune, S.M., et al., *Mycobacterium tuberculosis inhibits macrophage responses to IFN-gamma through myeloid differentiation factor 88-dependent and -independent mechanisms.* J Immunol, 2004. **172**(10): p. 6272-80.
71. Ernst, J.D., *Mechanisms of M. tuberculosis Immune Evasion as Challenges to TB Vaccine Design.* Cell Host Microbe, 2018. **24**(1): p. 34-42.
72. Jenkins, M.K. and R.H. Schwartz, *Antigen presentation by chemically modified splenocytes induces antigen-specific T cell unresponsiveness in vitro and in vivo.* J Exp Med, 1987. **165**(2): p. 302-19.
73. Bhatt, K., et al., *B7 costimulation is critical for host control of chronic Mycobacterium tuberculosis infection.* J Immunol, 2009. **182**(6): p. 3793-800.
74. Schreiber, H.A., et al., *Dendritic cells in chronic mycobacterial granulomas restrict local anti-bacterial T cell response in a murine model.* PLoS One, 2010. **5**(7): p. e11453.
75. Zhu, J., et al., *The transcription factor T-bet is induced by multiple pathways and prevents an endogenous Th2 cell program during Th1 cell responses.* Immunity, 2012. **37**(4): p. 660-73.
76. Zhu, J. and W.E. Paul, *Peripheral CD4+ T-cell differentiation regulated by networks of cytokines and transcription factors.* Immunol Rev, 2010. **238**(1): p. 247-62.
77. Eyerich, S., et al., *Th22 cells represent a distinct human T cell subset involved in epidermal immunity and remodeling.* J Clin Invest, 2009. **119**(12): p. 3573-85.
78. Fang, D. and J. Zhu, *Dynamic balance between master transcription factors determines the fates and functions of CD4 T cell and innate lymphoid cell subsets.* J Exp Med, 2017. **214**(7): p. 1861-1876.
79. Zhu, X. and J. Zhu, *CD4 T Helper Cell Subsets and Related Human Immunological Disorders.* Int J Mol Sci, 2020. **21**(21).
80. Chen, Y., et al., *Regulatory T cell clones induced by oral tolerance: suppression of autoimmune encephalomyelitis.* Science, 1994. **265**(5176): p. 1237-40.
81. Leung, S., et al., *The cytokine milieu in the interplay of pathogenic Th1/Th17 cells and regulatory T cells in autoimmune disease.* Cellular & Molecular Immunology, 2010. **7**(3): p. 182-189.
82. Cooper, A.M., et al., *Disseminated tuberculosis in interferon gamma gene-disrupted mice.* J Exp Med, 1993. **178**(6): p. 2243-7.
83. Cooper, A.M., et al., *Interleukin 12 (IL-12) is crucial to the development of protective immunity in mice intravenously infected with mycobacterium tuberculosis.* J Exp Med, 1997. **186**(1): p. 39-45.
84. Flory, C.M., R.D. Hubbard, and F.M. Collins, *Effects of in vivo T lymphocyte subset depletion on mycobacterial infections in mice.* J Leukoc Biol, 1992. **51**(3): p. 225-9.
85. Flynn, J.L., et al., *An essential role for interferon gamma in resistance to Mycobacterium tuberculosis infection.* J Exp Med, 1993. **178**(6): p. 2249-54.
86. Leveton, C., et al., *T-cell-mediated protection of mice against virulent Mycobacterium tuberculosis.* Infect Immun, 1989. **57**(2): p. 390-5.
87. Müller, I., et al., *Impaired resistance to Mycobacterium tuberculosis infection after selective in vivo depletion of L3T4+ and Lyt-2+ T cells.* Infect Immun, 1987. **55**(9): p. 2037-41.
88. Sullivan, B.M., et al., *Increased susceptibility of mice lacking T-bet to infection with Mycobacterium tuberculosis correlates with increased IL-10 and decreased IFN-gamma production.* J Immunol, 2005. **175**(7): p. 4593-602.
89. O'Garra, A., et al., *The Immune Response in Tuberculosis.* Annual Review of Immunology, 2013. **31**(1): p. 475-527.

90. Zhang, S.Y., et al., *Inborn errors of interferon (IFN)-mediated immunity in humans: insights into the respective roles of IFN-alpha/beta, IFN-gamma, and IFN-lambda in host defense.* Immunol Rev, 2008. **226**: p. 29-40.
91. Kalsdorf, B., et al., *HIV-1 Infection Impairs the Bronchoalveolar T-Cell Response to Mycobacteria.* American Journal of Respiratory and Critical Care Medicine, 2009. **180**(12): p. 1262-1270.
92. Eldholm, V., et al., *Impact of HIV co-infection on the evolution and transmission of multidrug-resistant tuberculosis.* eLife, 2016. **5**: p. e16644.
93. Du, G., et al., *TCR repertoire, clonal dominance, and pulmonary trafficking of mycobacterium-specific CD4+ and CD8+ T effector cells in immunity against tuberculosis.* J Immunol, 2010. **185**(7): p. 3940-7.
94. Zeng, G., G. Zhang, and X. Chen, *Th1 cytokines, true functional signatures for protective immunity against TB?* Cell Mol Immunol, 2018. **15**(3): p. 206-215.
95. Saito, S. and M. Nakano, *Nitric oxide production by peritoneal macrophages of Mycobacterium bovis BCG-infected or non-infected mice: regulatory role of T lymphocytes and cytokines.* J Leukoc Biol, 1996. **59**(6): p. 908-15.
96. Gutierrez, M.G., et al., *Autophagy is a defense mechanism inhibiting BCG and Mycobacterium tuberculosis survival in infected macrophages.* Cell, 2004. **119**(6): p. 753-66.
97. Russell, M.S., et al., *IFN-gamma expressed by T cells regulates the persistence of antigen presentation by limiting the survival of dendritic cells.* J Immunol, 2009. **183**(12): p. 7710-8.
98. Cruz, A., et al., *Cutting edge: IFN-gamma regulates the induction and expansion of IL-17-producing CD4 T cells during mycobacterial infection.* J Immunol, 2006. **177**(3): p. 1416-20.
99. Ahrends, T., et al., *CD4+ T Cell Help Confers a Cytotoxic T Cell Effector Program Including Coinhibitory Receptor Downregulation and Increased Tissue Invasiveness.* Immunity, 2017. **47**(5): p. 848-861.e5.
100. Lu, Y.-J., et al., *CD4 T cell help prevents CD8 T cell exhaustion and promotes control of Mycobacterium tuberculosis infection.* Cell Reports, 2021. **36**(11): p. 109696.
101. Sakai, S., et al., *Cutting Edge: Control of Mycobacterium tuberculosis Infection by a Subset of Lung Parenchyma–Homing CD4 T Cells.* The Journal of Immunology, 2014. **192**(7): p. 2965-2969.
102. Sakai, S., et al., *CD4 T Cell-Derived IFN-γ Plays a Minimal Role in Control of Pulmonary Mycobacterium tuberculosis Infection and Must Be Actively Repressed by PD-1 to Prevent Lethal Disease.* PLOS Pathogens, 2016. **12**(5): p. e1005667.
103. Barber, D.L., et al., *CD4 T cells promote rather than control tuberculosis in the absence of PD-1-mediated inhibition.* J Immunol, 2011. **186**(3): p. 1598-607.
104. Mahnke, Y.D., et al., *Selective expansion of polyfunctional pathogen-specific CD4(+) T cells in HIV-1-infected patients with immune reconstitution inflammatory syndrome.* Blood, 2012. **119**(13): p. 3105-12.
105. Filley, E.A., et al., *The effect of Mycobacterium tuberculosis on the susceptibility of human cells to the stimulatory and toxic effects of tumour necrosis factor.* Immunology, 1992. **77**(4): p. 505-9.
106. Gallegos, A.M., et al., *A Gamma Interferon Independent Mechanism of CD4 T Cell Mediated Control of M. tuberculosis Infection in vivo.* PLOS Pathogens, 2011. **7**(5): p. e1002052.
107. Tameris, M.D., et al., *Safety and efficacy of MVA85A, a new tuberculosis vaccine, in infants previously vaccinated with BCG: a randomised, placebo-controlled phase 2b trial.* Lancet, 2013. **381**(9871): p. 1021-8.
108. Van Dis, E., et al., *IFN-γ-independent control of M. tuberculosis requires CD4 T cell-derived GM-CSF and activation of HIF-1α.* PLoS Pathog, 2022. **18**(7): p. e1010721.
109. Arai, N., et al., *Complete nucleotide sequence of the chromosomal gene for human IL-4 and its expression.* The Journal of Immunology, 1989. **142**(1): p. 274-282.

110. D'Eustachio, P., et al., *The IL-4 gene maps to chromosome 11, near the gene encoding IL-3.* The Journal of Immunology, 1988. **141**(9): p. 3067-3071.
111. McKenzie, A.N., et al., *Structural comparison and chromosomal localization of the human and mouse IL-13 genes.* J Immunol, 1993. **150**(12): p. 5436-44.
112. Santangelo, S., et al., *DNA Methylation Changes at Human Th2 Cytokine Genes Coincide with DNase I Hypersensitive Site Formation During CD4⁺ T Cell Differentiation.* The Journal of Immunology, 2002. **169**(4): p. 1893-1903.
113. Williams, A., et al., *Hypersensitive site 6 of the Th2 locus control region is essential for Th2 cytokine expression.* Proceedings of the National Academy of Sciences, 2013. **110**(17): p. 6955-6960.
114. Lee, D.U. and A. Rao, *Molecular analysis of a locus control region in the T helper 2 cytokine gene cluster: A target for STAT6 but not GATA3.* Proceedings of the National Academy of Sciences of the United States of America, 2004. **101**(45): p. 16010-16015.
115. Koh, B.H., et al., *Th2 LCR is essential for regulation of Th2 cytokine genes and for pathogenesis of allergic asthma.* Proceedings of the National Academy of Sciences, 2010. **107**(23): p. 10614-10619.
116. van Panhuys, N., et al., *Basophils are the major producers of IL-4 during primary helminth infection.* J Immunol, 2011. **186**(5): p. 2719-28.
117. Seder, R.A., et al., *The presence of interleukin 4 during in vitro priming determines the lymphokine-producing potential of CD4+ T cells from T cell receptor transgenic mice.* J Exp Med, 1992. **176**(4): p. 1091-8.
118. Plaut, M., et al., *Mast cell lines produce lymphokines in response to cross-linkage of Fc epsilon RI or to calcium ionophores.* Nature, 1989. **339**(6219): p. 64-7.
119. Brown, M.A., et al., *B cell stimulatory factor-1/interleukin-4 mRNA is expressed by normal and transformed mast cells.* Cell, 1987. **50**(5): p. 809-818.
120. Nonaka, M., et al., *Distinct immunohistochemical localization of IL-4 in human inflamed airway tissues. IL-4 is localized to eosinophils in vivo and is released by peripheral blood eosinophils.* The Journal of Immunology, 1995. **155**(6): p. 3234-3244.
121. Yoshimoto, T. and W.E. Paul, *CD4pos, NK1.1pos T cells promptly produce interleukin 4 in response to in vivo challenge with anti-CD3.* J Exp Med, 1994. **179**(4): p. 1285-95.
122. Akbari, O., et al., *Essential role of NKT cells producing IL-4 and IL-13 in the development of allergen-induced airway hyperreactivity.* Nat Med, 2003. **9**(5): p. 582-8.
123. Ehrchen, J.M., et al., *Keratinocytes determine Th1 immunity during early experimental leishmaniasis.* PLoS Pathog, 2010. **6**(4): p. e1000871.
124. Seder, R.A. and W.E. Paul, *Acquisition of lymphokine-producing phenotype by CD4+ T cells.* Annu Rev Immunol, 1994. **12**: p. 635-73.
125. Ferrick, D.A., et al., *Differential production of interferon-gamma and interleukin-4 in response to Th1- and Th2-stimulating pathogens by gamma delta T cells in vivo.* Nature, 1995. **373**(6511): p. 255-7.
126. Nelms, K., et al., *The IL-4 receptor: signaling mechanisms and biologic functions.* Annu Rev Immunol, 1999. **17**: p. 701-38.
127. Zheng, W. and R.A. Flavell, *The transcription factor GATA-3 is necessary and sufficient for Th2 cytokine gene expression in CD4 T cells.* Cell, 1997. **89**(4): p. 587-96.
128. Jankovic, D., et al., *Single Cell Analysis Reveals That IL-4 Receptor/Stat6 Signaling Is Not Required for the In Vivo or In Vitro Development of CD4+ Lymphocytes with a Th2 Cytokine Profile.* The Journal of Immunology, 2000. **164**(6): p. 3047-3055.
129. Lowenthal, J.W., et al., *Expression of high affinity receptors for murine interleukin 4 (BSF-1) on hemopoietic and nonhemopoietic cells.* J Immunol, 1988. **140**(2): p. 456-64.
130. Miloux, B., et al., *Cloning of the human IL-13R alpha1 chain and reconstitution with the IL4R alpha of a functional IL-4/IL-13 receptor complex.* FEBS Lett, 1997. **401**(2-3): p. 163-6.

131. Andrews, A.L., et al., *Kinetic analysis of the interleukin-13 receptor complex.* J Biol Chem, 2002. **277**(48): p. 46073-8.
132. Hilton, D.J., et al., *Cloning and characterization of a binding subunit of the interleukin 13 receptor that is also a component of the interleukin 4 receptor.* Proceedings of the National Academy of Sciences of the United States of America, 1996. **93**(1): p. 497-501.
133. LaPorte, S.L., et al., *Molecular and structural basis of cytokine receptor pleiotropy in the interleukin-4/13 system.* Cell, 2008. **132**(2): p. 259-272.
134. Keegan, A.D., W.J. Leonard, and J. Zhu, *Recent advances in understanding the role of IL-4 signaling.* Fac Rev, 2021. **10**: p. 71.
135. Keegan, A.D. and J. Zamoran, *Regulation of gene expression, growth, and cell survival by IL-4: Contribution of multiple signaling pathways.* Cell Research, 1998. **8**(1): p. 1-13.
136. Kapsenberg, M.L., *Dendritic-cell control of pathogen-driven T-cell polarization.* Nature Reviews Immunology, 2003. **3**(12): p. 984-993.
137. Khader, S.A. and A.M. Cooper, *IL-23 and IL-17 in tuberculosis.* Cytokine, 2008. **41**(2): p. 79-83.
138. Leech, M.D. and R.K. Grencis, *Induction of enhanced immunity to intestinal nematodes using IL-9-producing dendritic cells.* J Immunol, 2006. **176**(4): p. 2505-11.
139. Martino, A., et al., *Dendritic cells derived from BCG-infected precursors induce Th2-like immune response.* J Leukoc Biol, 2004. **76**(4): p. 827-34.
140. Dwivedi, V.P., et al., *Mycobacterium tuberculosis directs T helper 2 cell differentiation by inducing interleukin-1β production in dendritic cells.* J Biol Chem, 2012. **287**(40): p. 33656-63.
141. Heuer, M., et al., *The 30-kDa and 38-kDa antigens from Mycobacterium tuberculosis induce partial maturation of human dendritic cells shifting CD4(+) T cell responses towards IL-4 production.* BMC Immunol, 2013. **14**: p. 48.
142. Agrewala, J.N. and R.J. Wilkinson, *Differential regulation of Th1 and Th2 cells by p91-110 and p21-40 peptides of the 16-kD alpha-crystallin antigen of Mycobacterium tuberculosis.* Clin Exp Immunol, 1998. **114**(3): p. 392-7.
143. Manca, C., et al., *Differential monocyte activation underlies strain-specific Mycobacterium tuberculosis pathogenesis.* Infect Immun, 2004. **72**(9): p. 5511-4.
144. North, R.J., *Mice incapable of making IL-4 or IL-10 display normal resistance to infection with Mycobacterium tuberculosis.* Clin Exp Immunol, 1998. **113**(1): p. 55-8.
145. Jung, Y.J., et al., *Evidence inconsistent with a negative influence of T helper 2 cells on protection afforded by a dominant T helper 1 response against Mycobacterium tuberculosis lung infection in mice.* Infect Immun, 2002. **70**(11): p. 6436-43.
146. Heitmann, L., et al., *The IL-13/IL-4Ralpha axis is involved in tuberculosis-associated pathology.* J Pathol, 2014. **234**(3): p. 338-50.
147. Harris, J., et al., *T Helper 2 Cytokines Inhibit Autophagic Control of Intracellular Mycobacterium tuberculosis.* Immunity, 2007. **27**(3): p. 505-517.
148. Martinez, F.O., L. Helming, and S. Gordon, *Alternative activation of macrophages: an immunologic functional perspective.* Annu Rev Immunol, 2009. **27**: p. 451-83.
149. Benoit, M., B. Desnues, and J.L. Mege, *Macrophage polarization in bacterial infections.* J Immunol, 2008. **181**(6): p. 3733-9.
150. Mills, C.D., et al., *M-1/M-2 Macrophages and the Th1/Th2 Paradigm1.* The Journal of Immunology, 2000. **164**(12): p. 6166-6173.
151. Stewart, D., et al., *GENETIC CONTRIBUTION TO THE SEPTIC RESPONSE IN A MOUSE MODEL.* Shock, 2002. **18**(4): p. 342-347.
152. Watanabe, H., et al., *INNATE IMMUNE RESPONSE IN TH1- AND TH2-DOMINANT MOUSE STRAINS.* Shock, 2004. **22**(5): p. 460-466.
153. Himmelrich, H., et al., *The IL-4 rapidly produced in BALB/c mice after infection with Leishmania major down-regulates IL-12 receptor beta 2-chain expression on CD4+ T cells resulting in a state of unresponsiveness to IL-12.* J Immunol, 1998. **161**(11): p. 6156-63.

154. Alleva, D.G., S.B. Kaser, and D.I. Beller, *Intrinsic defects in macrophage IL-12 production associated with immune dysfunction in the MRL/++ and New Zealand Black/White F1 lupus-prone mice and the Leishmania major-susceptible BALB/c strain.* J Immunol, 1998. **161**(12): p. 6878-84.
155. Franzblau, S.G., et al., *Comprehensive analysis of methods used for the evaluation of compounds against Mycobacterium tuberculosis.* Tuberculosis, 2012. **92**(6): p. 453-488.
156. Hernández-Pando, R., et al., *Correlation between the kinetics of Th1, Th2 cells and pathology in a murine model of experimental pulmonary tuberculosis.* Immunology, 1996. **89**(1): p. 26-33.
157. Hernandez-Pando, R., et al., *Pulmonary tuberculosis in BALB/c mice with non-functional IL-4 genes: changes in the inflammatory effects of TNF-alpha and in the regulation of fibrosis.* Eur J Immunol, 2004. **34**(1): p. 174-83.
158. van Crevel, R., et al., *Increased production of interleukin 4 by CD4+ and CD8+ T cells from patients with tuberculosis is related to the presence of pulmonary cavities.* J Infect Dis, 2000. **181**(3): p. 1194-7.
159. Roberts, T., et al., *Immunosuppression during active tuberculosis is characterized by decreased interferon- gamma production and CD25 expression with elevated forkhead box P3, transforming growth factor- beta , and interleukin-4 mRNA levels.* J Infect Dis, 2007. **195**(6): p. 870-8.
160. Dheda, K., et al., *In vivo and in vitro studies of a novel cytokine, interleukin 4delta2, in pulmonary tuberculosis.* Am J Respir Crit Care Med, 2005. **172**(4): p. 501-8.
161. Pooran, A., et al., *IL-4 subverts mycobacterial containment in Mycobacterium tuberculosis-infected human macrophages.* European Respiratory Journal, 2019. **54**(2): p. 1802242.
162. Holscher, C., et al., *A Mutation in IL4RA Is Associated with the Degree of Pathology in Human TB Patients.* Mediators Inflamm, 2016. **2016**: p. 4245028.
163. Guler, R., et al., *IL-4Rα-Dependent Alternative Activation of Macrophages Is Not Decisive for Mycobacterium tuberculosis Pathology and Bacterial Burden in Mice*, in *PLoS One*. 2015.
164. Hölscher, C., et al., *Impairment of alternative macrophage activation delays cutaneous leishmaniasis in nonhealing BALB/c mice.* J Immunol, 2006. **176**(2): p. 1115-21.
165. Herbert, D.R., et al., *Alternative macrophage activation is essential for survival during schistosomiasis and downmodulates T helper 1 responses and immunopathology.* Immunity, 2004. **20**(5): p. 623-35.
166. Maglione, P.J., J. Xu, and J. Chan, *B cells moderate inflammatory progression and enhance bacterial containment upon pulmonary challenge with Mycobacterium tuberculosis.* J Immunol, 2007. **178**(11): p. 7222-34.
167. Dubois Cauwelaert, N., et al., *Antigen presentation by B cells guides programing of memory CD4(+) T-cell responses to a TLR4-agonist containing vaccine in mice.* Eur J Immunol, 2016. **46**(12): p. 2719-2729.
168. Bosio, C.M., D. Gardner, and K.L. Elkins, *Infection of B cell-deficient mice with CDC 1551, a clinical isolate of Mycobacterium tuberculosis: delay in dissemination and development of lung pathology.* J Immunol, 2000. **164**(12): p. 6417-25.
169. Turner, J., et al., *The progression of chronic tuberculosis in the mouse does not require the participation of B lymphocytes or interleukin-4.* Exp Gerontol, 2001. **36**(3): p. 537-45.
170. Phuah, J., et al., *Effects of B Cell Depletion on Early Mycobacterium tuberculosis Infection in Cynomolgus Macaques.* Infect Immun, 2016. **84**(5): p. 1301-1311.
171. Houben, R.M.G.J. and P.J. Dodd, *The Global Burden of Latent Tuberculosis Infection: A Re-estimation Using Mathematical Modelling.* PLOS Medicine, 2016. **13**(10): p. e1002152.
172. Kiazyk, S. and T.B. Ball, *Latent tuberculosis infection: An overview.* Canada communicable disease report = Releve des maladies transmissibles au Canada, 2017. **43**(3-4): p. 62-66.

173. Radwanska, M., et al., *Deletion of IL-4Rα on CD4 T Cells Renders BALB/c Mice Resistant to Leishmania major Infection.* PLOS Pathogens, 2007. **3**(5): p. e68.
174. McFarlane, E., et al., *IL-4 Mediated Resistance of BALB/c Mice to Visceral Leishmaniasis Is Independent of IL-4Ralpha Signaling via T Cells.* Front Immunol, 2019. **10**: p. 1957.
175. Scibiorek, M., et al., *IL-4Rα signalling in B cells and T cells play differential roles in acute and chronic atopic dermatitis.* Sci Rep, 2023. **13**(1): p. 144.
176. Dewals, B., et al., *IL-4Ralpha responsiveness of non-CD4 T cells contributes to resistance in schistosoma mansoni infection in pan-T cell-specific IL-4Ralpha-deficient mice.* Am J Pathol, 2009. **175**(2): p. 706-16.
177. Schmidt, S., et al., *Nippostrongylus-Induced Intestinal Hypercontractility Requires IL-4 Receptor Alpha-Responsiveness by T Cells in Mice.* PLoS ONE, 2012. **7**: p. e52211.
178. Parihar, S.P., et al., *IL-4-Responsive B Cells Are Detrimental During Chronic Tuberculosis Infection in Mice.* Frontiers in immunology, 2021. **12**: p. 611673-611673.
179. Lindestam Arlehamn, C.S., et al., *Memory T cells in latent Mycobacterium tuberculosis infection are directed against three antigenic islands and largely contained in a CXCR3+CCR6+ Th1 subset.* PLoS Pathog, 2013. **9**(1): p. e1003130.
180. Lindestam Arlehamn, C.S., et al., *A Quantitative Analysis of Complexity of Human Pathogen-Specific CD4 T Cell Responses in Healthy M. tuberculosis Infected South Africans.* PLoS Pathog, 2016. **12**(7): p. e1005760.
181. Roy, S., et al., *Redefining the transcriptional regulatory dynamics of classically and alternatively activated macrophages by deepCAGE transcriptomics.* Nucleic Acids Res, 2015. **43**(14): p. 6969-82.
182. Jamaati, H., et al., *Nitric Oxide in the Pathogenesis and Treatment of Tuberculosis.* Front Microbiol, 2017. **8**: p. 2008.
183. Afzal, N., et al., *Percentage of CD4+ and CD8+ T-lymphocytes in blood of tuberculosis patients.* J Ayub Med Coll Abbottabad, 2010. **22**(4): p. 182-6.
184. Tanriverdi, H., et al., *Bronchoalveolar Lavage Fluid Characteristics of Patients With Sarcoidosis and Nonsarcoidosis Interstitial Lung Diseases: Ten-Year Experience of a Single Center in Turkey.* Iran Red Crescent Med J, 2015. **17**(10): p. e31103.
185. Sia, J.K. and J. Rengarajan, *Immunology of Mycobacterium tuberculosis Infections.* Microbiol Spectr, 2019. **7**(4).
186. Tsai, M.C., et al., *Characterization of the tuberculous granuloma in murine and human lungs: cellular composition and relative tissue oxygen tension.* Cell Microbiol, 2006. **8**(2): p. 218-32.
187. Flynn, J.L. and J. Chan, *Immunology of tuberculosis.* Annu Rev Immunol, 2001. **19**: p. 93-129.
188. Almeida, F.M., et al., *Hypervirulent Mycobacterium tuberculosis strain triggers necrotic lung pathology associated with enhanced recruitment of neutrophils in resistant C57BL/6 mice.* PLoS One, 2017. **12**(3): p. e0173715.
189. Niazi, M.K., et al., *Lung necrosis and neutrophils reflect common pathways of susceptibility to Mycobacterium tuberculosis in genetically diverse, immune-competent mice.* Dis Model Mech, 2015. **8**(9): p. 1141-53.
190. Lambrecht, B.N. and H. Hammad, *Biology of Lung Dendritic Cells at the Origin of Asthma.* Immunity, 2009. **31**(3): p. 412-424.
191. Desch, A.N., et al., *CD103+ pulmonary dendritic cells preferentially acquire and present apoptotic cell–associated antigen.* Journal of Experimental Medicine, 2011. **208**(9): p. 1789-1797.
192. Koh, V.H.Q., et al., *Role and contribution of pulmonary CD103+ dendritic cells in the adaptive immune response to Mycobacterium tuberculosis.* Tuberculosis, 2017. **102**: p. 34-46.
193. Lai, R., et al., *CD11b+ Dendritic Cell–Mediated Anti–Mycobacterium tuberculosis Th1 Activation Is Counterregulated by CD103+ Dendritic Cells via IL-10.* The Journal of Immunology, 2018. **200**(5): p. 1746-1760.

194. Vinuesa, C.G., et al., *Follicular B helper T cells in antibody responses and autoimmunity.* Nat Rev Immunol, 2005. **5**(11): p. 853-65.
195. Schneider, B.E., et al., *A role for IL-18 in protective immunity against Mycobacterium tuberculosis.* Eur J Immunol, 2010. **40**(2): p. 396-405.
196. Deretic, V., T. Saitoh, and S. Akira, *Autophagy in infection, inflammation and immunity.* Nat Rev Immunol, 2013. **13**(10): p. 722-37.
197. Dewals, B., et al., *Control of Schistosoma mansoni egg-induced inflammation by IL-4-responsive CD4+CD25−CD103+Foxp3− cells is IL-10-dependent.* European Journal of Immunology, 2010. **40**(10): p. 2837-2847.
198. Abdel Aziz, N., et al., *The Foxp3+ regulatory T-cell population requires IL-4Ralpha signaling to control inflammation during helminth infections.* PLoS Biol, 2018. **16**(10): p. e2005850.
199. Pace, L., C. Pioli, and G. Doria, *IL-4 Modulation of CD4+CD25+ T Regulatory Cell-Mediated Suppression1.* The Journal of Immunology, 2005. **174**(12): p. 7645-7653.
200. Yang, W.C., et al., *Interleukin-4 Supports the Suppressive Immune Responses Elicited by Regulatory T Cells.* Front Immunol, 2017. **8**: p. 1508.
201. Sullivan, B.M., et al., *Antigen-driven effector CD8 T cell function regulated by T-bet.* Proceedings of the National Academy of Sciences, 2003. **100**(26): p. 15818-15823.
202. Intlekofer, A.M., et al., *Effector and memory CD8+ T cell fate coupled by T-bet and eomesodermin.* Nature Immunology, 2005. **6**(12): p. 1236-1244.
203. Grant, N.L., et al., *Mycobacterium tuberculosis-Specific CD4 T Cells Expressing Transcription Factors T-Bet or RORγT Associate with Bacterial Control in Granulomas.* mBio, 2023. **14**(3): p. e00477-23.
204. DeGrendele, H.C., et al., *CD44 activation and associated primary adhesion is inducible via T cell receptor stimulation.* J Immunol, 1997. **159**(6): p. 2549-53.
205. Lefrançois, L. and J.J. Obar, *Once a killer, always a killer: from cytotoxic T cell to memory cell.* Immunol Rev, 2010. **235**(1): p. 206-18.
206. Winslow, G.M., et al., *Persistence and turnover of antigen-specific CD4 T cells during chronic tuberculosis infection in the mouse.* J Immunol, 2003. **170**(4): p. 2046-52.
207. Reiley, W.W., et al., *Distinct functions of antigen-specific CD4 T cells during murine Mycobacterium tuberculosis infection.* Proc Natl Acad Sci U S A, 2010. **107**(45): p. 19408-13.
208. Mueller, S.N., et al., *Memory T Cell Subsets, Migration Patterns, and Tissue Residence.* Annual Review of Immunology, 2013. **31**(1): p. 137-161.
209. Turner, D.L., et al., *Lung niches for the generation and maintenance of tissue-resident memory T cells.* Mucosal Immunology, 2014. **7**(3): p. 501-510.
210. Hoft, S.G., et al., *The Rate of CD4 T Cell Entry into the Lungs during Mycobacterium tuberculosis Infection Is Determined by Partial and Opposing Effects of Multiple Chemokine Receptors.* Infect Immun, 2019. **87**(6).
211. Moguche, A.O., et al., *ICOS and Bcl6-dependent pathways maintain a CD4 T cell population with memory-like properties during tuberculosis.* J Exp Med, 2015. **212**(5): p. 715-28.
212. Domingo-Gonzalez, R., et al., *Cytokines and Chemokines in Mycobacterium tuberculosis Infection.* Microbiology Spectrum, 2016. **4**(5): p. 10.1128/microbiolspec.tbtb2-0018-2016.
213. Monin, L. and S.A. Khader, *Chemokines in tuberculosis: the good, the bad and the ugly.* Semin Immunol, 2014. **26**(6): p. 552-8.
214. Darrah, P.A., et al., *Multifunctional TH1 cells define a correlate of vaccine-mediated protection against Leishmania major.* Nat Med, 2007. **13**(7): p. 843-50.
215. da Silva, M.V., et al., *Complexity and Controversies over the Cytokine Profiles of T Helper Cell Subpopulations in Tuberculosis.* J Immunol Res, 2015. **2015**: p. 639107.
216. Patankar, Y.R., et al., *Limited recognition of Mycobacterium tuberculosis-infected macrophages by polyclonal CD4 and CD8 T cells from the lungs of infected mice.* Mucosal Immunol, 2020. **13**(1): p. 140-148.

217. Caminero, J.A., et al., *Epidemiological evidence of the spread of a Mycobacterium tuberculosis strain of the Beijing genotype on Gran Canaria Island.* Am J Respir Crit Care Med, 2001. **164**(7): p. 1165-70.
218. Valway, S.E., et al., *An outbreak involving extensive transmission of a virulent strain of Mycobacterium tuberculosis.* N Engl J Med, 1998. **338**(10): p. 633-9.
219. López, B., et al., *A marked difference in pathogenesis and immune response induced by different Mycobacterium tuberculosis genotypes.* Clin Exp Immunol, 2003. **133**(1): p. 30-7.
220. Dunn, P.L. and R.J. North, *Virulence ranking of some Mycobacterium tuberculosis and Mycobacterium bovis strains according to their ability to multiply in the lungs, induce lung pathology, and cause mortality in mice.* Infect Immun, 1995. **63**(9): p. 3428-37.
221. Ordway, D., et al., *The hypervirulent Mycobacterium tuberculosis strain HN878 induces a potent TH1 response followed by rapid down-regulation.* J Immunol, 2007. **179**(1): p. 522-31.
222. Manca, C., et al., *Virulence of a Mycobacterium tuberculosis clinical isolate in mice is determined by failure to induce Th1 type immunity and is associated with induction of IFN-alpha /beta.* Proc Natl Acad Sci U S A, 2001. **98**(10): p. 5752-7.
223. Choreño-Parra, J.A., et al., *Mycobacterium tuberculosis HN878 Infection Induces Human-Like B-Cell Follicles in Mice.* J Infect Dis, 2020. **221**(10): p. 1636-1646.
224. Huang, L., et al., *Growth of Mycobacterium tuberculosis in vivo segregates with host macrophage metabolism and ontogeny.* J Exp Med, 2018. **215**(4): p. 1135-1152.
225. Huang, Z., et al., *Mycobacterium tuberculosis-Induced Polarization of Human Macrophage Orchestrates the Formation and Development of Tuberculous Granulomas In Vitro.* PLoS One, 2015. **10**(6): p. e0129744.
226. Refai, A., et al., *Mycobacterium tuberculosis Virulent Factor ESAT-6 Drives Macrophage Differentiation Toward the Pro-inflammatory M1 Phenotype and Subsequently Switches It to the Anti-inflammatory M2 Phenotype.* Front Cell Infect Microbiol, 2018. **8**: p. 327.
227. Shim, D., H. Kim, and S.J. Shin, *Mycobacterium tuberculosis Infection-Driven Foamy Macrophages and Their Implications in Tuberculosis Control as Targets for Host-Directed Therapy.* Front Immunol, 2020. **11**: p. 910.
228. Ramalingam, T.R., et al., *Unique functions of the type II interleukin 4 receptor identified in mice lacking the interleukin 13 receptor alpha1 chain.* Nat Immunol, 2008. **9**(1): p. 25-33.
229. Leonard, W.J., E.W. Shores, and P.E. Love, *Role of the common cytokine receptor gamma chain in cytokine signaling and lymphoid development.* Immunol Rev, 1995. **148**: p. 97-114.
230. Seah, G.T., G.M. Scott, and G.A.W. Rook, *Type 2 Cytokine Gene Activation and Its Relationship to Extent of Disease in Patients with Tuberculosis.* The Journal of Infectious Diseases, 2000. **181**(1): p. 385-389.
231. Smith, S.M., et al., *Decreased IFN- gamma and increased IL-4 production by human CD8(+) T cells in response to Mycobacterium tuberculosis in tuberculosis patients.* Tuberculosis (Edinb), 2002. **82**(1): p. 7-13.
232. Orme, I.M. and F.M. Collins, *Adoptive protection of the Mycobacterium tuberculosis-infected lung. Dissociation between cells that passively transfer protective immunity and those that transfer delayed-type hypersensitivity to tuberculin.* Cell Immunol, 1984. **84**(1): p. 113-20.
233. North, R.J., *Importance of thymus-derived lymphocytes in cell-mediated immunity to infection.* Cell Immunol, 1973. **7**(1): p. 166-76.
234. Ladel, C.H., S. Daugelat, and S.H. Kaufmann, *Immune response to Mycobacterium bovis bacille Calmette Guérin infection in major histocompatibility complex class I- and II-deficient knock-out mice: contribution of CD4 and CD8 T cells to acquired resistance.* Eur J Immunol, 1995. **25**(2): p. 377-84.
235. Urdahl, K.B., S. Shafiani, and J.D. Ernst, *Initiation and regulation of T-cell responses in tuberculosis.* Mucosal Immunol, 2011. **4**(3): p. 288-93.
236. Cooper, A.M., *Cell-mediated immune responses in tuberculosis.* Annu Rev Immunol, 2009. **27**: p. 393-422.

237. Carmona, J., et al., *Mycobacterium tuberculosis Strains Are Differentially Recognized by TLRs with an Impact on the Immune Response.* PLoS One, 2013. **8**(6): p. e67277.
238. Mourik, B.C., et al., *Mycobacterium tuberculosis clinical isolates of the Beijing and East-African Indian lineage induce fundamentally different host responses in mice compared to H37Rv.* Sci Rep, 2019. **9**(1): p. 19922.
239. Dunlap, M.D., et al., *Formation of Lung Inducible Bronchus Associated Lymphoid Tissue Is Regulated by Mycobacterium tuberculosis Expressed Determinants.* Frontiers in Immunology, 2020. **11**.
240. Khumalo, J., et al., *IL-4Rα signaling in CD4+CD25+FoxP3+ T regulatory cells restrains airway inflammation via limiting local tissue IL-33.* JCI Insight, 2020. **5**(20).
241. Mearns, H., et al., *Interleukin-4-promoted T helper 2 responses enhance Nippostrongylus brasiliensis-induced pulmonary pathology.* Infect Immun, 2008. **76**(12): p. 5535-42.
242. LaMarche, N.M., et al., *An IL-4 signalling axis in bone marrow drives pro-tumorigenic myelopoiesis.* Nature, 2023.
243. Tan, S.Y. and M.A. Krasnow, *Developmental origin of lung macrophage diversity.* Development, 2016. **143**(8): p. 1318-27.
244. Pisu, D., et al., *Dual RNA-Seq of Mtb-Infected Macrophages In Vivo Reveals Ontologically Distinct Host-Pathogen Interactions.* Cell Rep, 2020. **30**(2): p. 335-350.e4.
245. Aegerter, H., B.N. Lambrecht, and C.V. Jakubzick, *Biology of lung macrophages in health and disease.* Immunity, 2022. **55**(9): p. 1564-1580.
246. Davis, J.M. and L. Ramakrishnan, *The Role of the Granuloma in Expansion and Dissemination of Early Tuberculous Infection.* Cell, 2009. **136**(1): p. 37-49.
247. Huang, S.C., et al., *Cell-intrinsic lysosomal lipolysis is essential for alternative activation of macrophages.* Nat Immunol, 2014. **15**(9): p. 846-55.
248. Kramnik, I. and G. Beamer, *Mouse models of human TB pathology: roles in the analysis of necrosis and the development of host-directed therapies.* Semin Immunopathol, 2016. **38**(2): p. 221-37.
249. Barnes, P.F., et al., *Predictors of Short-Term Prognosis in Patients with Pulmonary Tuberculosis.* The Journal of Infectious Diseases, 1988. **158**(2): p. 366-371.
250. Martineau, A.R., et al., *Neutrophil-mediated innate immune resistance to mycobacteria.* The Journal of Clinical Investigation, 2007. **117**(7): p. 1988-1994.
251. Lowe, D.M., et al., *Neutrophils in tuberculosis: friend or foe?* Trends in Immunology, 2012. **33**(1): p. 14-25.
252. Orme, I.M., R.T. Robinson, and A.M. Cooper, *The balance between protective and pathogenic immune responses in the TB-infected lung.* Nat Immunol, 2015. **16**(1): p. 57-63.
253. Lyadova, I.V. and A.V. Panteleev, *Th1 and Th17 Cells in Tuberculosis: Protection, Pathology, and Biomarkers.* Mediators Inflamm, 2015. **2015**: p. 854507.
254. Torrado, E. and A.M. Cooper, *IL-17 and Th17 cells in tuberculosis.* Cytokine Growth Factor Rev, 2010. **21**(6): p. 455-62.
255. Kanhere, A., et al., *T-bet and GATA3 orchestrate Th1 and Th2 differentiation through lineage-specific targeting of distal regulatory elements.* Nature Communications, 2012. **3**(1): p. 1268.
256. Hölscher, C., et al., *The IL-27 Receptor Chain WSX-1 Differentially Regulates Antibacterial Immunity and Survival during Experimental Tuberculosis 1.* The Journal of Immunology, 2005. **174**(6): p. 3534-3544.
257. Skapenko, A., et al., *The IL-4 receptor alpha-chain-binding cytokines, IL-4 and IL-13, induce forkhead box P3-expressing CD25+CD4+ regulatory T cells from CD25-CD4+ precursors.* J Immunol, 2005. **175**(9): p. 6107-16.
258. Yang, W.-C., et al., *Interleukin-4 Supports the Suppressive Immune Responses Elicited by Regulatory T Cells.* Frontiers in Immunology, 2017. **8**.

259. Woodworth, J.S., et al., *Protective CD4 T Cells Targeting Cryptic Epitopes of Mycobacterium tuberculosis Resist Infection-Driven Terminal Differentiation.* The Journal of Immunology, 2014. **192**(7): p. 3247-3258.
260. Sallin, M.A., et al., *Th1 Differentiation Drives the Accumulation of Intravascular, Non-protective CD4 T Cells during Tuberculosis.* Cell Rep, 2017. **18**(13): p. 3091-3104.
261. Bull, N.C., et al., *Enhanced protection conferred by mucosal BCG vaccination associates with presence of antigen-specific lung tissue-resident PD-1+ KLRG1− CD4+ T cells.* Mucosal Immunology, 2019. **12**(2): p. 555-564.
262. Gopal, R., et al., *IL-23-dependent IL-17 drives Th1-cell responses following Mycobacterium bovis BCG vaccination.* Eur J Immunol, 2012. **42**(2): p. 364-73.
263. Alcantara, C.A., et al., *Neutrophils in Mycobacterium tuberculosis.* Vaccines, 2023. **11**(3): p. 631.
264. Pedrosa, J., et al., *Neutrophils play a protective nonphagocytic role in systemic Mycobacterium tuberculosis infection of mice.* Infect Immun, 2000. **68**(2): p. 577-83.
265. Aujla, S.J., P.J. Dubin, and J.K. Kolls, *Th17 cells and mucosal host defense.* Semin Immunol, 2007. **19**(6): p. 377-82.
266. Elkington, P.T. and J.S. Friedland, *Matrix metalloproteinases in destructive pulmonary pathology.* Thorax, 2006. **61**(3): p. 259-66.
267. Basile, J.I., et al., *Mycobacteria-Specific T Cells Are Generated in the Lung During Mucosal BCG Immunization or Infection With Mycobacterium tuberculosis.* Frontiers in Immunology, 2020. **11**.
268. Gail, D.P., et al., *Mycobacterium tuberculosis impairs human memory CD4(+) T cell recognition of M2 but not M1-like macrophages.* iScience, 2023. **26**(9): p. 107706.
269. Leal, I.S., et al., *Failure to induce enhanced protection against tuberculosis by increasing T-cell-dependent interferon-gamma generation.* Immunology, 2001. **104**(2): p. 157-61.
270. Shafiani, S., et al., *Pathogen-specific regulatory T cells delay the arrival of effector T cells in the lung during early tuberculosis.* J Exp Med, 2010. **207**(7): p. 1409-20.
271. Tchilian, E.Z., et al., *Simultaneous immunization against tuberculosis.* PLoS One, 2011. **6**(11): p. e27477.
272. Beverley, P.C.L., et al., *Harnessing local and systemic immunity for vaccines against tuberculosis.* Mucosal Immunology, 2014. **7**(1): p. 20-26.
273. Sacks, D. and N. Noben-Trauth, *The immunology of susceptibility and resistance to Leishmania major in mice.* Nat Rev Immunol, 2002. **2**(11): p. 845-58.
274. Adam, L., et al., *Early Resistance of Non-virulent Mycobacterial Infection in C57BL/6 Mice Is Associated With Rapid Up-Regulation of Antimicrobial Cathelicidin Camp.* Frontiers in Immunology, 2018. **9**.
275. Wakeham, J., J. Wang, and Z. Xing, *Genetically Determined Disparate Innate and Adaptive Cell-Mediated Immune Responses to Pulmonary Mycobacterium bovis BCG Infection in C57BL/6 and BALB/c Mice.* Infection and Immunity, 2000. **68**(12): p. 6946-6953.
276. Wang, J., et al., *Macrophages are a significant source of type 1 cytokines during mycobacterial infection.* J Clin Invest, 1999. **103**(7): p. 1023-9.
277. Shibuya, K., et al., *IL-1 alpha and TNF-alpha are required for IL-12-induced development of Th1 cells producing high levels of IFN-gamma in BALB/c but not C57BL/6 mice.* J Immunol, 1998. **160**(4): p. 1708-16.
278. de Martino, M., et al., *Immune Response to Mycobacterium tuberculosis: A Narrative Review.* Front Pediatr, 2019. **7**: p. 350.